TECHNICAL REPORT STANDARD TITLE PAGE

1. Report No.	2. Government Accession No.	3. Recipient's Catalog No.
FHWA/TX-78/07+196-1F		

4. Title and Subtitle	5. Report Date
DESIGN OF REINFORCEMENT FOR NOTCHED ENDS OF PRESTRESSED CONCRETE GIRDERS	August 1977
	6. Performing Organization Code

7. Author(s)	8. Performing Organization Report No.
Gangadharan Menon and Richard W. Furlong	Research Report 196-1F

9. Performing Organization Name and Address	10. Work Unit No.
Center for Transportation Research The University of Texas at Austin Austin, Texas 78712	11. Contract or Grant No. Research Study 3-5-76-196
	13. Type of Report and Period Covered

12. Sponsoring Agency Name and Address	14. Sponsoring Agency Code
Texas State Department of Highways and Public Transportation; Transportation Planning Division P. O. Box 5051 Austin, Texas 78763	Final

15. Supplementary Notes

Study conducted in cooperation with the U. S. Department of Transportation, Federal Highway Administration. Research Study Title: "Optimum Reinforcement for Notched Ends of Prestressed Concrete Girders"

16. Abstract

This study was intended to analyze the shear strength of the notched ends of prestressed concrete girders and to evaluate the ultimate shear capacity by testing a model with reinforcing details simpler than those currently adopted in practice. Various discrete element analyses by a computer program showed that it is possible to identify the most highly stressed regions of an end block and also to predict a likely crack pattern that would occur before failure.

One specimen with two different end block details was tested to failure. The failure of the specimen did not occur at either notch, and the notch capacity with uncongested reinforcement was shown to be adequate for the intended load. The end block with the provision of a hanger strap assembly and reinforcement welded to the bearing plate behaved well during the test. As concluded from the observation of crack widths, such a design with hanger straps seems to possess a higher degree of serviceability than a design based on the provision of large web plates embedded at the notched end.

A design procedure derived from two potential failure modes has been suggested. The two failure modes involved are (a) a shear friction separation parallel to the inclined hanger strap reinforcement and (b) a shear compression separation from the corner of the notch into the flexural compression zone of the end block. An example design for the end block of a standard highway bridge stringer has been given to illustrate the design procedure.

17. Key Words	18. Distribution Statement
prestressed concrete, girder, notched ends, shear strength, reinforcement, hanger strap assembly	No restrictions. This document is available to the public through the National Technical Information Service, Springfield, Virginia 22161.

19. Security Classif. (of this report)	20. Security Classif. (of this page)	21. No. of Pages	22. Price
Unclassified	Unclassified	166	

Form DOT F 1700.7 (8-69)

DESIGN OF REINFORCEMENT FOR NOTCHED ENDS OF PRESTRESSED CONCRETE GIRDERS

by

Gangadharan Menon
Richard W. Furlong

Research Report Number 196-1F

Optimum Reinforcement for Notched Ends
of Prestressed Concrete Girders

Research Project 3-5-76-196

conducted for

Texas
State Department of Highways and Public Transportation

in cooperation with
U. S. Department of Transportation
Federal Highway Administration

by the

CENTER FOR TRANSPORTATION RESEARCH
BUREAU OF ENGINEERING RESEARCH
THE UNIVERSITY OF TEXAS AT AUSTIN

August 1977

The contents of this report reflect the views of the authors, who are responsible for the facts and the accuracy of the data presented herein. The contents do not necessarily reflect the official views or policies of the Federal Highway Administration. This report does not constitute a standard, specification, or regulation.

There was no invention or discovery conceived or first actually reduced to practice in the course of or under this contract, including any art, method, process, machine, manufacture, design or composition of matter, or any new and useful improvement thereof, or any variety of plant which is or may be patentable under the patent laws of the United States of America or any foreign country.

ABSTRACT

This study was intended to analyze the shear strength of the notched ends of prestressed concrete girders and to evaluate the ultimate shear capacity by testing a model with reinforcing details simpler than those currently adopted in practice. Various discrete element analyses by a computer program showed that it is possible to identify the most highly stressed regions of an end block and also to predict a likely crack pattern that would occur before failure.

One specimen with two different end block details was tested to failure. The failure of the specimen did not occur at either notch, and the notch capacity with uncongested reinforcement was shown to be adequate for the intended load. The end block with the provision of a hanger strap assembly and reinforcement welded to the bearing plate behaved well during the test. As concluded from the observation of crack widths, such a design with hanger straps seems to possess a higher degree of serviceability than a design based on the provision of large web plates embedded at the notched end.

A design procedure derived from two potential failure modes has been suggested. The two failure modes involved are (a) a shear friction separation parallel to the inclined hanger strap reinforcement and (b) a shear compression separation from the corner of the notch into the flexural compression zone of the end block. An example design for the end block of a standard highway bridge stringer has been given to illustrate the design procedure.

SUMMARY

Standard size prestressed concrete bridge beams can span across an opening no greater than about 130 ft. The flexibility of deformations would be excessive if the largest girders were supported at greater distances. Consequently the maximum width of opening across which the girders can be used would be 130 ft unless the girder support points could be extended an additional distance outward from the limits of the opening.

Girders can be extended outward as suggested in Fig A in order to make possible an opening more than 160 ft wide without changing the basic standard girder configuration. The sketch of Fig A does show that a notch or shelf must be used at the connection between girders.

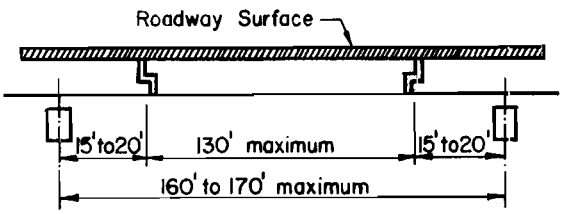

FIGURE A

Extra reinforcement must be placed in the region of the notched end in order to maintain shear capacity after half the depth of the girder is removed at the notch. The analysis and physical tests reported here indicate that only two principal types of reinforcement must be added at the notch. In addition to stirrups that are needed even without a notch, a strap-type hanger mechanism plus supplementary longitudinal steel for maintaining shear friction at the throat of the notch can be used effectively without congesting the notch region. Concrete is not difficult to place if the accumulated reinforcement can be kept uncongested.

Design procedures and an example problem are presented in order to implement recommendations derived from the project.

IMPLEMENTATION STATEMENT

The research study reported herein revealed that there are only two major failure mechanisms that need to be considered for the proportioning of extra reinforcement in notched ends of prestressed concrete beams. Simple and direct design procedures are expressed in the form of a strength equation which expresses resistance to the formation of a diagonal shear failure and another equation for resistance to a shear friction failure at the notch.

An analytic effort was developed which required the use of a discrete element model and a computer program for predicting crack propagation and probable load paths. The analysis was considered more sophisticated and no more accurate than the direct formulation of strength in the failure mechanism that describes diagonal cracking or that describes shear friction at the notch.

Notched ends can be reinforced for adequate strength and for control of cracking at service loads by means of longitudinal bars welded to a bearing plate at the notch and by a diagonal strap hanger mechanism, each of which must be used in addition to the "normal" quantity of stirrups that would be used in the absence of the notch. The extra reinforcement does not create unusual congestion in the region of the notch.

Notched end beams can be fabricated at costs which are insignificantly greater than costs associated with beams that are not notched. Clear span openings for bridge prestressed stringer composite beam structures can be extended from 130 ft to 160 to 170 ft without requiring the creation of new, deeper forms for larger standard beam cross sections.

TABLE OF CONTENTS

CHAPTER 5. DISCUSSION OF TEST RESULTS

CHAPTER 6. SHEAR STRENGTH OF NOTCHED END

CHAPTER 7. RECOMMENDATIONS

APPENDICES

NOTATION

a	Distance from the vertical face of a notch to the centroid of the reaction at the notched end
A_{cr}	Area of a shear plane
A_{vf}	Area of tension reinforcement necessary to insure enough normal force to develop shear friction strength
c	Distance from compression face of a member to its neutral axis
C	Compression force on a beam cross section
d_{cr}	Horizontal projection of length of a diagonal shear compression crack
d	Distance from compression face of a member to the centroid of tensile forces on a cross section
E_c	Modulus of elasticity of concrete
E_s	Modulus of elasticity of steel
F	Friction force
f'_c	Compression ultimate stress of standard concrete cylinders
f'_{ci}	Compression ultimate stress of concrete when prestress strands are released
f_p	Stress created by prestress force
F_p	Force in prestress strand
f_{ps}	Stress developed in strand from end of member to the shear friction crack
L	Distance between supports of a simply supported beam
N	Force normal (perpendicular) to a cross section
N_i	Specific component i of normal force N

n	Modular ratio between steel and concrete stiffness E_s/E_c
P_u	Force applied normal to a shear friction crack
R	Reaction or force applied at the reaction of a notched end beam
s	Spacing of reinforcement
T	Tension force in reinforcement
v	Shear stress
V_{ag}	Vertical shear capacity attributed to aggregate interlock
v_c	Shear stress capacity of concrete
V_{cz}	Vertical shear force capacity of concrete
V_d	Vertical shear force attributed to dowel action of longitudinal reinforcement
V_s	Vertical shear force attributed to stirrups
V_u	Ultimate shear force capacity
v_u	Ultimate shear stress capacity
α	Angle between horizontal axis and diagonal shear compression crack
Δ	Vertical displacement
Δ_{cc}	Deformation of extreme fibers of concrete across d_{cr} length
Δ_{st}	Deformation of tensile reinforcement across d_{cr} length
μ	Sliding friction coefficient
μ'	Modified sliding friction coefficient
ϕ	Capacity reduction factor

CHAPTER 1. INTRODUCTION

1.1 General

The maximum span of prestressed concrete bridge stringers is limited by the flexural strength and flexural stiffness of the stringers. If simple span members are incorporated into a cantilever system, as illustrated in Fig 1.1, the distance between the required supports can be increased by approximately 20 percent in the end span and by 40 percent in the interior span without any increase in the required flexural capacity of the stringers. However, the reduction in shear capacity at the end block regions where the simple span members rest on the cantilever members has posed problems in design since the re-entrant notch reduces the effective depth in this region to less than half the overall depth. A typical arrangement at this portion of the structure is shown in Fig 1.2.

A high concentration of stresses is known to exist at these notched end locations. The mechanisms of shear failure, even in simple cases involving beams of constant cross section, have not been defined adequately for precise analysis as yet. With more indeterminate factors that cause stresses such as those near a notched support region, the designer is inclined to be oversafe in his provision of reinforcement for shear strength. This excess steel poses problems in detailing, fabrication, and placing as well as congestion which inhibits good placement of concrete around and within the reinforcement patterns.

1.2 Objective of Study

The purpose of this study is to analyze the internal distribution of forces in notched end blocks and to determine experimentally end block reinforcement details that can be constructed with no unusual congestion of reinforcement and which are structurally more efficient than those presently under consideration. A supplementary objective will be the improvement of analytical capability of the problem. Various

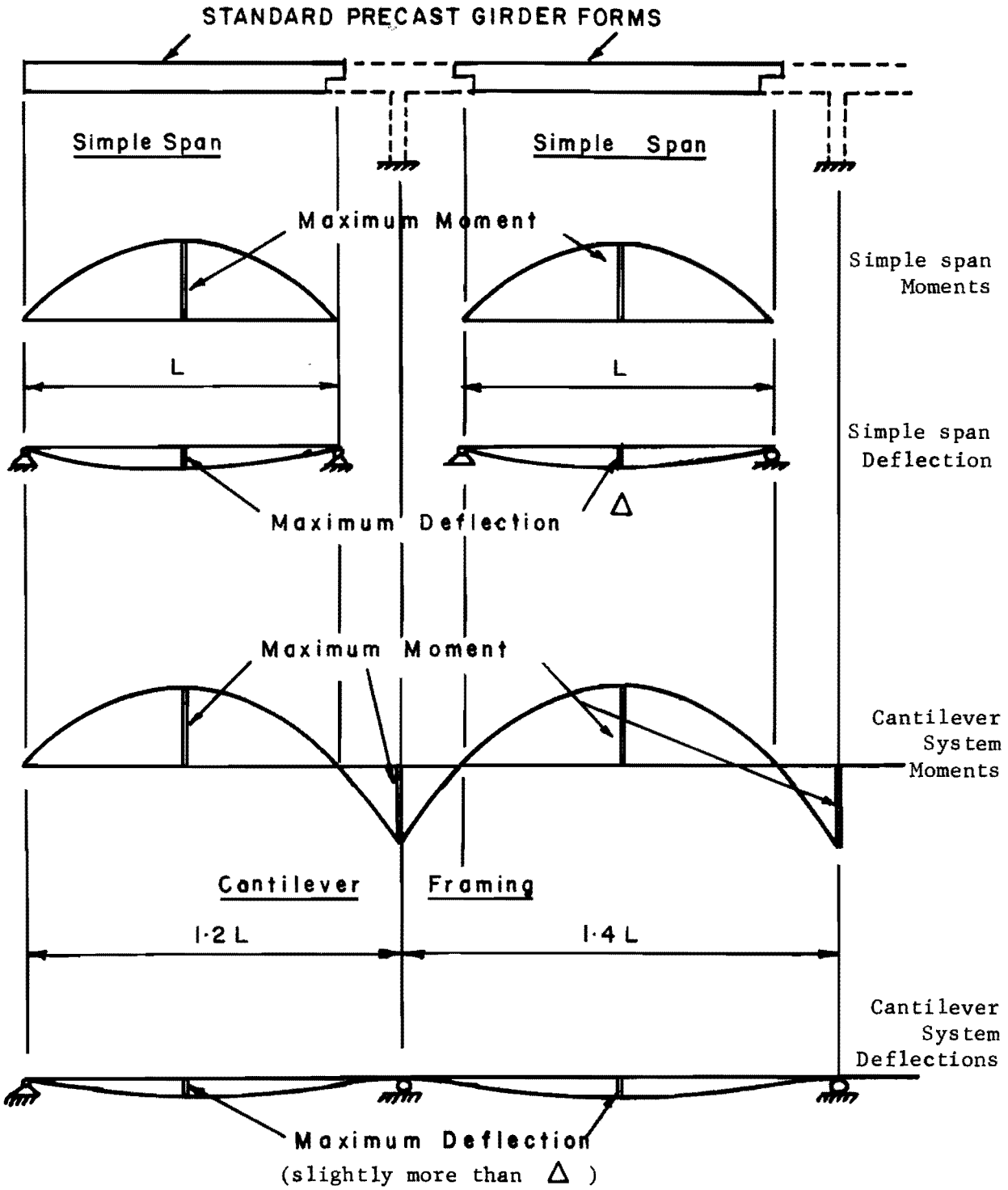

Fig 1.1. Cantilever and simple framing.

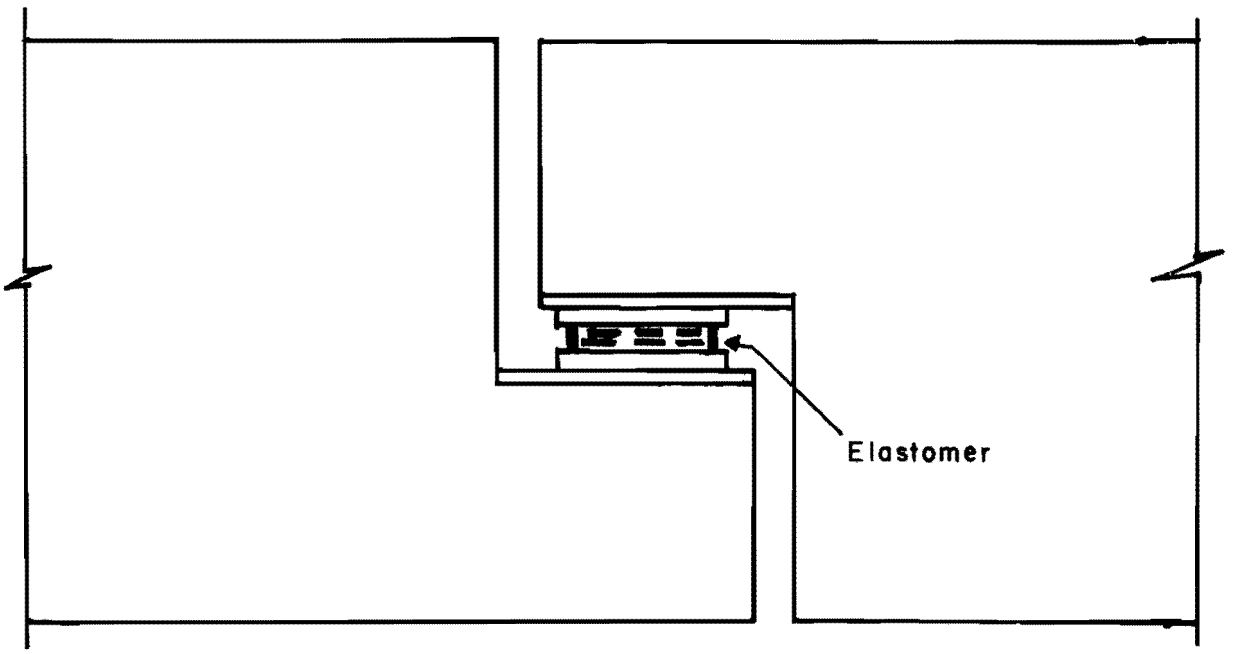

Fig 1.2. Arrangements at notched end.

analytical models of the end block will be tried for a computer aided study.

1.3 Scope of Work

The scope of the work on this investigation consists of

(a) a preliminary study of stress distribution at the notched end with the aid of an available computer program for plane frames,

(b) selection of two types of design details based on the initial appraisal of the problem and on the above study,

(c) design of the specimen for testing in the laboratory,

(d) establishing the degree of efficiency of computer aided analysis, and

(e) suggestion of a simple design procedure for notched end reinforcement.

1.4 Previous Studies

Very few reports have been published regarding studies of problems connected with notched end stress conditions. The following brief summary of some of the relevant works published in this area will help describe the problem.

1.4.1 Work done by Ali A. Hamoudi et al (1)

The state of stress near the root of the notched end was derived on the basis of an elastic equilibrium plane stress analysis. Calculated stresses were compared with experimental data. Eight prestressed concrete T-beams were fabricated and tested. Spanning 30 ft each, these beams were pretensioned with 1/2-in. strands. Web reinforcement at notched ends consisted of (1) 1/2-in.-diameter Stressteel (145 ksi) post-tensioned bars, (2) vertical and horizontal rebar stirrups, and (3) rebars inclined at 30^{o} to the horizontal. The authors concluded that prestressing the notched ends with inclined high strength steel provided a satisfactory method for web reinforcement and furthermore prevented shear cracking in this area at working loads.

1.4.2 Work done by M. J. N. Priestley (12)

Tests were carried out on four specimens in the Central Laboratories, New Zealand, to check the shear strength of the notched ends of beams which were to be built in an overpass. All specimens were post-tensioned. Shear reinforcement at notched ends consisted of vertical stirrups closely spaced and light horizontal stirrups. None of the specimens failed in shear at the notched end. However, the notched ends were found to possess capacities much greater than their design strength. Though cracking occurred at low levels of load, the crack widths remained very small until the flexural capacity of the beams was reached. No design method was presented in this report. The crack pattern and stress contours of the specimens are suggestive of a truss action by which load is transferred from the notched end to the full section of the beam.

1.4.3 Work done by M. P. Werner and W. H. Dilger (14)

This study was aimed at finding (1) the shear force required to form a crack at the re-entrant corner of the notched end and (2) whether the cracking shear could be taken as the contribution of concrete to total shear strength. Based on a finite element analysis and experimental data from five beams tested, the authors suggested that the shear cracking load can be predicted with reasonable accuracy and that this could be taken as the concrete strength in shear. All the beams tested were post-tensioned and it is possible that anchor plates could have had an effect on the stress distribution in the end zone, a condition which does not exist in pretensioned beams.

1.4.4 Work done by J. R. Gaston and L. B. Kriz (7)

A similar problem of scarf joints used in precast frames for buildings was investigated at the Research and Development Laboratories of the Portland Cement Association. These tests were conducted mainly for studying flexural behavior, but the mode of failure reported is consistent with what could be expected in the shear problem of girders with notched ends, i.e., a failure initiated from cracking at a re-entrant corner. (See Fig 1.3). These tests were conducted for connections (a) without stirrups 1 and 2, (b) with stirrup 1 only, and (c) with stirrups 1 and 2. In

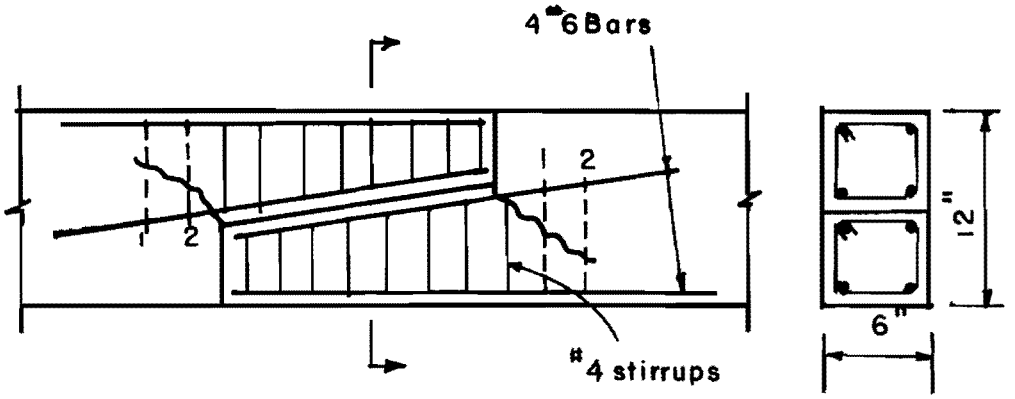

Fig 1.3. Scarf joint (from study of Ref 7).

the first two cases the inclined #6 bars were very short and in the third case these were well anchored. The capacities were found to be 25 percent higher and 70 percent higher than (a) for (b) and (c) respectively. The tests clearly established the importance of providing stirrups that cross potential cracks, and also illustrated the role of anchorage requirements.

CHAPTER 2. PRELIMINARY STUDY

2.1 Mechanism of Shear Failure

Research on shear failure in reinforced concrete and prestressed concrete members has been carried out by many people all over the world for decades, but the phenomenon of shear failure has not been analytically explained in all its aspects. Concepts on the mechanism of shear failure have undergone various stages, from Morsch's Truss Theory through Kani's Concrete Teeth concept (9). The present thinking as opposed to these earlier theories is directed mainly towards analysis of forces which are present along or across a crack where a shear failure is imminent.

Figure 2.1 shows the various internal forces by which shear is transmitted across a shear crack in a beam subjected to shear force. These are mainly (a) shear stress carried by concrete, V_c or V_{cz}, (b) interface shear transfer or the aggregate interlock V_{ag}, (c) dowel action V_d, a vertical force in the longitudinal reinforcement as it is bent across the crack, and (d) force V_s in the vertical stirrups. When the beam is prestressed the capacity of concrete to take shear is enhanced by the longitudinal compression which delays formation of cracks. Discussion of these internal forces and the effects of prestressing are contained in the following paragraphs.

2.2 Mechanism of Shear Failure at Notched End

2.2.1 Distribution of internal shears

Since the most adverse combination of shear stress and flexural tensile stress due to the moment $R \times a$ (Fig 2.3a) exists in the uncracked member at the junction of the notched end, it is obvious that cracking should commence at the root of the notch. Once the concrete strength is overcome, various internal forces come into play in succession to resist a failure.

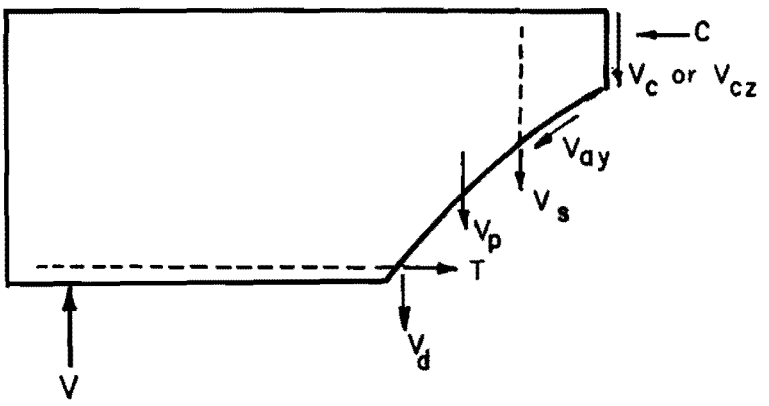

Fig 2.1. Forces at an inclined crack.

The distribution of internal forces as they occur in a reinforced beam with web reinforcement has been discussed extensively in the report by the ASCE-ACI Committee 426 on Shear and Diagonal Tension (8). In the case of a prestressed concrete beam with shear reinforcement, the distribution of internal shears can be described at various load stages as follows.

The internal shear can be related to the applied shear diagrammatically as shown in Fig 2.2. As the external loading applied to the beam is increased, the precompressed concrete resists the tension that is induced below the neutral axis of the cross section until the load is large enough to nullify the compressive stress at the bottom fiber. This stage is represented by the zone ab of Fig 2.2. Thereafter, the shear is carried by concrete alone by virtue of its shear strength V_{cz} until the occurrence of flexural cracking. From this stage onwards the behavior is identical to a reinforced concrete beam, except for the effects of the vertical component V_p of the prestress in draped strands. Between flexural cracking and the inclined cracking, shear is resisted by the concrete V_{cz}, the interface shear transfer V_{ay}, the dowel action V_d and the vertical component of the prestressing forces. After formation of inclined cracks the shear reinforcement carries part of the shear, V_s. As the cracks widen the interface shear transfer decreases forcing V_{cz}, V_d, and V_s to increase until failure occurs either by compression failure of concrete or splitting failure of the longitudinal reinforcement or yielding of shear reinforcement.

2.2.2 Effect of prestressing

As can be seen from the distribution of internal shears, the horizontal component of the prestressing force delays the flexural cracking and the vertical component delays the inclined cracking. In addition to this the compression prestress forces a shear crack into a more horizontal orientation resulting in longer crack lengths than in a reinforced concrete beam. This is advantageous because with an increased crack length more vertical stirrups share the shear resistance.

The flat orientation of cracks when there is prestressing can be explained by analyzing the stress conditions on an element as shown in Fig 2.3. At the neutral axis the forces caused by applied bending moments

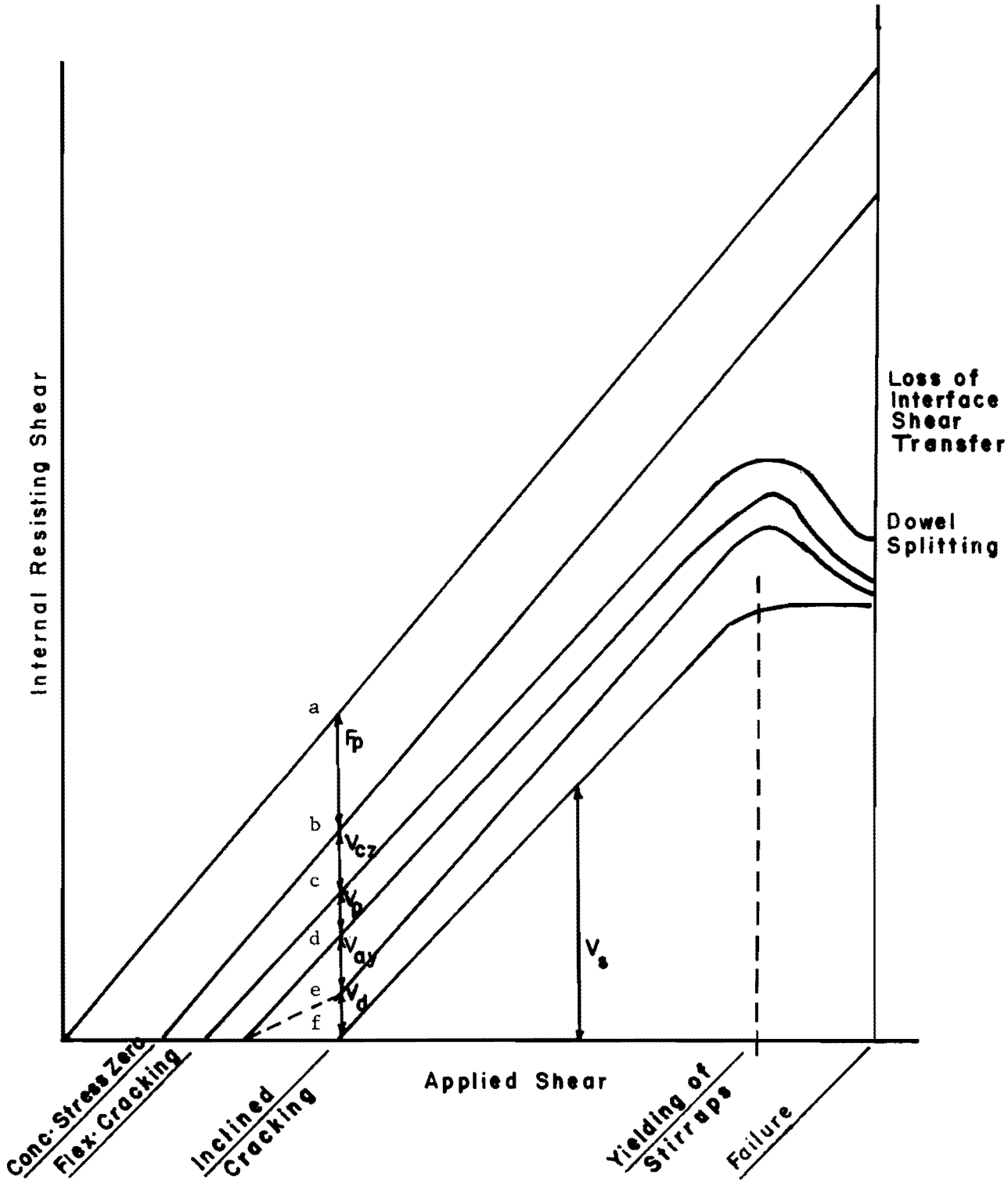

Fig 2.2. Distribution of internal shears in a prestressed concrete beam.

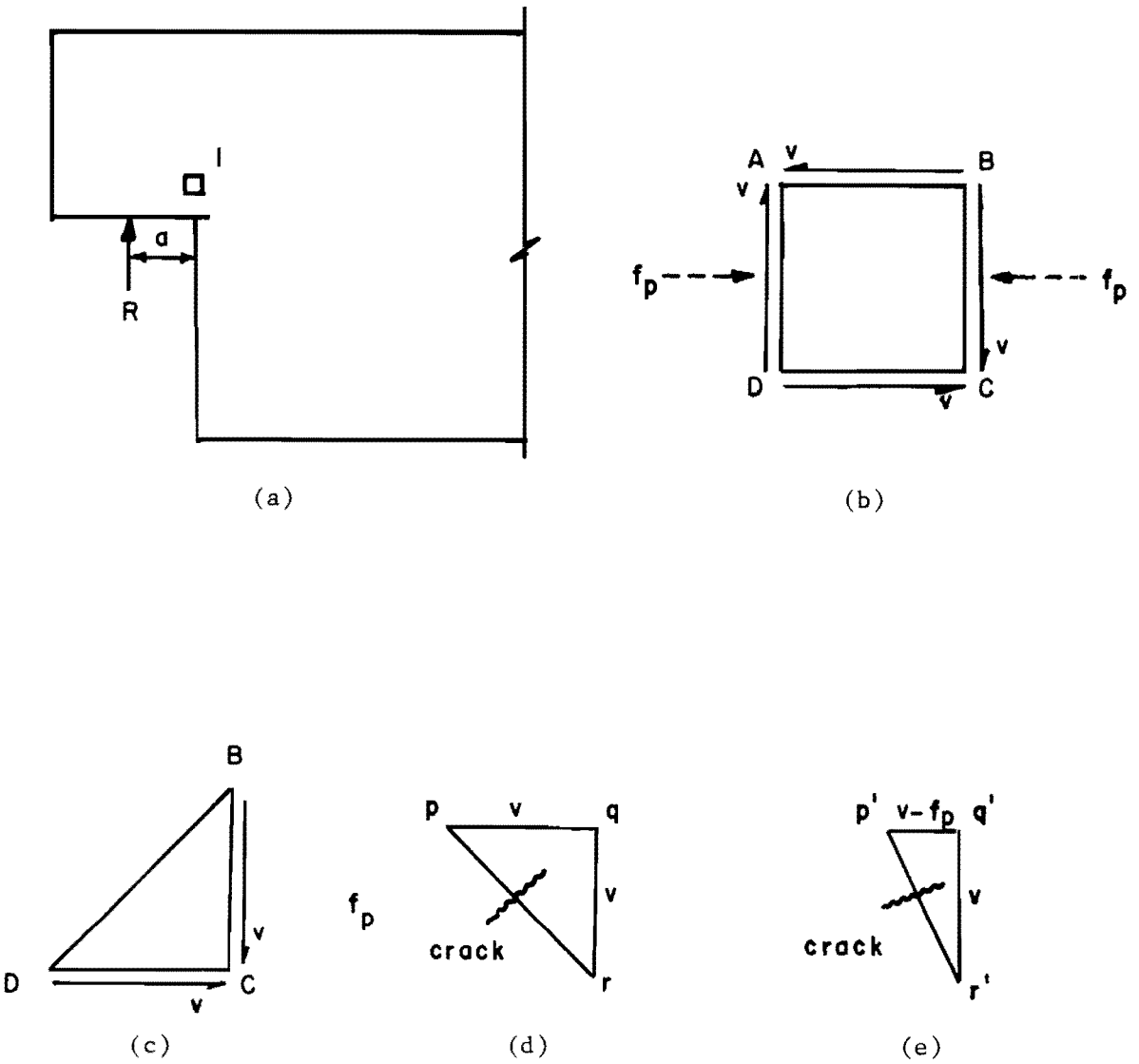

Fig 2.3. Effect of prestress on crack orientation.

are zero, and the element would be subjected to pure shear v if there were no prestressing. The tensile principal stress occurs at 45^{o} from the vertical as the sum of the shear forces on the element BDC and is represented by pr in the triangle of forces pqr (Fig 2.3d). If a prestress f_p is introduced, the resultant will be p'r' (Fig 2.3e), which is closer to the vertical than pr . Since cracks form approximately perpendicular to the direction of the principal tensile stress the effect of prestressing is to make the crack less steep.

2.3 Load Paths at Notched End Region

The notched end region of a beam has been analyzed as an elastic continuum (16) in order to identify regions of maximum principal tensile or shear stress before cracking. After cracking occurs the continuum must be redefined, and a finite element representation becomes complicated by the need to employ dissimilar elements, some representing concrete and others representing reinforcement. An alternate analytic representation of the notched end region can be composed of truss elements that, if pin connected, possess only the capacity to resist axial forces. If connected as homogeneous, continuous elements, the "truss" members possess also the capacity to resist shear forces between the ends of the elements. Individual elements can be modeled to represent the stiffness and strength of the steel reinforcement or they can be made less stiff to represent concrete. In order to model cracking, elements that appear to be in tension high enough to fracture concrete can be eliminated, and the analytical procedure can be repeated.

A frame analysis program named 'LINFIX' was used for the truss analysis. This program is capable of analyzing the axial load, moment, and shear forces, rotations, and deflections of all members of a two-dimensional frame with member connections that may be specified as pinned or continuous.

A typical end block of a beam, shown in Fig 2.4, was chosen for the initial study of load paths. Figure 2.5 shows the pattern of the analytical model adopted for this end block. The end block is divided into 132 members with 50 node points all serially numbered from right to left. Each member is designated by the number indicated adjoining the member. Prestressing is represented by external loads applied at node

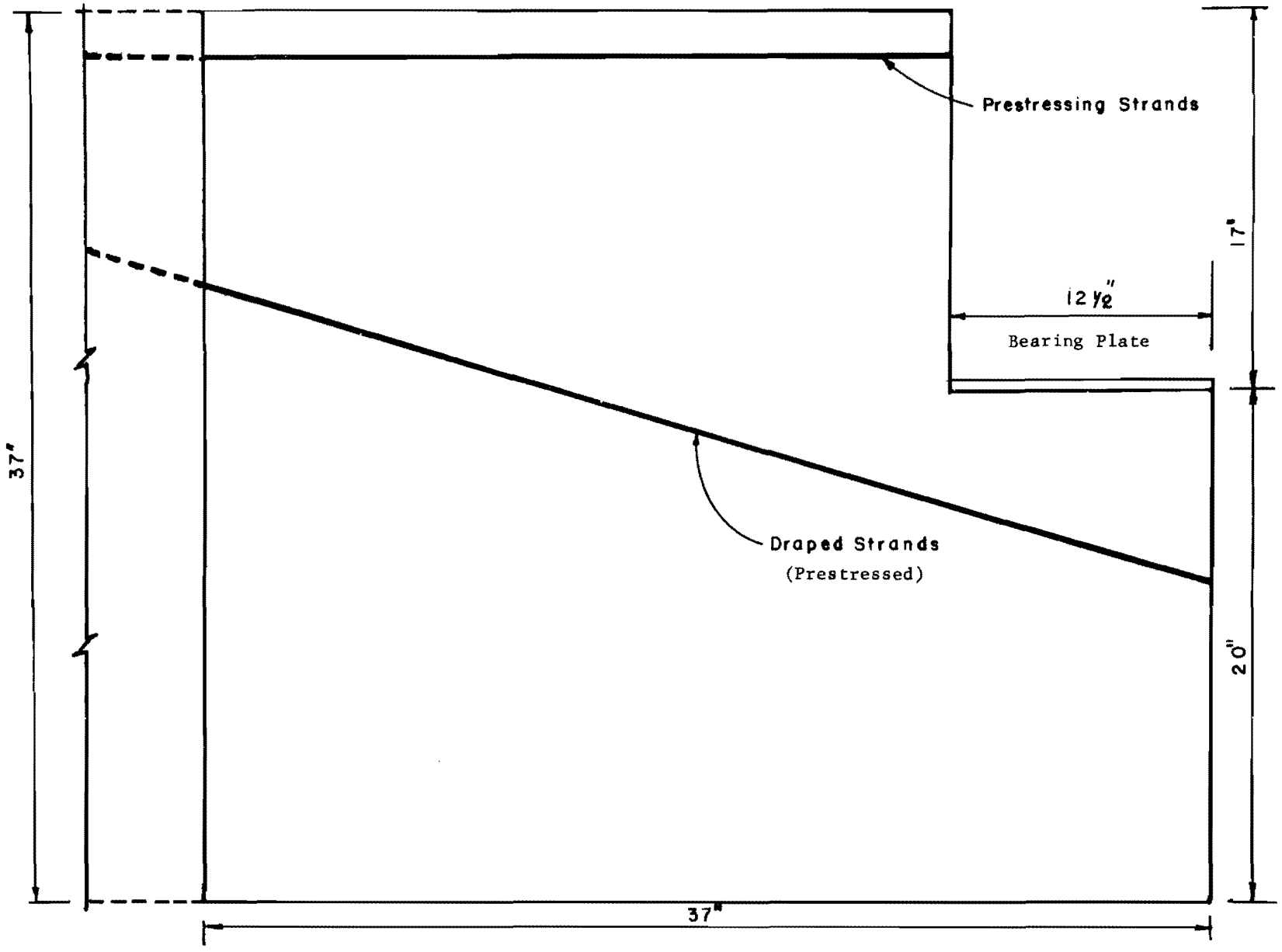

Fig 2.4. End block details for preliminary analysis.

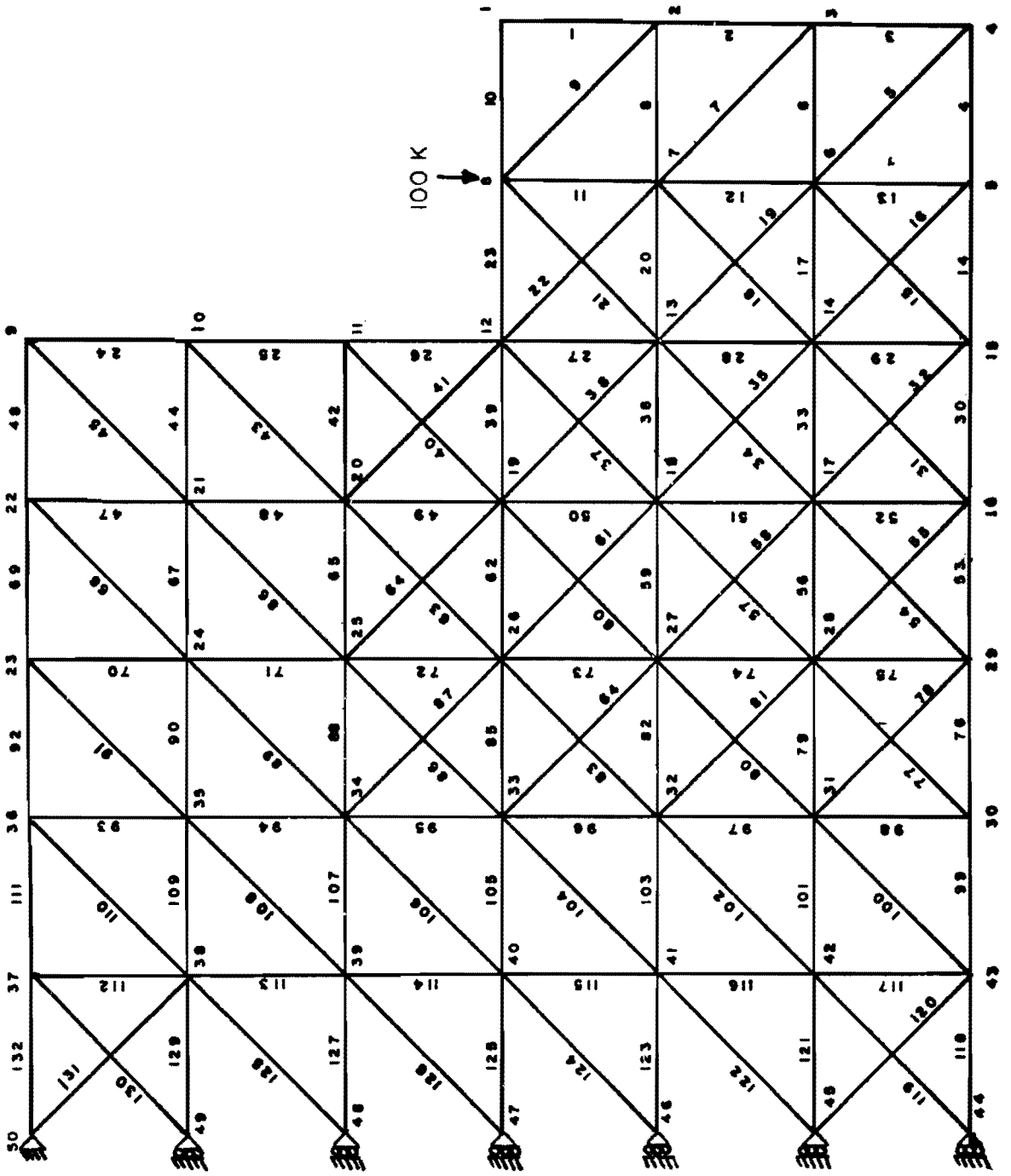

Fig 2.5. Analytical model.

points within the development length of the prestressing strands. The area and stiffness of the members are taken as that of the concrete around them.

A load of 100K was applied at Joint 8. The axial stresses in the members as obtained by the computer analysis are given in Appendix G. The members with tensile stresses which exceeded the capacity of concrete (taken as $7.5\sqrt{f'c}$) were removed or replaced by reinforcing members.

Figures 2.6(a) through 2.6(c) show progressive development of excessive tension in members on application of load. The members whose stresses exceeded the concrete capacity in tension and assumed to be cracked are shown with hatched lines. Figure 2.6(d) shows all the members cracked when 100K load is applied. The study showed that tensile stresses are predominant on vertical as well as inclined members adjacent to the notched end junction. Obviously such zones would require reinforcement to resist tensile forces. In view of this the following conclusions were made:

(1) A diagonal steel bar was needed as a hanger bar for tension, starting below the notch extending to the flexural compression zone above the notched region.

(2) Both vertical and horizontal web reinforcement is required near the notch.

(3) Flexural tension parallel to the bearing plate requires reinforcement that is attached to the bearing plate.

(4) The prestressing force on draped strands helps reduce deformed bar reinforcement that is needed near the notch.

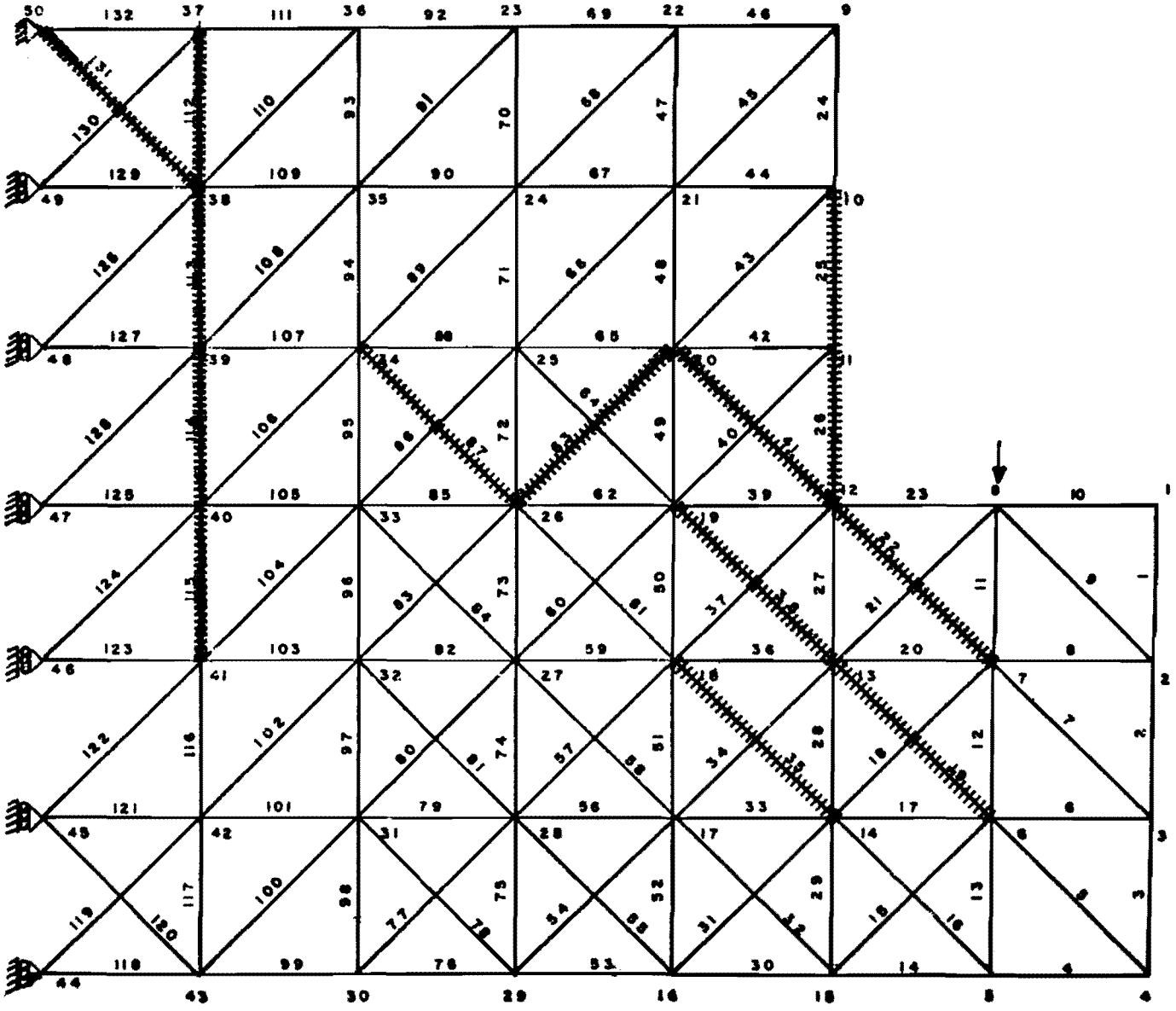

Fig 2.6(a). Members cracked, first stage (all members concrete).

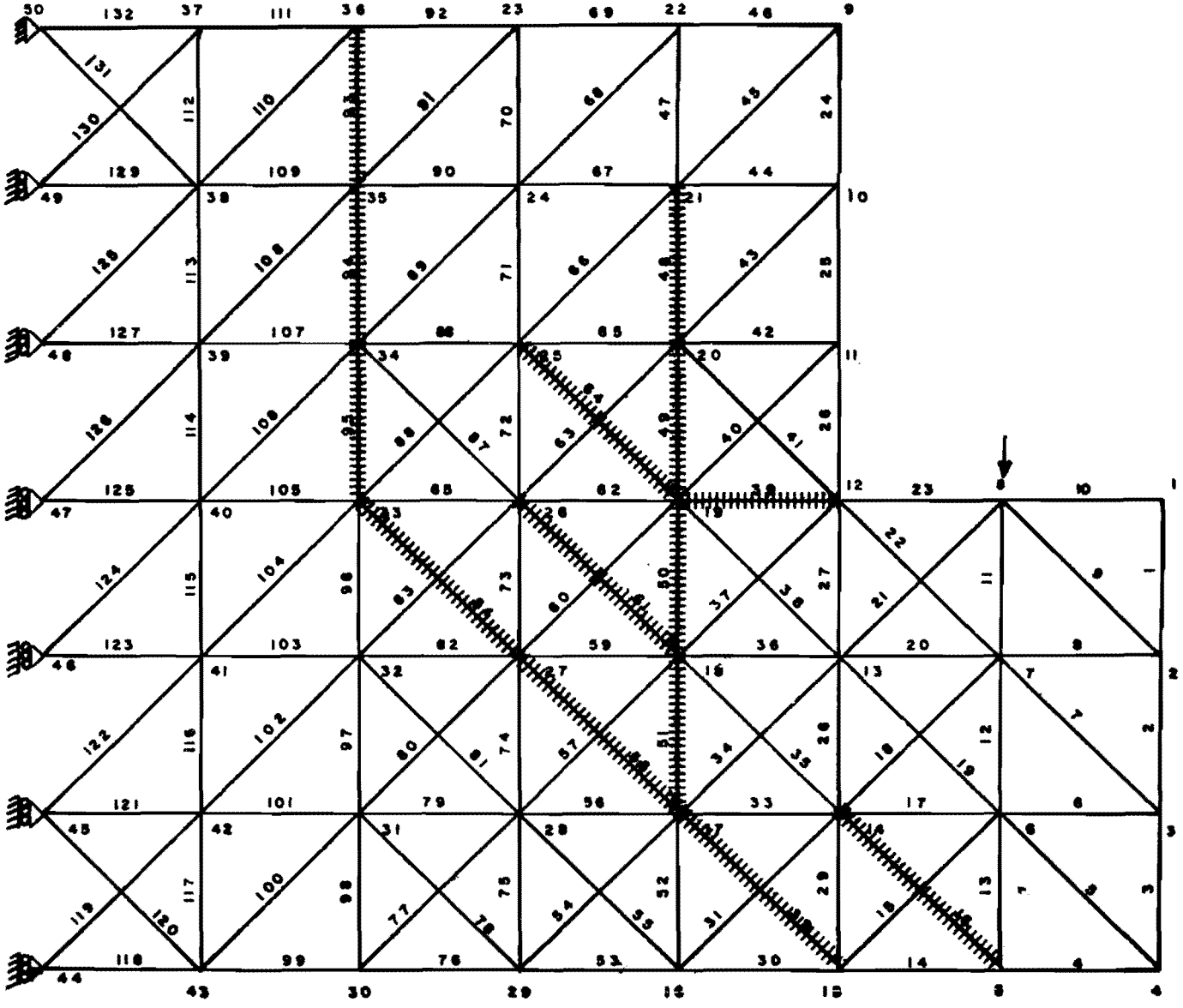

Fig 2.6(b). Members cracked, second stage.

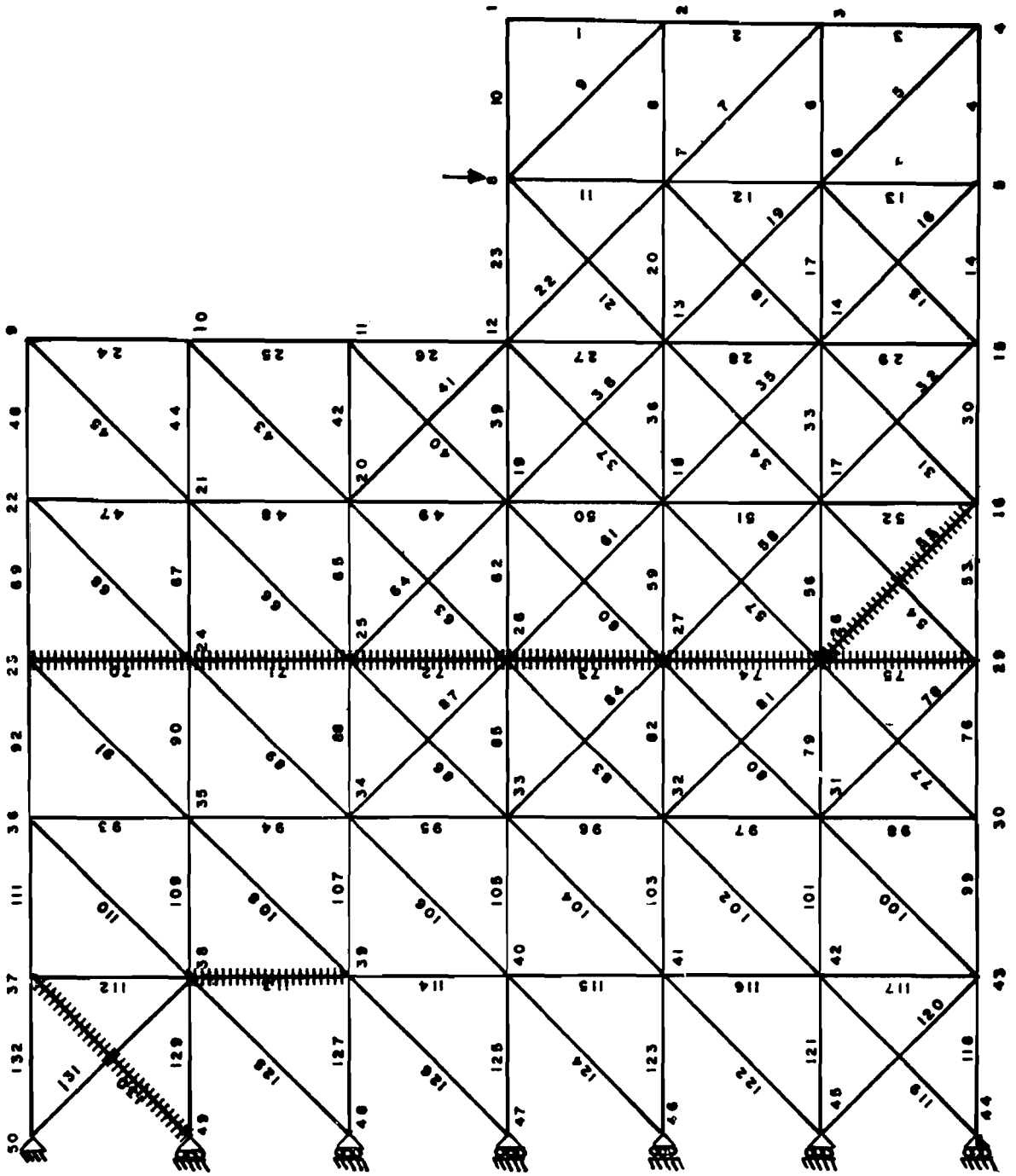

Fig 2.6(c). Members cracked, third stage.

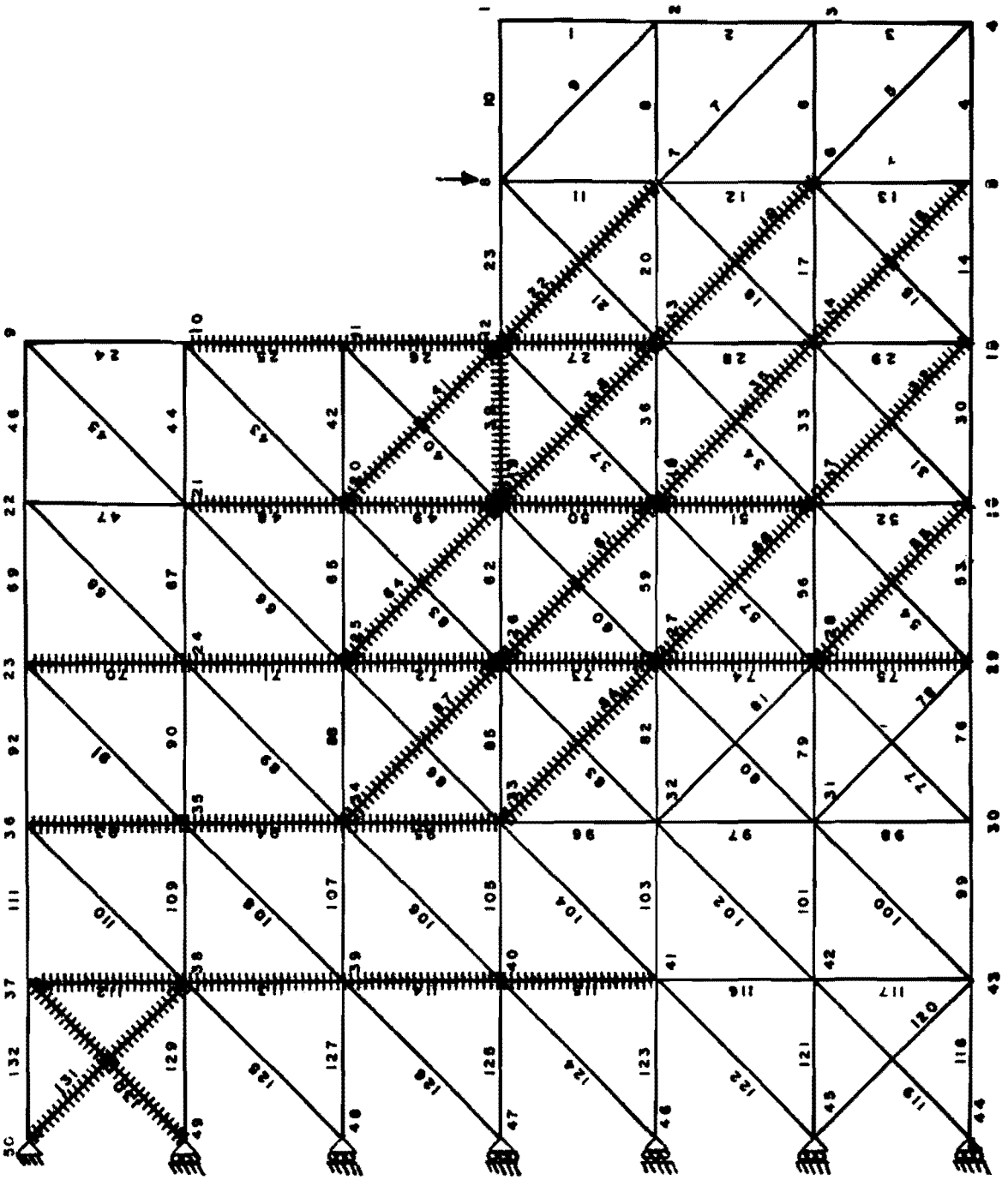

Fig 2.6(d). Showing all cracked members.

CHAPTER 3. THE SPECIMEN

3.1 Design of the Specimen

For the design of the test specimen, the 54-inch-deep standard beam of the State Department of Highways and Public Transportation was selected as a prototype. Figure 3.1 shows details at the notched end of the 54-in. beam as proposed by one of the district offices of the Department. This beam with composite action offered by the deck slab on top is supposedly designed for a service load reaction of 178 k and an ultimate load reaction of 300 k. Calculations for this load are based on a girder spacing of 7.5 ft for a standard lane loading of HS-20-44 and are given in Appendix A.

With the data from the discrete element truss analysis at hand, a critical study of the design of the beam described above was made. The proposed reinforcement for this beam, as shown in Fig 3.1, calls for heavy steel bars horizontal and vertical, and one set of four diagonal straps near the reentrant corner of the notched end. The congestion caused by the reinforcement makes concrete placement difficult. For examining the effectiveness of the reinforcement provided at different locations the notched end was analyzed by the computer program as a truss model with elements continuous at joints. Details of this analysis are given in Chapter 6. The computations led to the conclusion that most of the horizontal reinforcement does not get stressed on application of load at the notched end. Hence a reduction of steel is possible in such locations. Accordingly, one end of the specimen was designed with reduced reinforcement. A design for the other end of the specimen was developed with reinforcement that is based on a different concept. Embedded web plates intended to resist shear at the notched end and to transfer the load from the notch to the full cross section of the beam, were selected. The shape and position of these web plates can be seen in Figs 3.2 and 3.3(a) and (d).

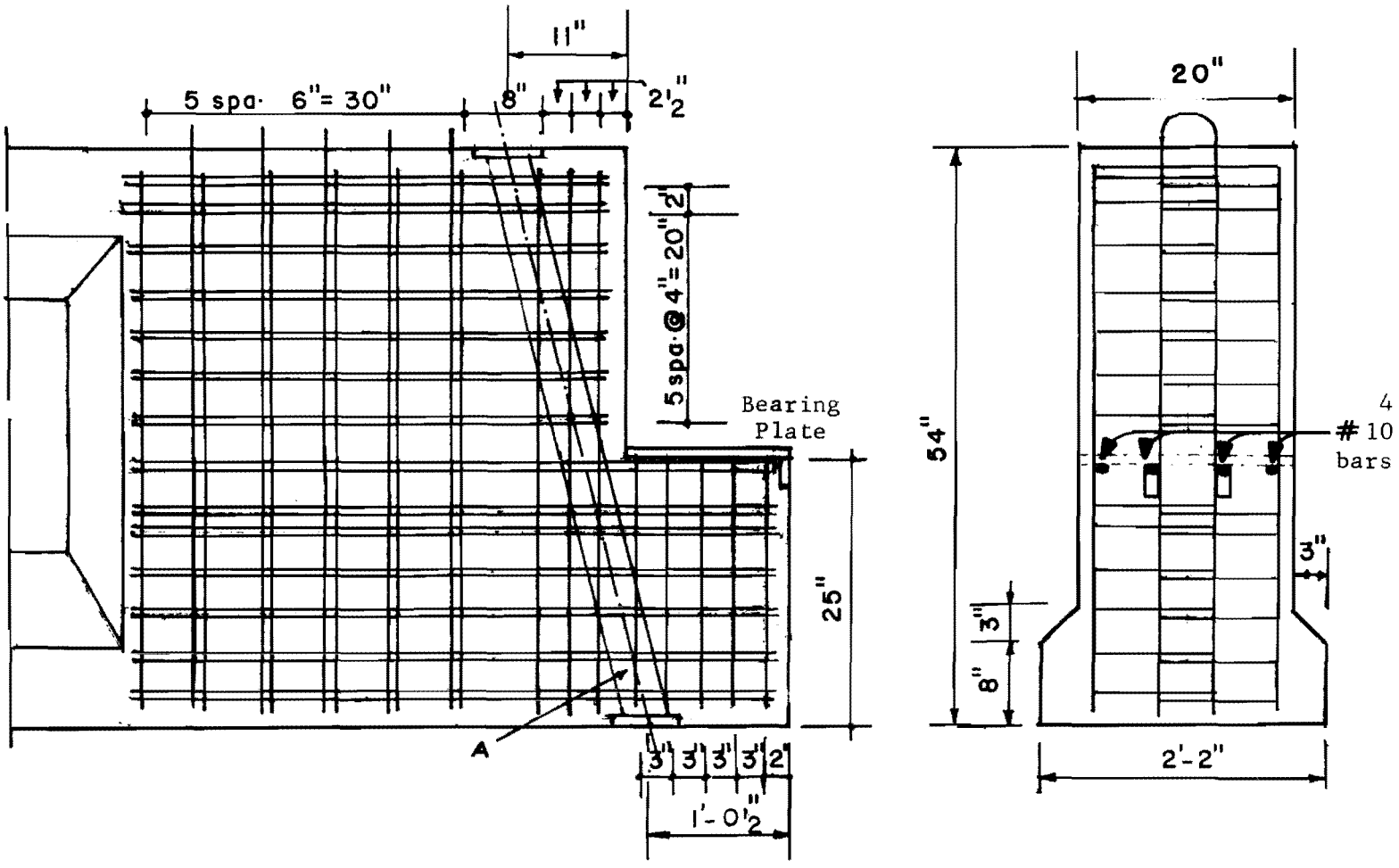

A - 4, 4-in. × 1/2-in. flat bars

All stirrups are #4 bars

Fig 3.1. End block reinforcement - as currently in practice.

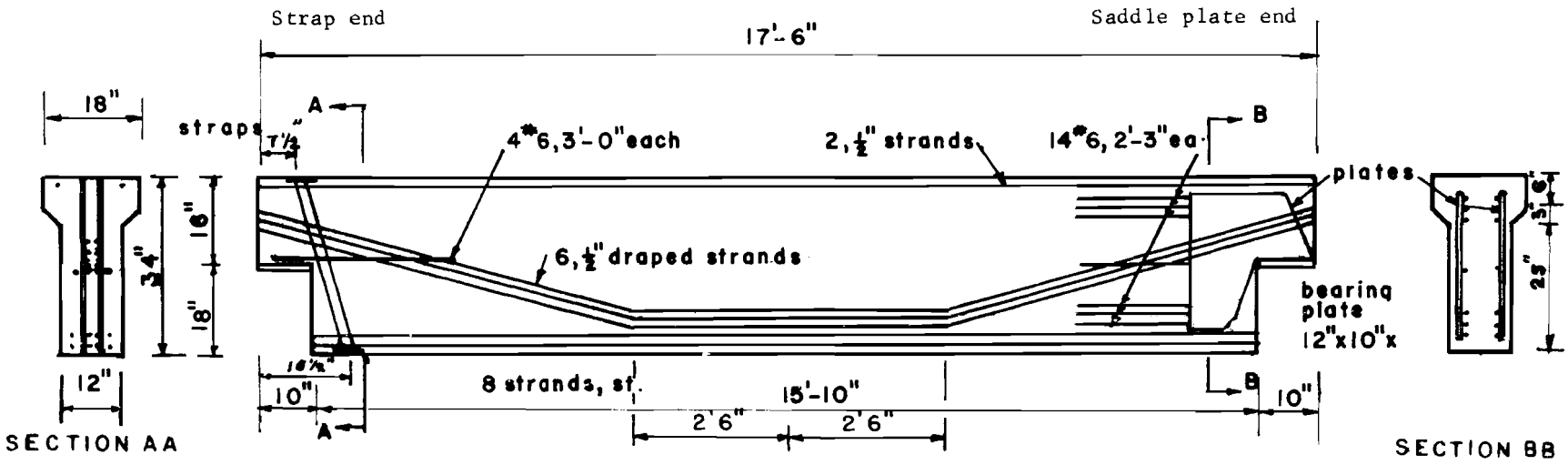

Details showing strands, straps and plates

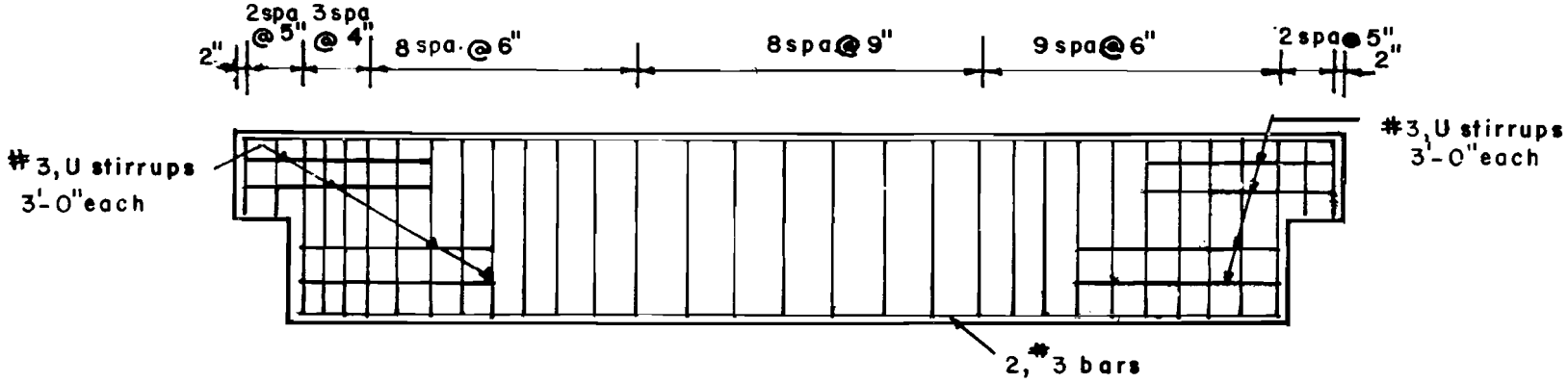

Details showing stirrups

Fig 3.2. Details of specimen.

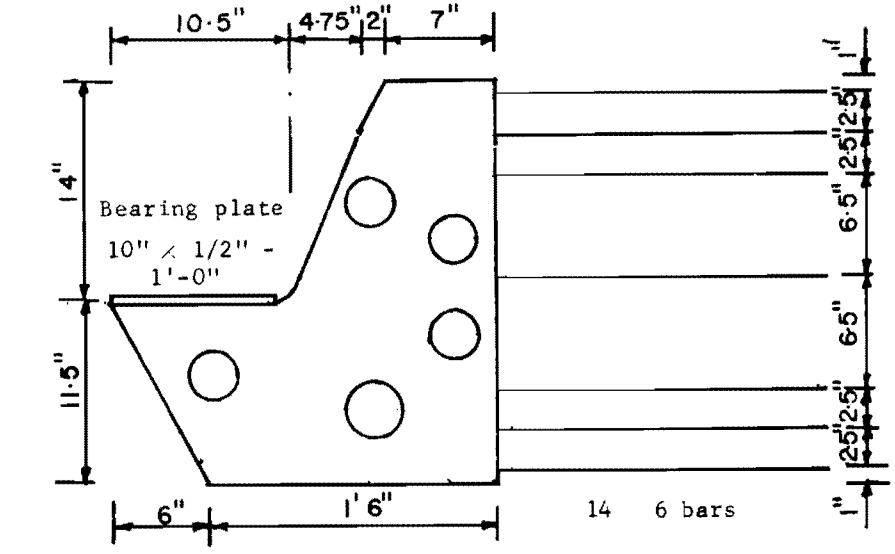

Elevation

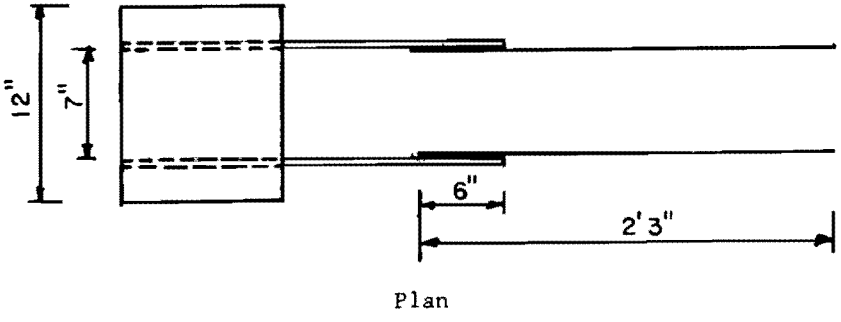

Plan

Fig 3.3(a). Saddle plate.

Fig 3.3(b). Strap.

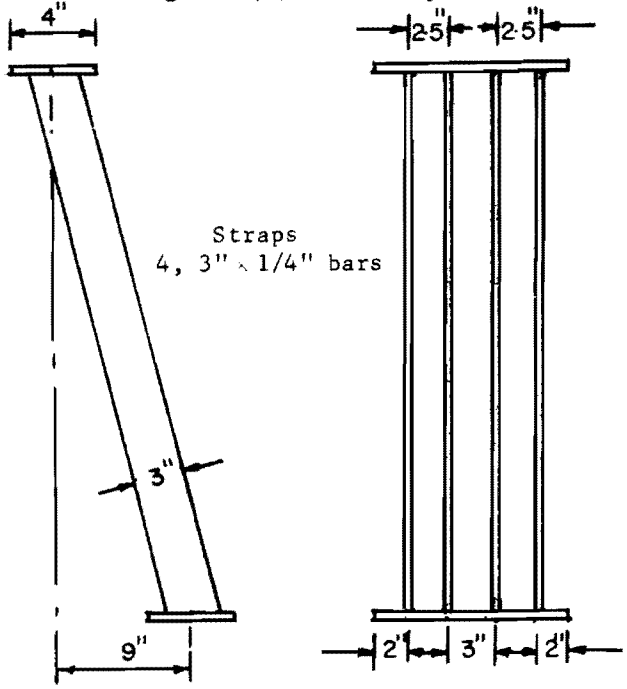

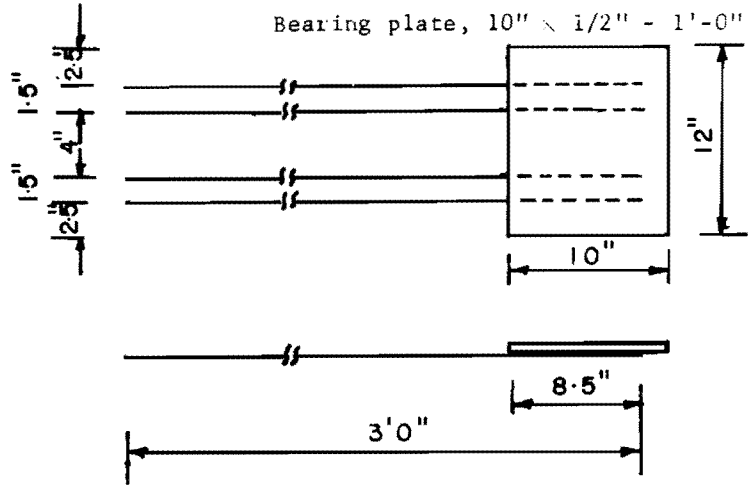

Fig 3.3(c). Bearing plate with reinforcements welded.

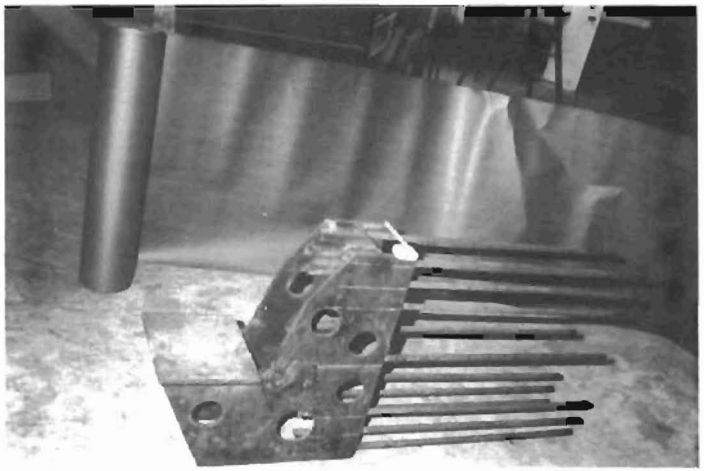

Saddle plate.

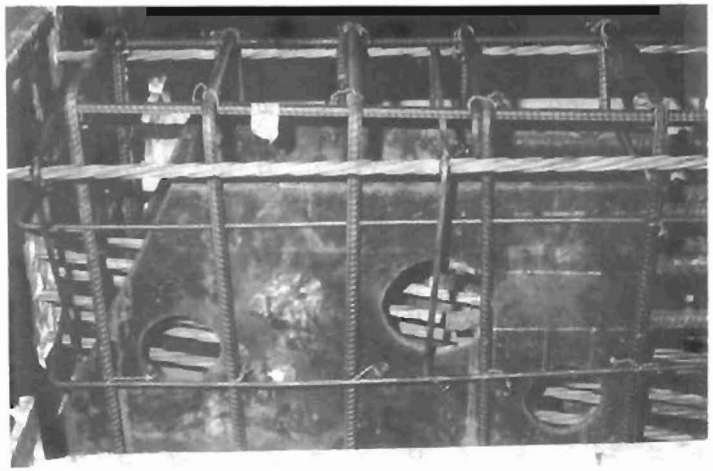

Saddle plate in position.

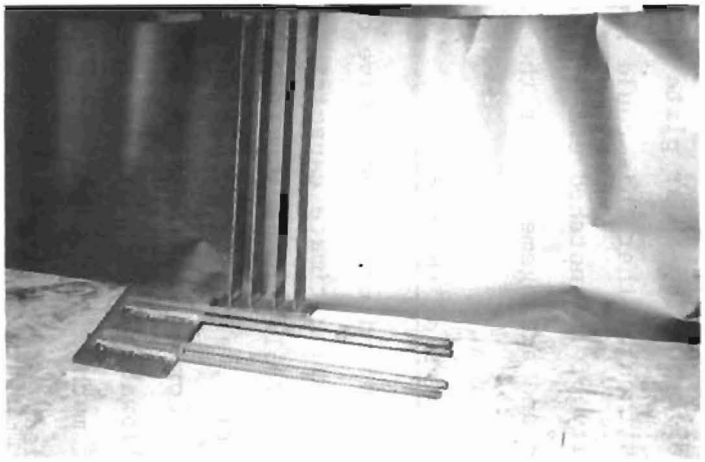

Strap and bearing plate with bars welded.

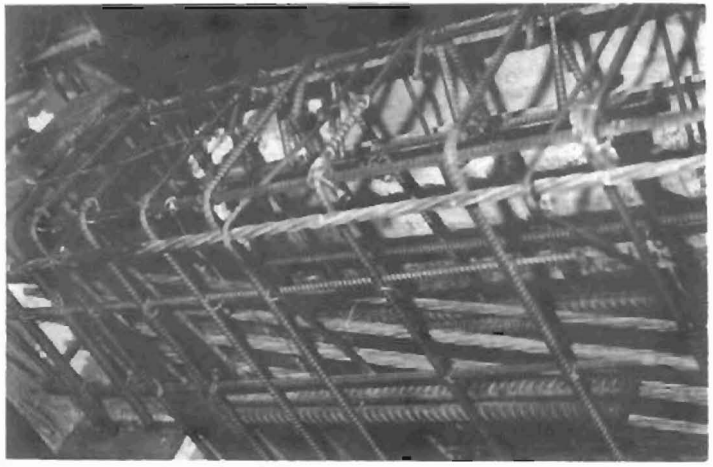

Strap in position.

Fig 3.3(d)

3.2 Scale of the Model

A scale of 0.5 was adopted for modeling the specimen. This unusually large scale for a model was chosen in order to have a better understanding of the behavior of the beam under field conditions than could be possible with a smaller model. Figure 3.2 shows detailed dimensions of the model. Figures 3.3(a) to (d) show the different component parts used at the notched ends. A comparison of dimensions between prototype and model is given in Table 3.1. It can be seen that the quantity of horizontal stirrups is reduced considerably and has a ratio of only 0.085. The area ratio for the specimen has been maintained at an average of 0.4.

Calculations for the moment capacity and stresses at different stages of loading for the 54-in.-deep beam are contained in Appendix B. The shear strength of the notched end of the 54-in. beam was estimated as 500 k, based on the ACI Code method of calculating shear capacity v_c of prestressed concrete beams. Details of calculations are given in Appendix C. According to the scale adopted the shear capacity of the model should be approximately $0.4 \times 500 = 200$ k . The capacity was estimated using the ACI Code equations, which gave a value of 185 k for the strap end and 189 k for the shear plate end. Calculations are given in Appendix E. It was thought that this could represent an upper-bound value of the shear capacity of the notched end of the model and was taken as a guide for the design and arrangements for the loading frame for the test.

3.3 Design of the Model

Appendices B and D give detailed calculations for the service load stresses and ultimate capacities for the prototype and the model respectively. Table 3.2 gives a comparison of the loading conditions, flexural capacities, and stresses at different stages of the prototype and the model. For the model, tensile stress in concrete at transfer is more than the allowable stress of $3\sqrt{f'_{ci}}$ stipulated by the ACI Code but considered not of much significance since the tensile capacity of the concrete is not exceeded. Moreover, this stage of stress conditions remains for a very short period of time.

Calculations for arriving at a load-deflection relationship for the model are contained in Appendix D. Following the methods suggested by

TABLE 3.1

Situation	Dimensions and Areas		Ratio
	Prototype	Model	
Span (support to free end, c/c distance)	14 ft 0 in.	8 ft 9 in.	.625
Depth	54 in.	34 in.	.63
Depth at notched end	24-1/4 in.	16 in.	.66
Top width	20 in.	12 in.	.60
Bottom width	26 in.	18 in.	.69
Area of end block	1137 $in.^2$	445.5 $in.^2$	.392
Area of strands (1/2 in., 270 ksi)	6.273 $in.^2$ (41 strands)	2.45 $in.^2$ (16 strands)	.390
Inclined straps A36	8 $in.^2$	3 $in.^2$	.375
Horizontal bars welded to base plate Grade 60	5.08 $in.^2$	1.76 $in.^2$	.345
Vertical stirrups at notched end Grade 60	.8 $in.^2/ft$	.33 $in.^2/ft$	.41
Horizontal stirrups Grade 60	26#4 U-type	4#3 U-type	.085

TABLE 3.2. COMPARATIVE STATEMENT OF STRESSES IN PROTOTYPE AND MODEL

Beam	Initial Prestressing Force, k	Service Load At Notched End, k	Concrete Stresses, ksi				Ultimate Capacity in Bending, in-k	Ultimate Capacity in Shear (Estimated), k
			At Transfer		At Service Load			
			Top Fiber	Bottom Fiber	Top Fiber	Bottom Fiber		
Prototype	1185	178	-.33	3.34	2.6	-.612	47570	500
Model	400	71	-.403	2.23	2.113	-.86	14728	185

Burns (4) the Moment Curvature relationships at different sections of the beam were computed taking into account the variation in effective depth in relation to the draping of strands. Deflections are computed based on these moment curvature relationships with the cracking stress for concrete assumed as $7.5\sqrt{f'_c}$. These calculations for load-deflection relationship were made in order to compare them with the observed values during the test.

3.4 Prestressing

The specimen was fabricated at the Civil Engineering Structures Research Laboratory of The University of Texas at Austin. The specimen was cast in an inverted position with respect to its anticipated position in service in order to keep the widest portion (the bottom flange) in the top of the form. Only one specimen was made and tested, but each end employed different notch reinforcement. The arrangements and set up for pretensioning are shown in Figs 3.4a and b. Two horizontal beams, each made up of two W 10×39 sections, were used to take the thrust of the 400K prestressing force. End frames were made up of (a) two vertical posts with two C 9×15 3-1/2 in. apart with 1/2-in. stiffeners welded in between and (b) two horizontal beams of I-sections with 1-in. plates welded to them. These members were designed for any combination of loading which could occur during stressing operations.

The ends of the two horizontal beams were not square, and a 1/2-in. gap for grouting was used between the frames and the beam ends. Hydrostone grout in the gap was added after alignment in the horizontal as well as the vertical direction was satisfactory. After hardening of hydrostone, all connecting bolts were tightened with a pneumatic wrench.

The reinforcement, web plates, strap bars, and bearing plates were placed in position resting on the bottom of the form. Strands were threaded through one end of the frame and held in position temporarily by chucks. Strands were tensioned by hydraulic jacks, one strand at a time. Draping was achieved by using cast iron hold-down devices with 1-in.-dia. A-490 high strength bolts anchored to the laboratory floor. Details can be seen in the photograph of Fig 3.5.

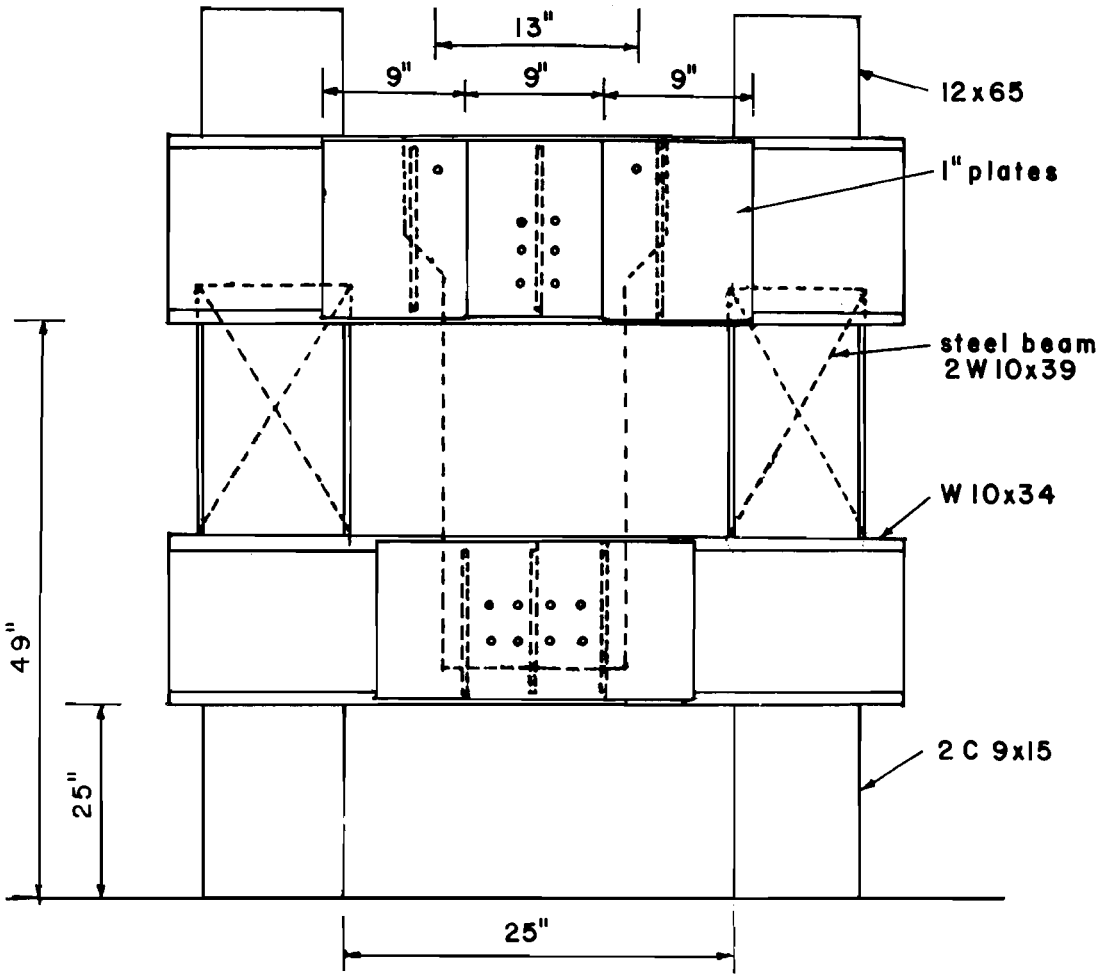

END VIEW OF PRESTRESSING FRAME

Fig 3.4(a). Prestressing end frame.

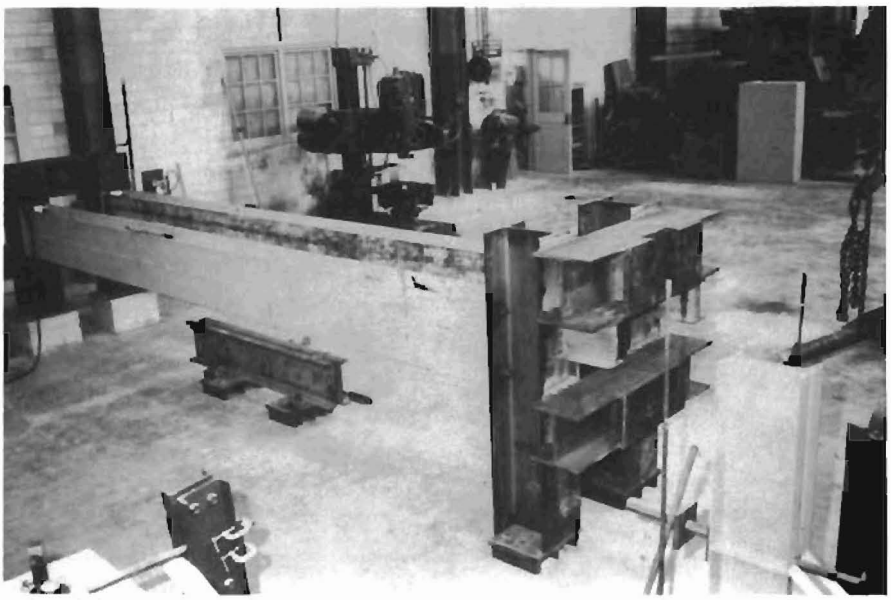

Fig 3.4(b). Prestressing frame.

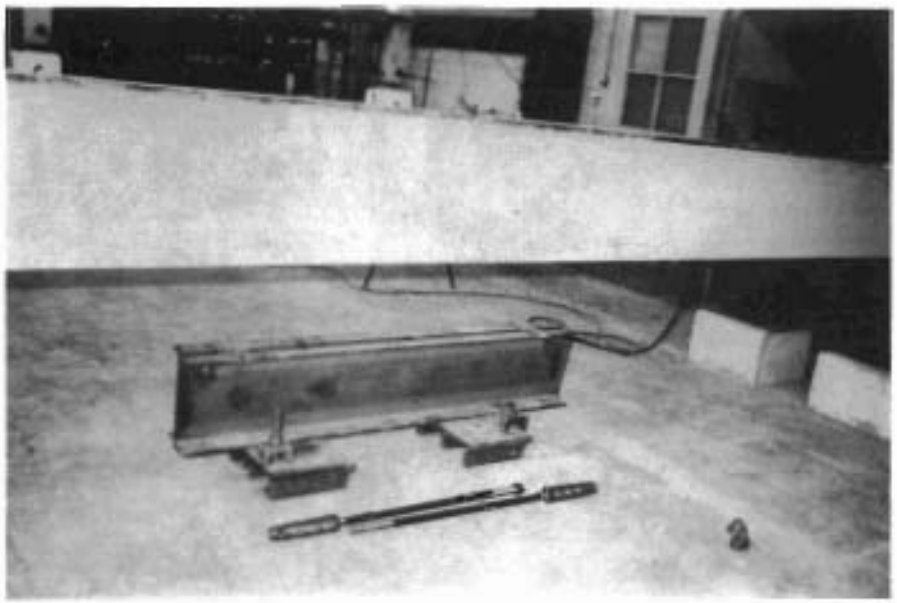

Fig 3.5. Draping device.

Since the grid used for strands was 2 in. and strands were to be pulled one at a time, a special "chair" was made so that it could be placed against any strand without interference with anchor chucks and free ends of strands already stressed. A plate within the chair prevented chucks from moving away from the bearing plate while the strands were stressed. Allowance was made for the extra load required for the slip of grips into the chuck on release of pressure in the hydraulic jack. The prestressing force applied was calculated such that the net force after release of strands should be equal to the prestress corresponding to field conditions - i.e., after all losses, including time-dependent losses, have occurred. Calculations for this are given in Appendix D. According to these calculations the load to be applied on one strand was 30 k to get the required stress of 163 ksi after stressing operations were complete.

Strands were stressed in a sequence that caused minimum eccentricity on the frames. After all the strands were stressed, loads in three strands were measured to find out whether any immediate losses have occurred, possibly, by creep in steel or by overall shortening of the frame, after all strands had been stressed. This was done by measuring the hydraulic pressure required to pull the strand to an extent just sufficient to cause separation of grips from the chuck holding the strand. The following are the values of the retensioning forces on the three strands checked.

(1) 22.6 k
(2) 23.5 k } Average 23 k Desired = 24.4 k
(3) 23.2 k

For the two straight strands at the top of the cross section, bond was destroyed for the 18-in. end region of the strand in order to eliminate the undesirable effects of prestressing force. Bond was prohibited by application of grease and paper wrapping.

3.5 Concrete

The mix for the concrete used is given below:

Cement	6-1/2 sacks
Coarse aggregate	1780 lb
Fine aggregate	1600 lb
Water	30 gal
Airsene	50 oz/sack

The above mix was designed to yield a strength of 6000 psi. slump obtained was 4 in. The beam was cured for 10 days by covering with polythene sheets. This concrete resulted in the following strengths at different ages of the specimen.

Days After Casting	Strength Recorded	Average	Remarks
7	(1) 5446 psi (2) 5305 psi (3) 4102 psi	4951 psi	
26	(1) 6330 psi (2) 5765 psi (3) 4456 psi	5517 psi	Release of strands
46	(1) 7215 psi (2) 5871 psi (3) 7427 psi (4) 6402 psi (5) 6119 psi (6) 6867 psi	6667 psi	Test of specimen

3.6 Release of Strands

Strand forces were released by burning each strand 26 days after concrete casting. The hold-down bolts for draped strands were released by loosening the nuts on the holding mechanism. The projecting portions of the hold-down bolts were burned off later.

CHAPTER 4. SPECIMEN LOAD TEST

4.1 General

The test set-up is shown in Fig 4.1. After stripping of forms and burning of protruding strands and hold-down bolts the specimen was transferred to the test area with an overhead crane. The supports consisted of two reinforced concrete blocks 20 in. by 18 in. by 20 in. high, with 2-in.-thick bearing plates. The specimen was centered and levelled on these supports such that the c/c distance of supports measured 16 ft 10 in. The hold-down points for draped strands were the same as the location of loading points. Loads were applied through 1-in.-thick plates with rollers. This arrangement allowed the rams to remain always vertical even when the specimen developed large deformations from loading. One 100-ton hydraulic ram was used at each loading point as shown in Fig 4.2(a).

Three dial gages capable of measuring deflections up to .001 in. were used, one at midspan and one each at the ends of the specimen 12 in. from the supports. Fourteen strain meters, 12 for measurement of shear compression strains of concrete at ends and two for tensile strains for the inclined straps, were fixed. The strain meters used were of 20-in. gage length, surface strain meters. A sketch of the strain meter is given in Fig 4.3. Calibration data for one of the strain meters are given in Table 4.1. Strain meters were pretensioned for measurement of compressive strains but were used without any pretensioning for tensile strains. Figure 4.2 shows position of strain gages on the specimen.

4.2 First Stage

Load was applied in small increments initially until there was a force of 10K on each ram. Thereafter, load increments of 10K were used. Strains and deflections were monitored for every increment. The first shear crack appeared at the saddle plate end when the load on each ram

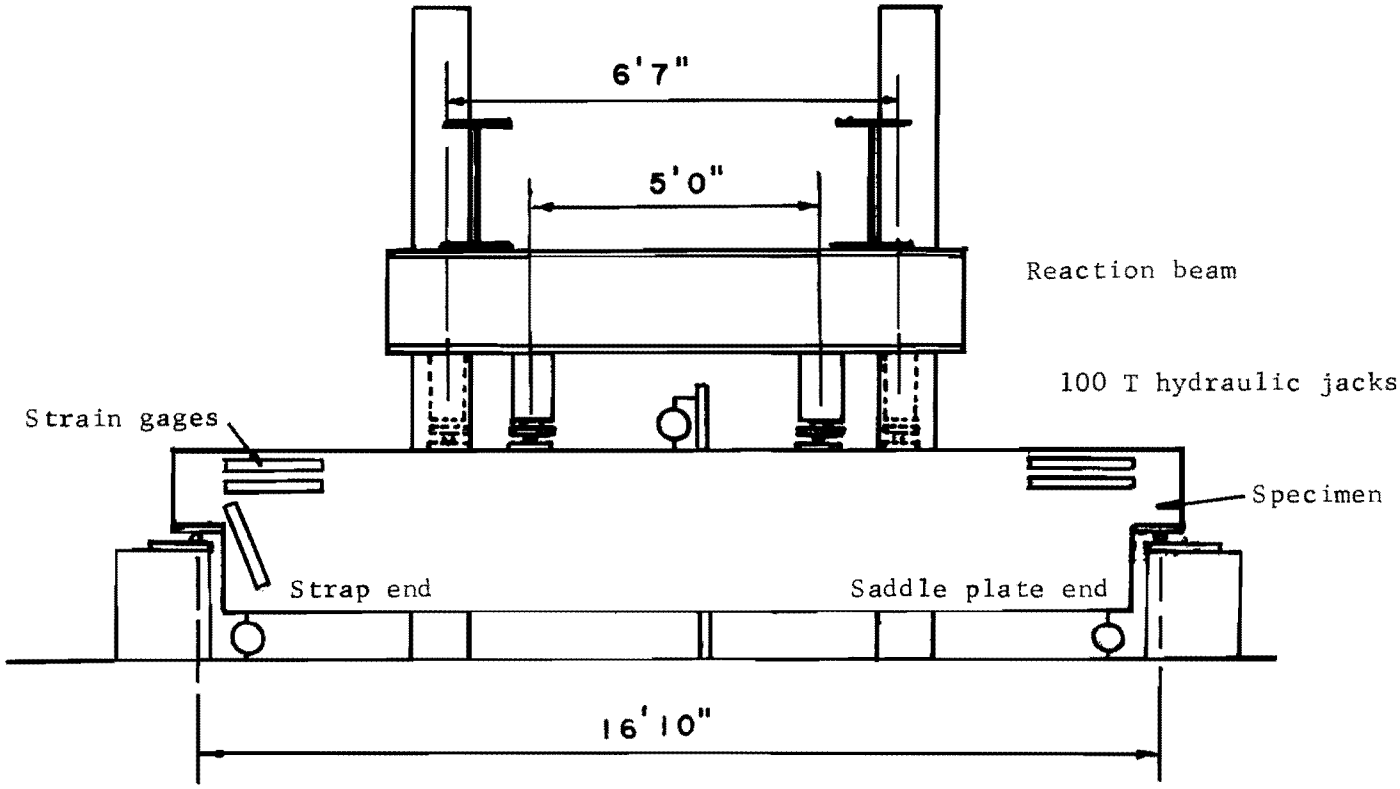

Fig 4.1. Test set-up.

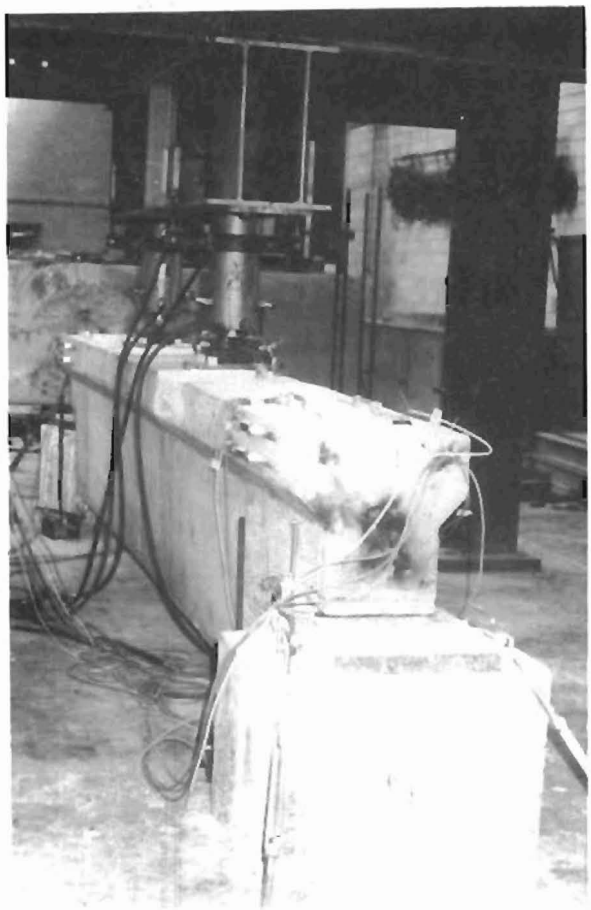

Fig 4.2(a). Test set-up for Stage 1.

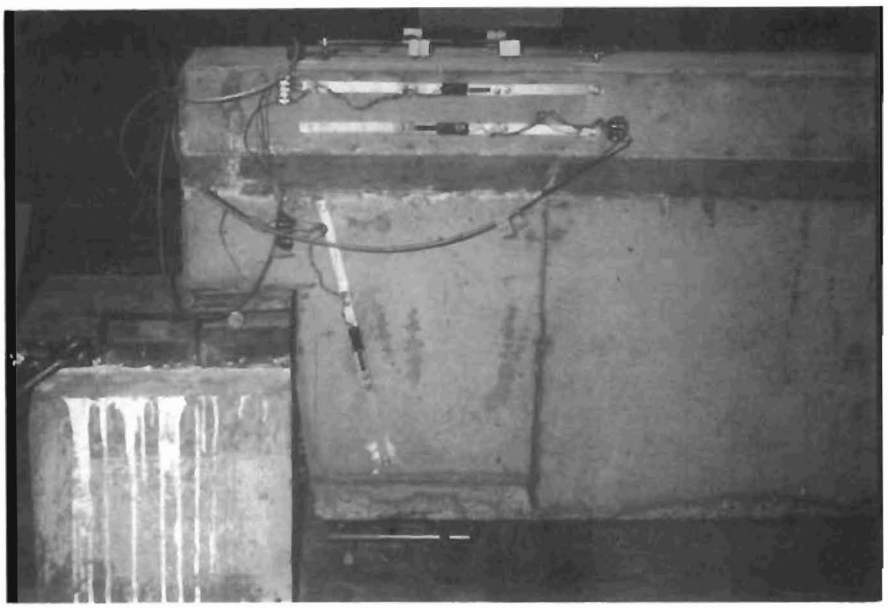

Fig 4.2(b). Strap end - arrangement of strain gages.

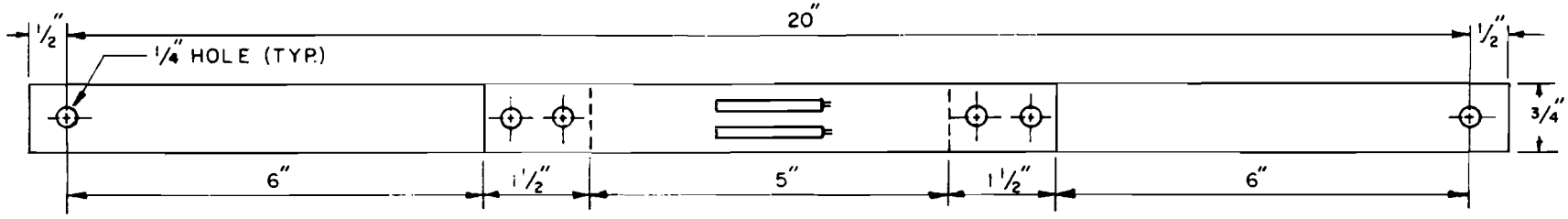

TOP VIEW

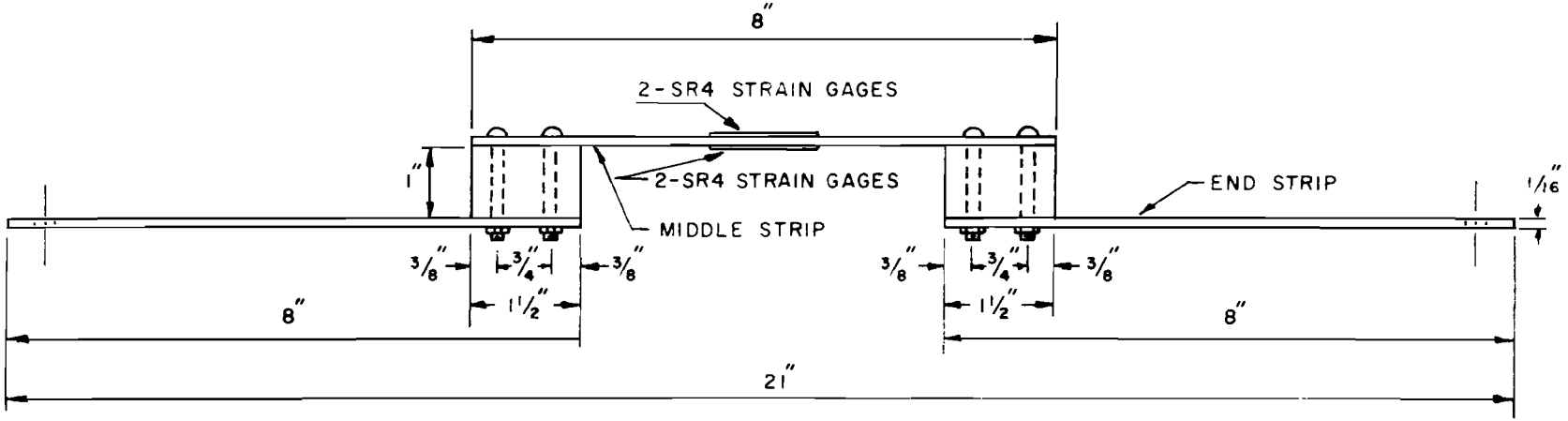

SIDE VIEW

Fig 4.3. Strain meter.

TABLE 4.1. CALIBRATION DATA FOR STRAIN METER

Gage Factor Setting 2.00 — Strain Meter No. SM3

Gage Length 20.20 inches — Tension Test No. 1

Dial Gage Reading	Displacement in. $\times 10^{-3}$	Unit Strain $\times 10^{-4}$ in./in.	Indicator Reading	Indicator Reading (Reverse)	Average Increment	Increment Sum	Remark
0	0	0	0	+ 2	0	0	
90	10	5	222	238	229	229	
80	20	10	453	470	232	461	
70	30	15	689	710	238	699	
60	40	20	930	946	238	927	
50	50	25	1171	1190	242	1169	
40	60	30	1420	1430	245	1414	
30	70	35	1669	1681	250	1664	
20	80	40	1910	1923	247	1911	
10	90	45	2160	2170	248	2159	
0	100	50	2410	2410	245	2404	

S.M. Factor = (Sum of Average Increment) / Sum of Unit Strain

= 13037 / 275 = 47.4×10^{-4} in./in.

was 80K. Subsequently a crack of minor nature appeared at the strap end at 100K loading. The first flexural crack was observed at 120K on each ram. As the load was increased, more cracks developed at midspan, spreading in areas beyond load points with inclinations characteristic of flexural cracks in any beam loaded in this manner. No new cracks developed at the saddle plate end between the stages of 110K and 160K loading. After the 160K stage of loading, additional cracks started appearing. Cracks at the strap end did not appear to be so significant as did those at the plate end.

At the 170K load a crack developed from the bottom of the specimen and reached within 8 inches of the top of the specimen. The location of this crack was at the plate end, about 6 ft from the reaction. The specimen appeared very stable, and there was no suggestion of failure. The testing was temporarily stopped at the next load stage, i.e., 180K on each ram, because 90 percent of the capacity of the rams had been reached, and it was felt that the loading frame and floor anchor bolts had to be strengthened before application of additional load.

Results of this first stage are discussed in Chapter 5. The crack widths at the ends and deflections at midspan were measured on release of loads and again after two days and were recorded.

4.3 Second Stage

The testing frame was reinforced by attaching cross channels at the end of the reaction girder and anchoring them to the floor. This attachment could share one-fifth of the total load. Control of load sharing by the two systems could be modified by loosening or tightening the nuts provided for the bolts connecting the channels to the floor. Two rams of 100-ton capacity each were used on either side of the midspan for the second stage loading. The additional rams were positioned 9-1/2 in. away from the first two rams on either side. These are indicated by dashed lines in Fig 4.1.

All measurements were recorded as before for each increment of loading. No new cracks appeared until 180K load had been restored. At this stage fresh cracks appeared at the notched ends as well as the flexural cracking zone. Figures 4.4 and 4.5 show portions of the cracked

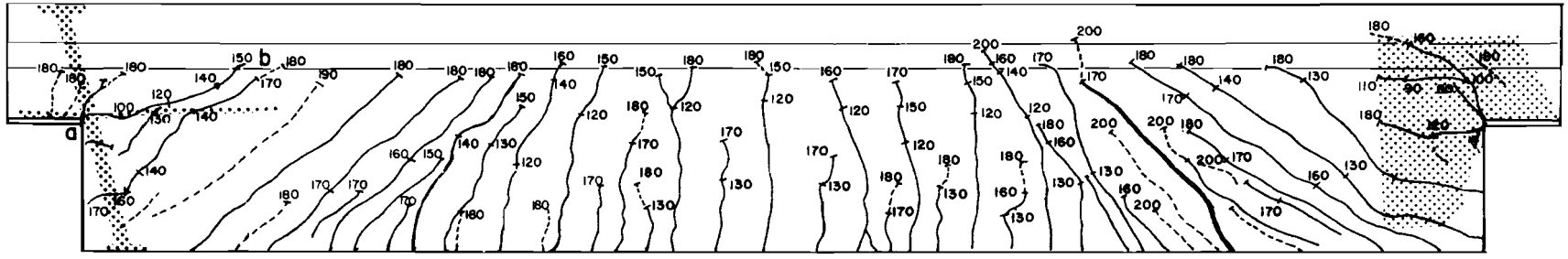

Fig 4.4. The cracked specimen.

(a). Cracks at strap end.

(b). Cracks at plate end.

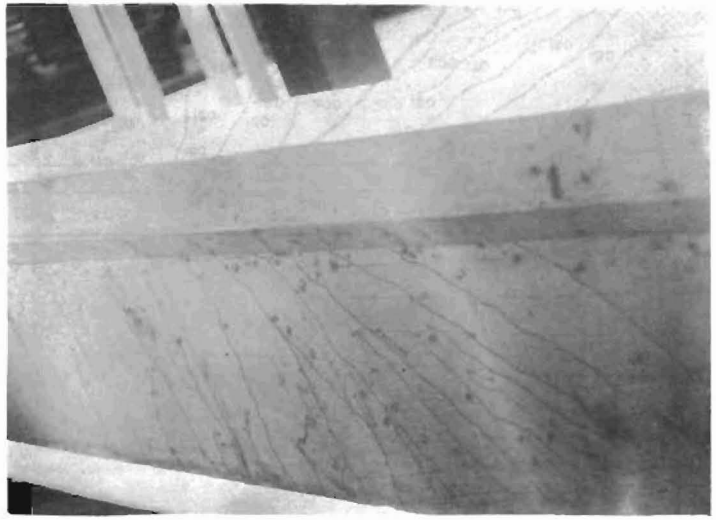

(c). Cracks in the middle.

Fig 4.5

specimen in detail. The dashed lines shown in Fig 4.4 are the cracks which appeared during the second stage of the test. When the load on each side was 200K the crack which had formed at 170K during the first stage started widening rapidly. The position of this crack was approximately 6 ft from the saddle plate end. A general shear failure occurred along this particular crack when the load on each side was 210K. At the same end another crack had lengthened as much as to encroach the flange portion of the specimen to an extent of about 2 in. when the load was only 180K, but it propagated no further.

CHAPTER 5. DISCUSSION OF TEST RESULTS

5.1 General

Deflection gage readings and crack width measurements are shown in Tables 5.1 and 5.2. A sketch of the specimen with cracks marked for various loading stages was shown in Fig 4.4. Cracks shown as solid lines or as dashed lines distinguish the first stage and second stage of the test, respectively. As mentioned in Chapter 4, at the saddle plate end a crack extended into the flange portion at 180K load, but it was not a part of the failure. Various cracks developed at both ends below the notch as loads increased from 130K to 180K. Most cracks closed up almost immediately after the specimen was unloaded before stage 2 loads were applied.

5.2 Deflections

Deflections at midspan are plotted against loading as shown in Fig 5.1. Maximum variation between the theoretical and measured relationship exists at the onset of cracking. The actual response was less stiff than the analysis suggested prior to the reloading stage. For loads above 190K in the reloading stage, the actual response was more stiff than that predicted, but the ultimate load predicted was about the same as that which was actually resisted. Measured data points are plotted and a line marks the loading sequence. The solid line represents an analytical prediction of deformation. Details of the analysis are given in Appendix D.

Deflections that were measured near ends are plotted against loads in Fig 5.2. In the first stage of the test, deflections are larger at the strap end than at the plate end initially, but the reverse was observed at later stages. In the second stage of the test the strap end deflections are consistently larger. Deflections at these points were relatively small, and, since they involve a combined effect of shear and bending deformations, no analytical data were derived for comparison. At the load level of observed flexural cracking, the rate of deformation increased in

TABLE 5.1. DEFLECTIONS, STAGE 1 - TEST DATA

	Load Stage	Load One Side kips i.e., one ram)	Δ Midspan (inch)			Δ Plate End (inch)		Δ Strap End		Crack Widths			
			Dial Gage Reading	Δ + Camber (.066")	Δ (net)	Dial Gage Reading	Δ	Dial Gage Reading	Δ	Plate End		Strap End	
										1	2	3	4
	1	0	1.730	0	-.066	.550	0	.180	0				
	2	2.1	1.728	.002	-.064	.550	0	.180	0				
	3	4.3	1.724	.006	-.060	.550	0	.180	0				
	4	9.3	1.716	.014	-.052	.550	0	.182	.002				
	5	19.7	1.700	.030	-.036	.553	.003	.187	.007				
	6	28.6	1.688	.042	-.024	.557	.007	.191	.011				
	7	38.4	1.674	.056	-.010	.562	.012	.195	.015				
	8	48.7	1.659	.071	.005	.566	.016	.201	.021				
	9	58.8	1.643	.087	.021	.571	.021	.208	.028				
	10	68.8	1.627	.103	.037	.576	.026	.211	.031				
	11	78.4	1.609	.121	.055	.581	.031	.216	.036				
	12	88.4	1.588	.142	.076	.587	.037	.222	.042	.003	.004		
	13	98.6	1.560	.170	.104	.592	.042	.230	.050	.006	.005	.002	.003
	14	107.8	1.518	.212	.146	.601	.051	.238	.058	.006	.005	.002	.004
	15	118.4	1.459	.271	.205	.614	.064	.249	.069	.01	.01	.002	.004
	16	128.6	1.382	.348	.282	.629	.079	.262	.082	.01	.01	.002	.005
	17	138.2	1.290	.440	.374	.659	.109	.282	.102	.012	.013	.003	.006
	18	148.1	1.197	.533	.467	.674	.124	.300	.120	.018	.014	.003	.008
	19	158.3	1.110	.620	.554	.692	.142	.315	.135	.018	.017	.004	.008
	20	167.8	0.994	.736	.670	.718	.168	.336	.156	.02	.018	.004	.009
	21	177.8	0.837	.893	.827	.747	.197	.367	.187	.025	.02	.005	.010
Dec 2	22	0	1.640	.090	.024	.586	.036	.210	.030				
Dec 3	23	0	1.655	.075	.009	.570	.020	.205	.025				
Dec 7	24	0	1.660	.070	.004	.570	.020	.203	.023	.006	.005	.003	.001

TABLE 5.2. DEFLECTIONS, STAGE 2 - TEST DATA

Load Stage	Load on One Side kips (i.e., two rams)	Δ Midspan inches			Δ Plate End (inch)		Δ Strap End (inch)		Crack Widths			
		Dial Gage Reading	Δ + Camber	Δ , in. Net Deflection	Dial Gage Reading	Δ	Dial Gage Reading	Δ	Plate End		Strap End	
									1	2	3	4
1	0	1.630	0	.004	.780	0	.200	0	.007	.005	.002	.001
2	5.0	1.621	.009	.013	.783	.003	.205	.005	.007	.005	.002	.001
3	10.0	1.618	.012	.016	.784	.004	.207	.007	.007	.005	.002	.001
4	40.0	1.570	.06	.064	.799	.019	.224	.024				
5	60.0	1.532	.098	.102	.810	.03	.236	.036				
6	80.0	1.479	.151	.155	.823	.043	.250	.050	.015	.014		
7	100.0	1.390	.24	.244	.842	.062	.268	.068				
8	120.0	1.272	.358	.362	.865	.085	.292	.092	.019		.003	
9	140.0	1.145	.485	.489	.890	.11	.316	.116	.021		.003	
10	160.0	1.016	.614	.618	.914	.134	.339	.139	.021			
11	180.0	0.885	.745	.749	.936	.156	.378	.178	.026		.004	
12	190.0	0.808	.822	.826	.952	.172	.378	.178	.026		.005	
13	200.0	0.704	.926	.930	.975	.195	.397	.197	.027		.006	
14	210.0	0.637	.993	.997	.991	.211	.401	.201	.029		.007	
	0								.008		.002	

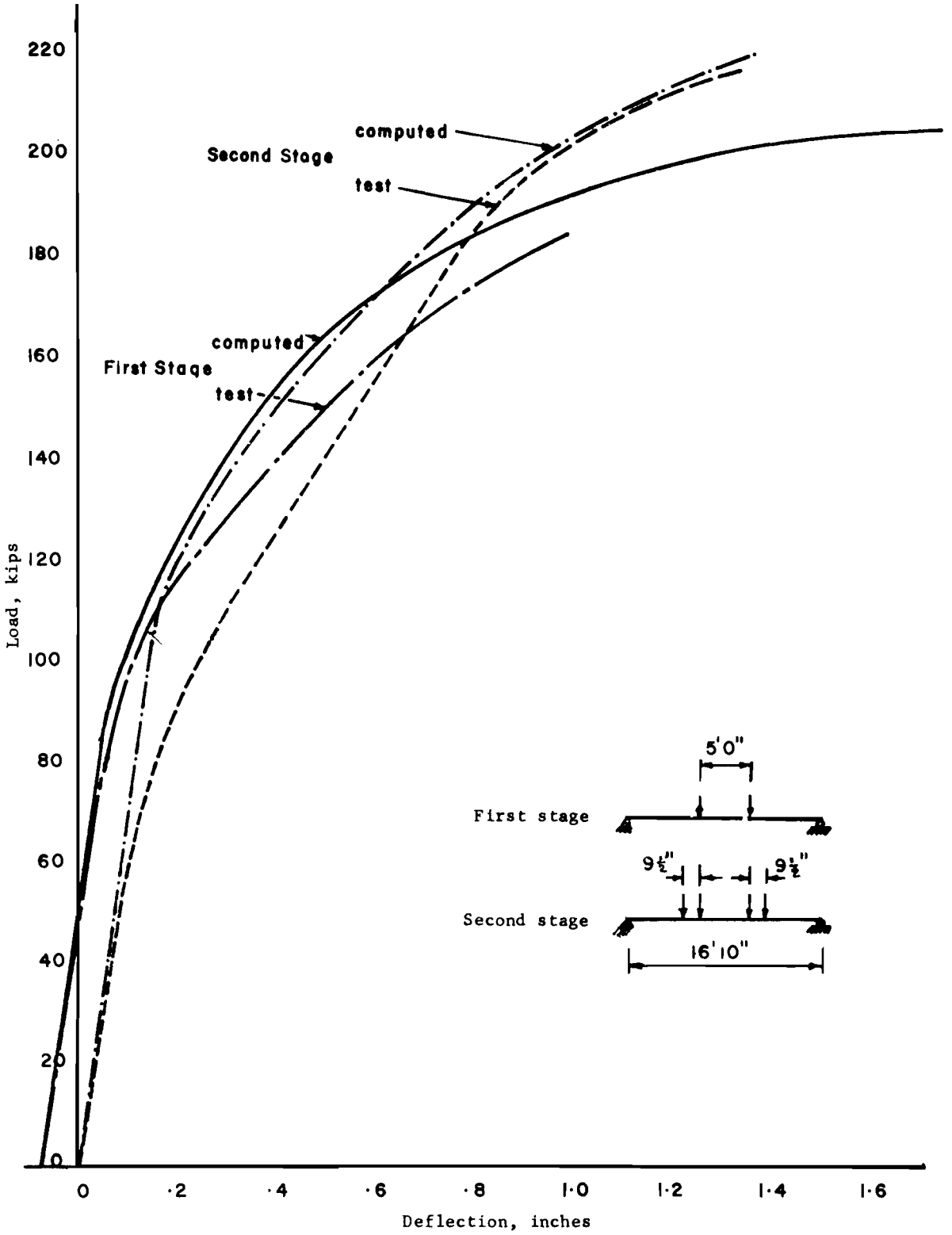

Fig 5.1. Deflection at midspan versus load.

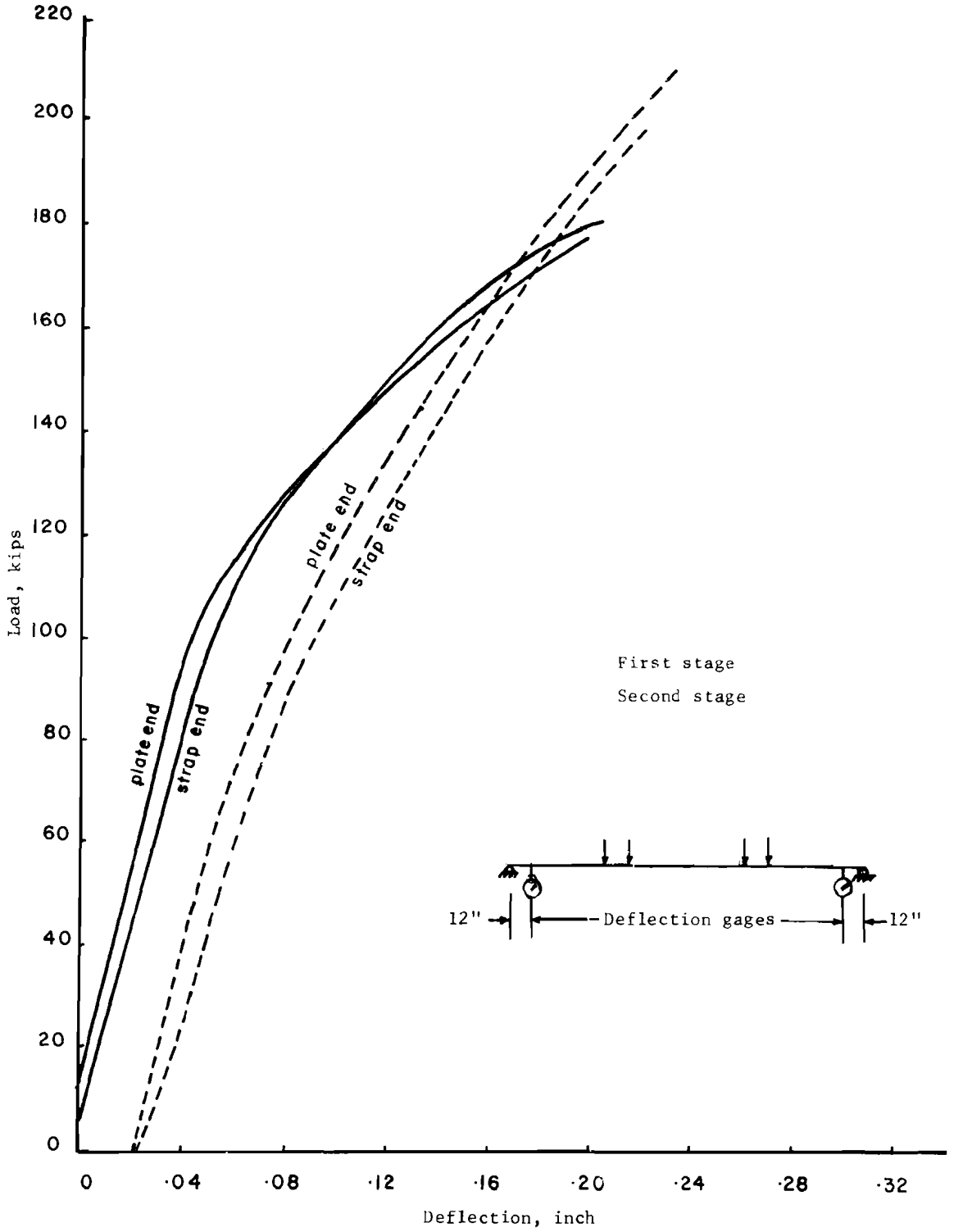

Fig 5.2. Deflection near ends versus load.

end regions, suggesting that cracking in end regions permitted larger deflections than uncracked end regions.

5.3 Crack Widths

A graph showing crack widths at the notched ends versus load is given in Fig 5.3. Crack widths appear to increase almost linearly with load. The crack at the plate end increased in width more than twice as much as the crack at the strap end under the same increase in load. The rebar and strap arrangement appears to be more effective in controlling cracks than are the web plates.

5.4 Strains

5.4.1 Steel strains

The relationship between the strains sustained by the straps are shown as a function of load in Fig 5.4. In the first stage of the test the function is distinctly different in two parts. The initial steep portion indicates the small degree of contribution of steel to the shear resistance. During this stage the concrete is uncracked and is effective in resisting shear. The first crack in this region was observed at a 110K load and the load-strain curve retained its steepness up to this load. After cracking, the straps had to resist most of the shear load, and the graph displays a slope about one-sixth of the uncracked region. At about 175K load the stress in the strap would have reached 38 ksi, corresponding to a measured strain of 0.132 percent. On release of load a residual strain of .044 percent was observed for the strap, suggesting that the strap had yielded before load was removed.

In the second stage of the test, the strap with an initial strain of .044 percent revealed a linear load-strain function. It remained linear to loads above 175K, suggesting that strain hardening may have occurred. Since concrete was already cracked before the second load stage, the strap probably had no range of load in which concrete shared force during the reloading stage.

The second stage of the test started with initially cracked shear zones. The cracks which formed at the final loads of the first stage of

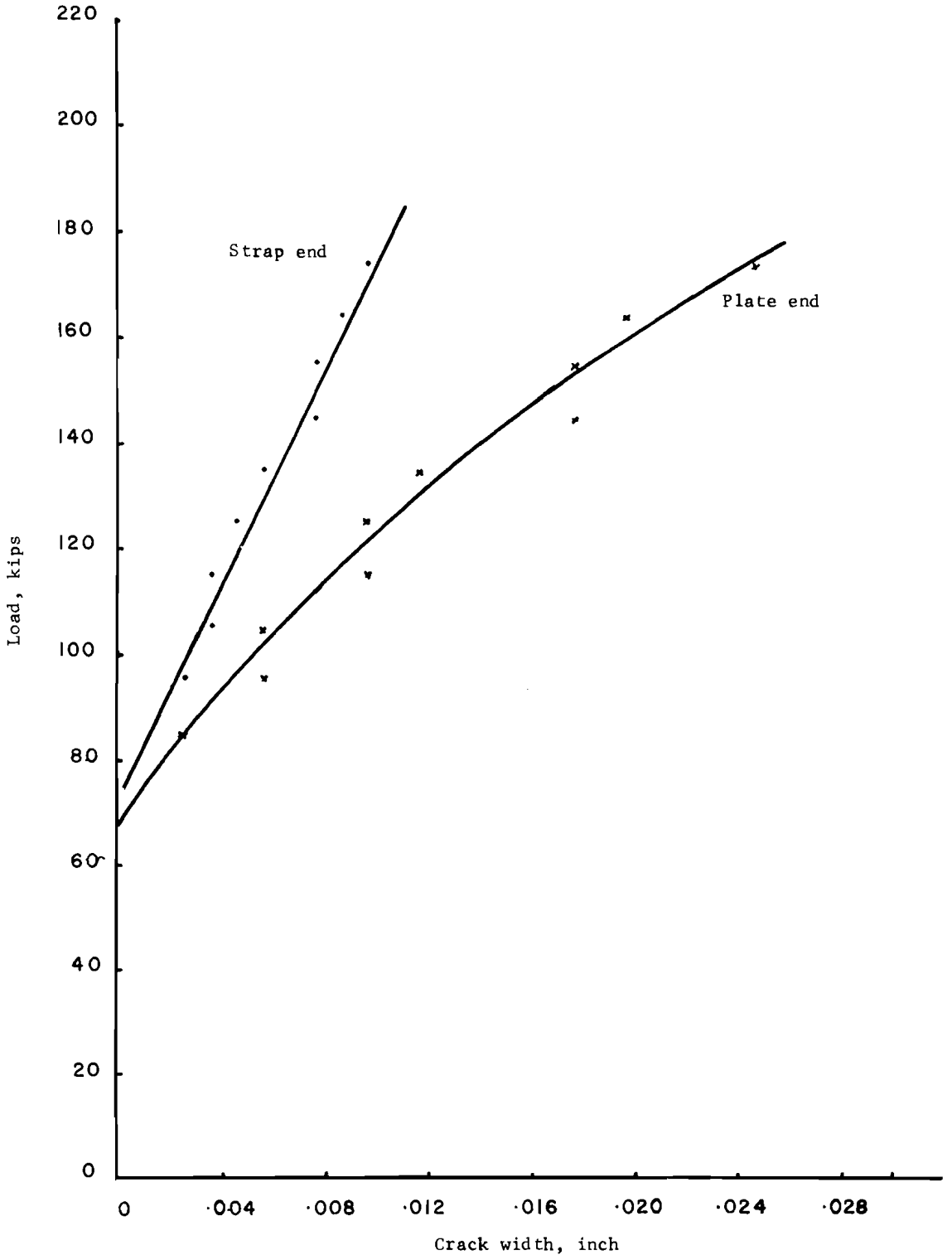

Fig 5.3. Maximum crack widths at notched ends versus load.

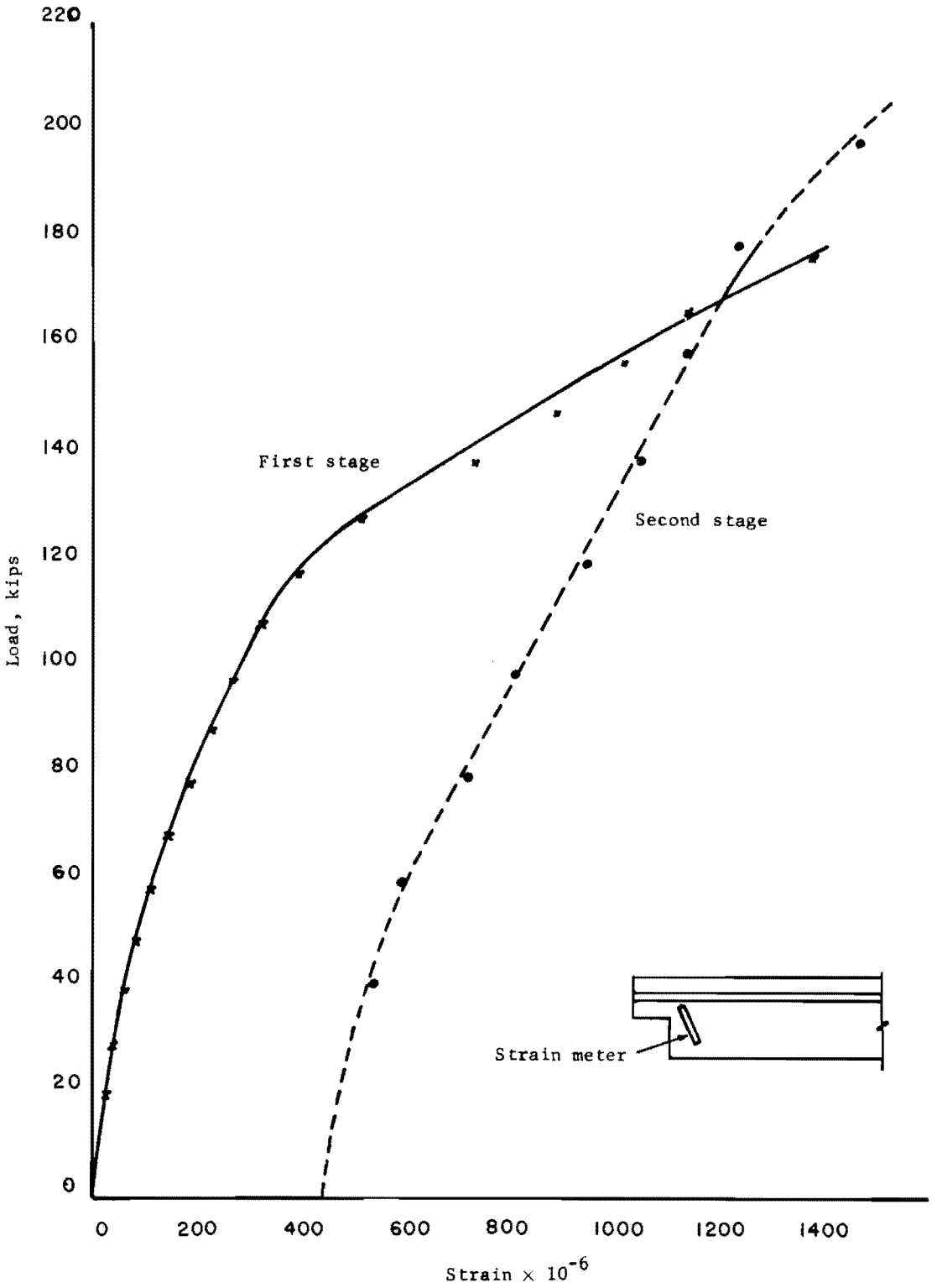

Fig 5.4. Strain at straps versus load.

the test existed across the draped strands. The strands, whose contribution to shear resistance was not significant in the first stage of the test, had to resist in the second stage forces trying to enlarge the crack. The horizontal stirrups also probably started to resist forces at cracks immediately upon reloading. Rebar reinforcement may have shared enough force at the straps to inhibit them from straining, making it appear that the straps were stiffer in the second stage.

5.4.2 Concrete strains

Compression strains in concrete in the shear compression zone were measured and are plotted against load in Fig 5.5. The maximum strains reached were 0.0004 at the saddle plate end and 0.00024 at the strap end. At each end the compression strains increased linearly with load. The lower strain in concrete at the strap end implies that the bar reinforcement helped resist flexural compression near the notch more effectively than did the saddle plates at the opposite end.

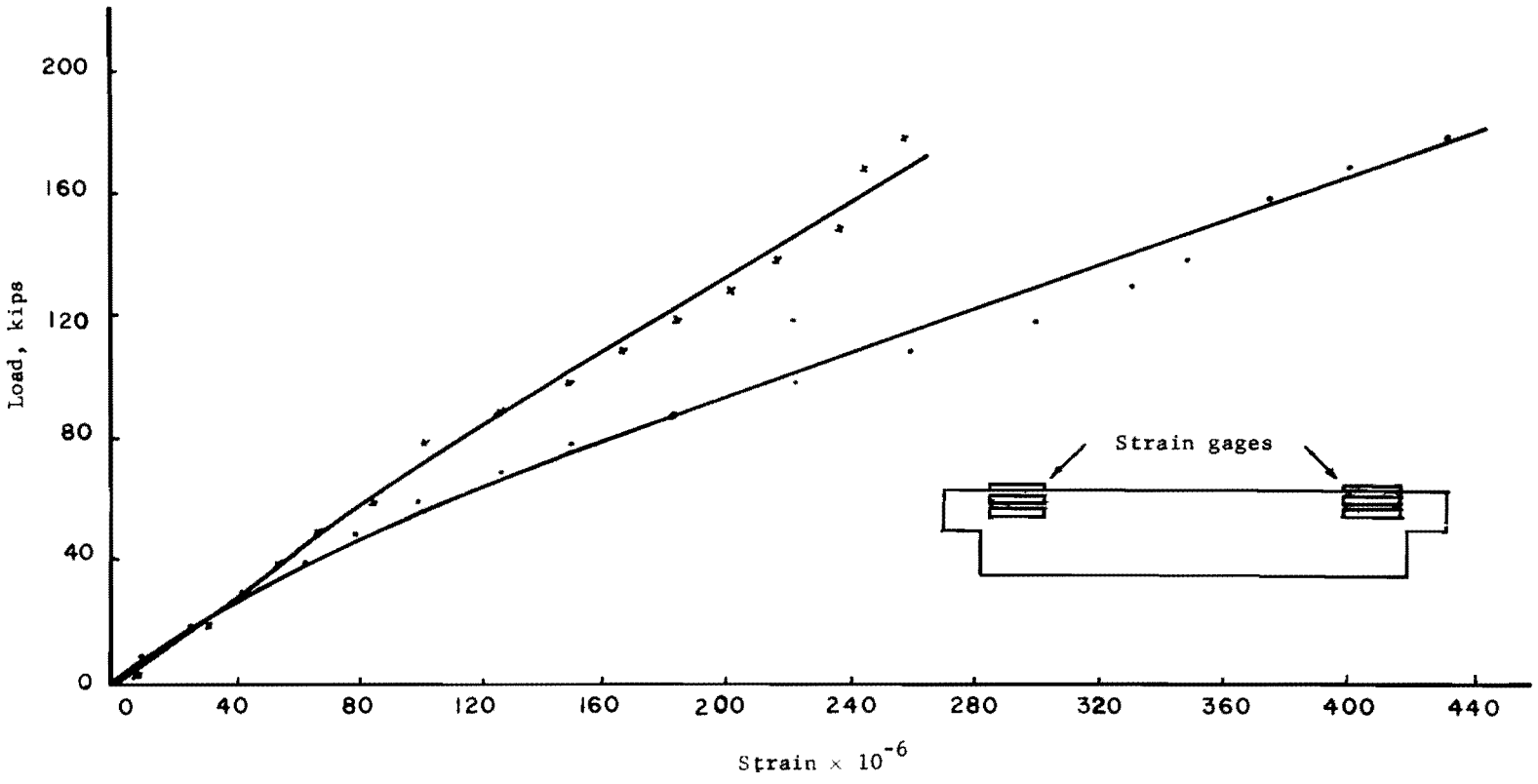

Fig 5.5. Concrete strain at notched ends versus load.

CHAPTER 6. SHEAR STRENGTH OF NOTCHED END

6.1 Shear Friction

6.1.1 The concept

The theory of shear friction is based on the concept that shear is resisted by sliding resistance between the interfaces of concrete along a potential surface for a shear failure. This hypothesis was originally suggested by Phillip W. Birkeland and Halvard W. Birkeland as a tool for the design of connections between two heavily loaded structural members where a sliding shear interface can exist (3). As indicated in Figs 6.1a, 6.1b, and 6.1c, a failure by sliding is considered to be resisted by a frictional force which can be taken as the product of the normal force N and a coefficient of sliding friction μ. Reinforcement that crosses the shear face provides the normal force N. The values of μ suggested by Birkeland were 1.7 for monolithic concrete, 1.4 for artificially roughened construction joints, .8 to 1.0 for smooth concrete construction joints and concrete to steel interfaces. On the basis of further investigations, ACI 318-71 stipulates the following values for μ.

Concrete cast monolithically	1.4
Concrete placed against hardened concrete	1.0
Concrete placed against as-rolled structural steel	0.7

The Building Code also restricts the yield strength of reinforcement to a maximum of 60 ksi in the determination of the steel capacity to maintain the normal force N.

6.1.2 Application to the notched end

In the notched end that contained hanger straps, there are principally three reinforcement systems penetrating the shear plane as shown in Fig 6.1d. These are (1) the hanger straps inclined at an angle of 15^{o} from the vertical, (2) horizontal #6 bars welded to the bearing

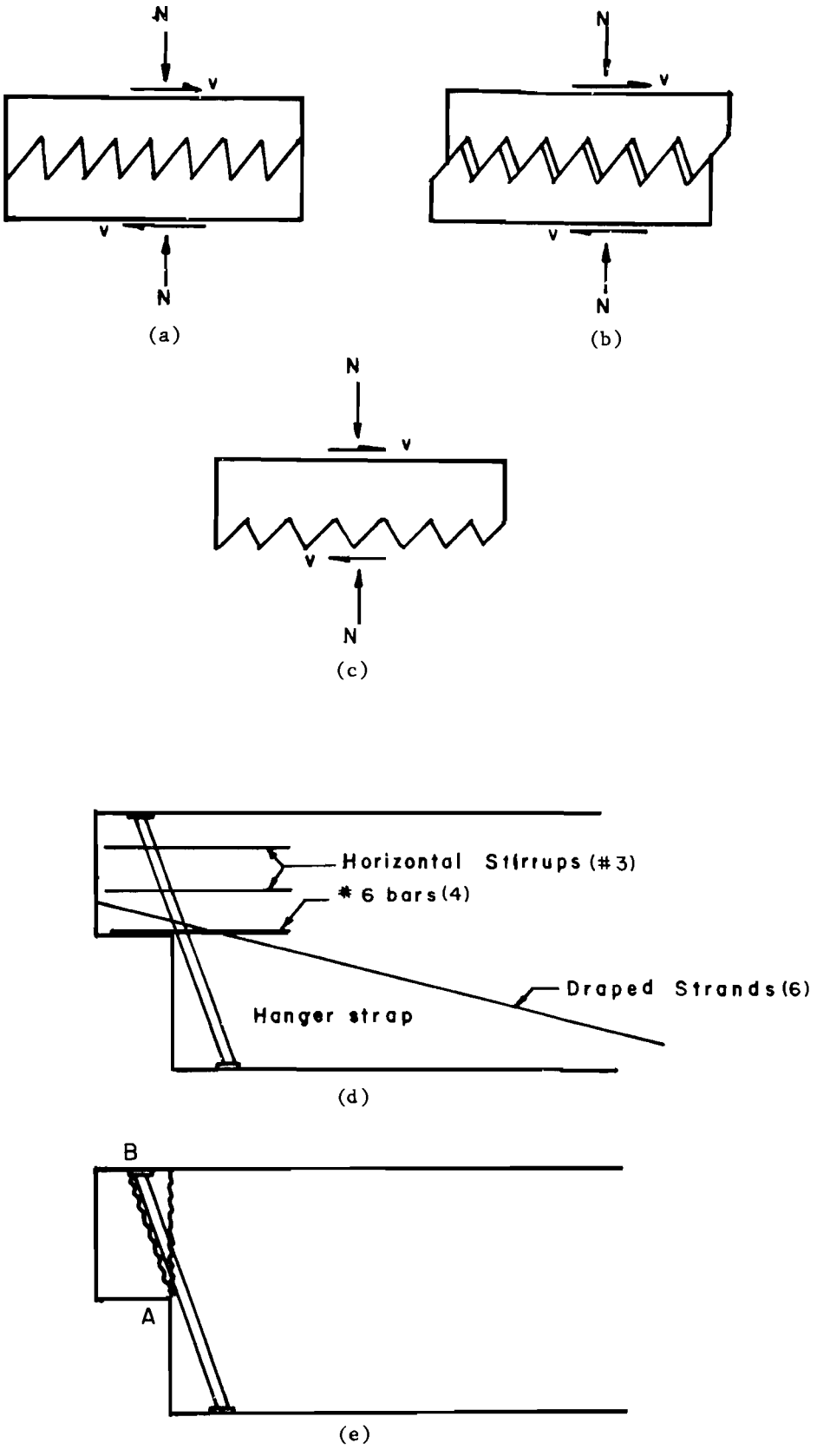

Fig 6.1. Shear friction analysis.

plate and #3 horizontal stirrups, and (3) the draped prestressing strands. A vertical shear plane with a crack starting at the notch (Fig 6.1e) is unlikely to form a crack since all major systems of reinforcement cross it. In contrast the plane AB parallel to the straps is penetrated only by the #6 bearing plate bars and the strands. It is the most likely plane at which a crack could be assumed for a shear friction analysis. The value of μ would be 0.7 at the edge of straps, but it could be 1.4 everywhere else. The edge of straps occupies 1/12th of the width. A weighted average value for μ can be taken as $\frac{1}{12} \times .7 + \frac{11}{12} \times 1.4 = 1.34$ or 1.3 to be conservative.

Modification for the value of the friction coefficient μ has been suggested in the PCI Design Handbook, Eq 6.5, reproduced below:

$$\mu' = \mu \left(\frac{300\mu}{v_u} + 0.5\right) \qquad \text{where}$$

μ' = modified value of the friction coefficient.

$v_u = V_u / \phi A_{cr}$

A_{cr} = area of the shear plane

The above modification is possible only if v_u is known. In the case under discussion, assuming $V_u = 200K$,

$$v_u = \frac{200 \times 1000}{237} = 844 \text{ psi}$$

$$\mu' = 1.34 \left(\frac{300 \times 1.34}{844} + .5\right)$$

$$= 1.3$$

The beam ordinarily will be subjected to a longitudinal force in addition to the vertical reaction R . This longitudinal force is created by shrinkage and creep of the superstructure of the bridge, drag due to vehicle movement, and the resistance of frictional force at the bearings. A minimum value equal to 20 percent of the vertical reaction is advised by the ACI Building Code, and that value will be used in the calculations.

The force N normal to the assumed failure plane can be calculated as follows:

N_1 from #6 bars = $(4 \times .44 \times 60) \cos 15^\circ$ = 102 k

N_2 from #3 stirrups = $(2 \times .22 \times 60) \cos 15^\circ$ = 25.5 k

N_3 from strands = $(6 \times .153 \times 60) \sin 63^\circ$ = 49.0 k

N_4 from reaction R and longitudinal force = $(R \sin 15^\circ - .2R \cos 15^\circ)$ = $.066R$ k

Total Normal force N = $(176.5 + .066R)$ k

Frictional force F = $1.3\ (176.5 + .066R)$ = $(229.5 + .0858R)$ k

Equating F to the component of the applied load parallel to the shear plane, $(229.5 + .0858R) = R \cos 15^\circ$

$R = 260$ k > 205 k measured maximum value from test

The above calculation indicates that failure along a shear friction plane would have been unlikely even with a longitudinal force. The number of #6 bars welded to the bearing plate appears to have been excessive for the laboratory model which did not involve a longitudinal force.

The above procedure with the shear friction hypothesis could be used as a first step in estimating the area of horizontal steel that is to be welded to the bearing plate.

6.2 Diagonal Tension

6.2.1 Mode of failure

A diagonal crack that starts at the re-entrant corner of the notch could extend towards the compression face of the beam. The specific diagonal angle at which the crack propagates will follow the path of least resistance. Several possible cracks can be studied in terms of a distance d_{cr} measured from the corner of the notch longitudinally along the beam to

the assumed end of the diagonal crack. The diagonal crack should be assumed to terminate in the flexural compression zone of the beam. The free body sketch of Fig 6.2 illustrates the top, separating portion of the notched end.

Equilibrium of moments about the right end of the free body diagram of Fig 6.2 illustrates how all forces across the crack must be resisted by reinforcement. The shear resisted by the compression concrete is not a part of the moment equation.

6.2.2 Length and direction of crack

The position of the top end of the shear crack depends upon various factors such as reinforcement ratio, extent of prestressing and configuration of the beam particularly the widened portion at the top. Nevertheless, for the calculations that follow the length of crack has been taken as that of the crack which could have caused failure at the notched end in the specimen tested. It will be shown later that the estimate of failure load is not sensitive to the precise value of crack length, and a range within which the end of the crack could be assumed can be fixed without appreciable errors in the strength calculation.

6.2.3 Neutral axis depth

Various theories have been suggested by different authors with regard to establishing a neutral axis depth to define the compression zone of concrete in regions of shear compression failures. One theory proposed by Bjuggren and Regan is given below (14).

The depth c (Fig 6.3) from the compression face to a neutral axis in shear compression differs from the flexural neutral axis location because the assumption that plane sections remain plane after deformation may not apply near a large diagonal crack. At the same time it is not equal to the ultimate neutral axis depth for the simple reason that tension steel has not yielded at the time of shear failure at the section considered. Theoretically it is necessary to satisfy compatibility of finite deformations along the part of the beam affected by shear cracking. Compatibility conditions can be expressed as explained below.

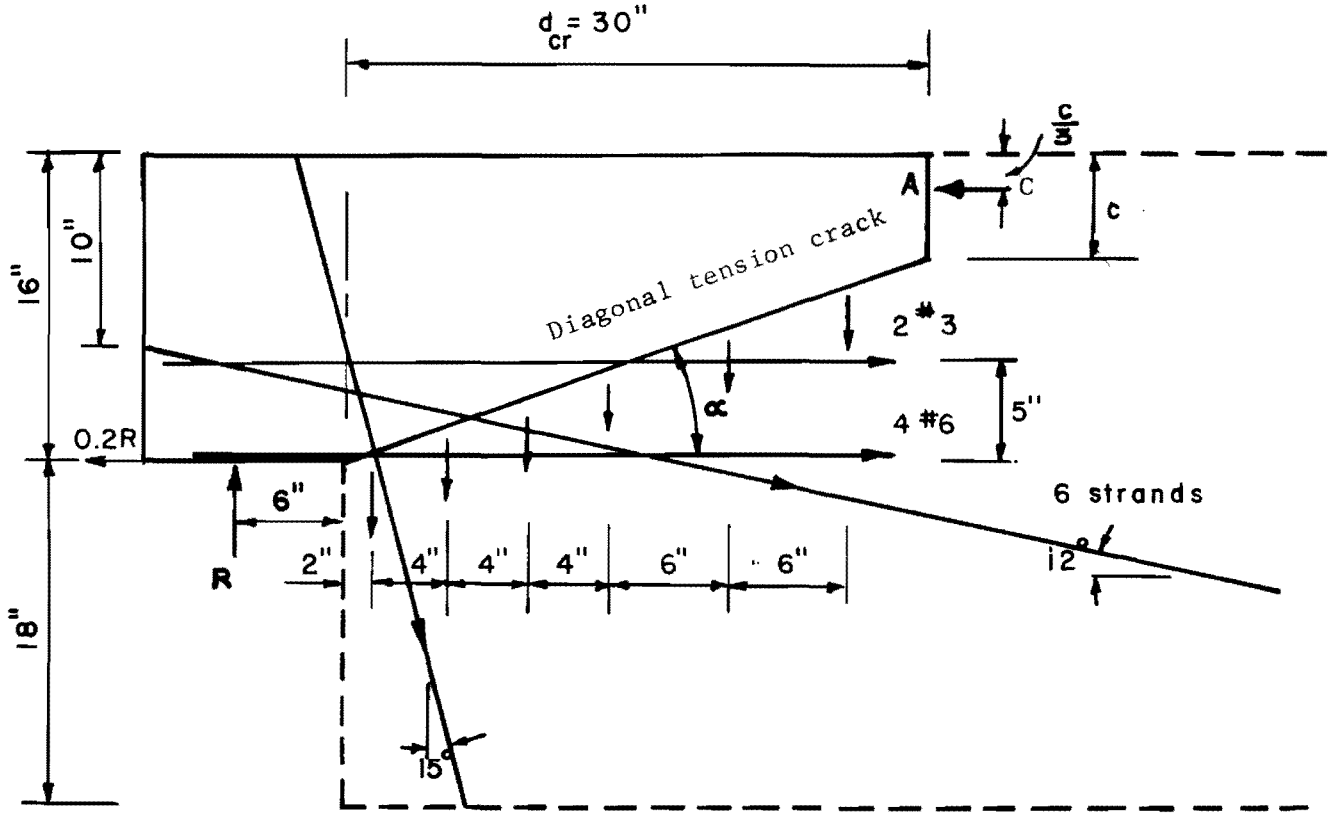

Fig 6.2. Forces acting on free body.

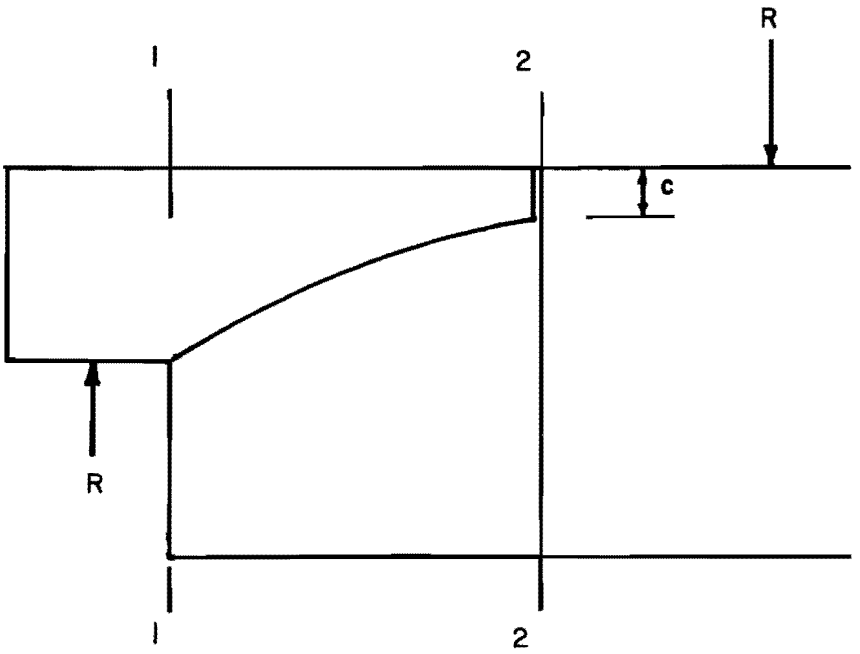

Fig 6.3. Depth of neutral axis (referenced in 6.2.3).

Since section 1-1 as shown in Fig 6.3 undergoes only negligible deformation during loading and section 2-2 is a plane section which remains plane, the neutral axis depth c at section 2-2 is given by the equation

$$\frac{c}{1-c} = \frac{\Delta cc}{\Delta st}$$

where

Δcc = deformation of extreme concrete fiber between sections 1 and 2 and

Δst = deformation of tension steel between sections 1 and 2.

By the above definition the value of c can be calculated from measurements of strains in concrete and steel where these data are known.

The end of the beam is required to resist moments that are not adequate to cause flexural steel to yield nor flexural concrete stress to reach very large values. Consequently an analysis of cross section properties at section 2-2 based on the elastic behavior of a cracked section should be relevant at a distance of perhaps one beam depth away from the notch. Cross section properties and calculations for the location of a neutral axis are illustrated in Fig 6.4. The modular ratio n was taken as 6.3.

6.2.4 Calculation of capacity R

In the calculations that follow, it is assumed that all steel across the crack except the strands yield before failure. Near the end of the beam the strand may not be able to develop its full yield strength, and the strand stress should be limited to the developable amount. The development length of the 1/2-inch strand was taken as 50 diameters or 25 inches. Therefore the allowable stress in the strands is calculated as

$$\text{Modular Ratio } n = \frac{E_s}{E_c}$$

$$= \frac{29000}{4635}$$

$$= 6.3$$

Taking moments of areas of concrete and transformed area of steel about the neutral axis,

$$18 \times c \times \frac{c}{2} = .918 \times 6.3\ (18.53 - c) + 1.224 \times 6.3\ (31 - c)$$

$$9c^2 = 344 - 13.1 \times c$$

$$c = 5.48 \text{ in.}$$

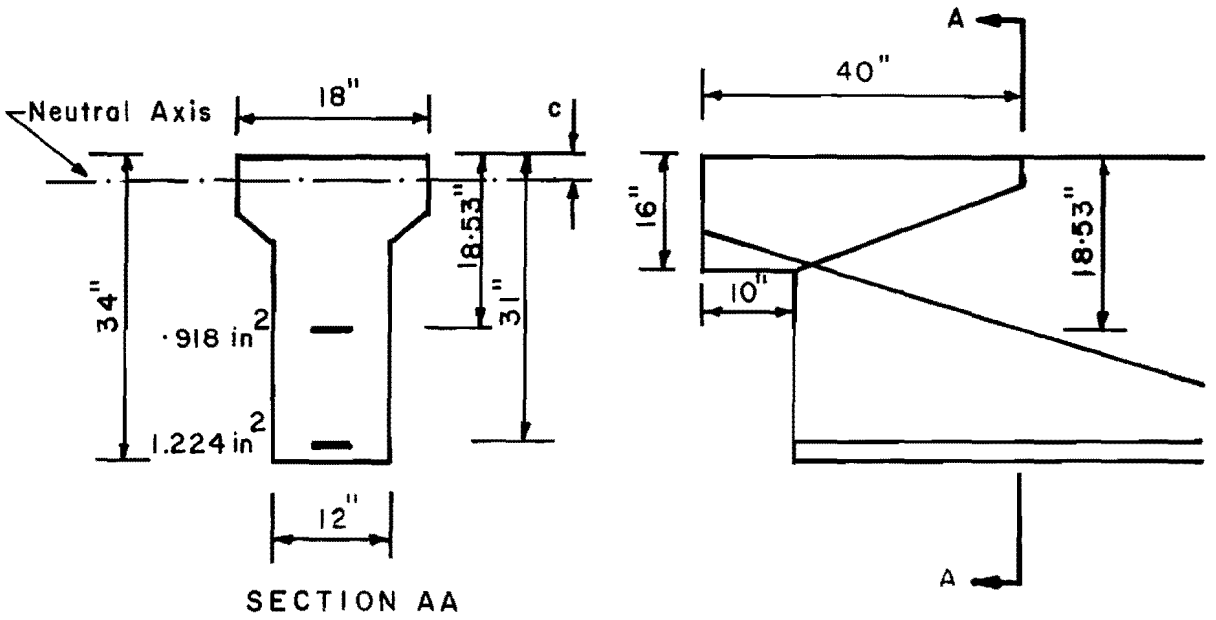

Fig 6.4. Depth of neutral axis.

$$f_{ps} = \frac{\text{Yield strength} \times \text{distance from end to the crack}}{\text{Development length}}$$

$$= .85 \times 270 \times \frac{16.5}{25}$$

$$= 152 \text{ ksi}$$

From the actual crack patterns of the specimen after failure (Fig 4.4) the length of the potential crack which would cause a failure at the notched end with straps, can be estimated. Judged from the orientation of this crack (marked ab in Fig 4.4) the distance d_r has been taken as 30 inches.

Taking moments of forces about A, the center of gravity of the compressive force in concrete and using reinforcement sketched in Fig 6.2:

(1) Moment due to R and L = 36 R + .2R (16 - 1.83)
= 38.83R

(2) Moment due to tension in strap = $3 \times 36 \times 32.5 \cos 15^{o}$
= 3390 in-kips

(3) Moment due to #6 bars = 1.76×60 (16 - 1.83)
= 1496 in-kips

(4) Moment due to #3 horizontal bars = $.22 \times 60$ (9.17)
= 121 in-kips

(5) Moment due to strands = $.918 \times 152$ (40 tan 12^{o} + 10 - 1.83) cos 12^{o} = 2276 in-kips

For design, it is recommended that the effective component of strand force be restricted to the f_y value that is assumed to exist in tensile bars welded to the base plate. Limiting to f_y the tensile stress effective in strand will have the effect of limiting the possible size of crack prior to failure.

(6) Moment due to vertical stirrups = $.22 \times 60$ (28 + 24 + 20 + 16 + 10 + 4)
= 1347 in-kips

$$38.83R = 3390 + 1496 + 121 + 2276 + 1347 = 8630$$

$$R = 222 \text{ k}$$

The value of R increases to 240K if L , the longitudinal force, is not present.

6.2.5 Effect of neutral axis depth

Though the depth of neutral axis is an important parameter so far as the compressive force in concrete is concerned its influence is minor in the above calculations. To illustrate this, values of R for values of c were calculated and are given below.

c, in.	Moment, in-kips						R, kips
	1	2	3	4	5	6	
3	39 R	3390	1584	132	2378	1347	226
5.48	38.83R	3390	1496	121	2276	1347	222
7	38.73R	3390	1443	114	2197	1347	219

It can be seen that variation in the values of R over a range of possible values of c is small enough to be insignificant.

6.2.6 Effect of d_{cr}

Values of R for a range of crack lengths are given below:

d_{cr}, in.	Moments, in-k						R, k
	1	2	3	4	5	6	
10	R×18.83	1303	1496	121	1688	158	253
20	R×28.83	2347	1496	121	1977	633	228
30	R×38.83	3390	1496	121	2276	1347	222
40	R×48.83	4434	1496	121	2554	2244	223
60	R×68.83	6520	1496	121	3131	4382	227

From the above values of R it is evident that for crack lengths d_{cr} greater than the notched depth of 16 in. the results are not very sensitive to crack length. The variation as plotted in Fig 6.5 shows that a d_{cr} value of 2h gives minimum values for R . The notched end

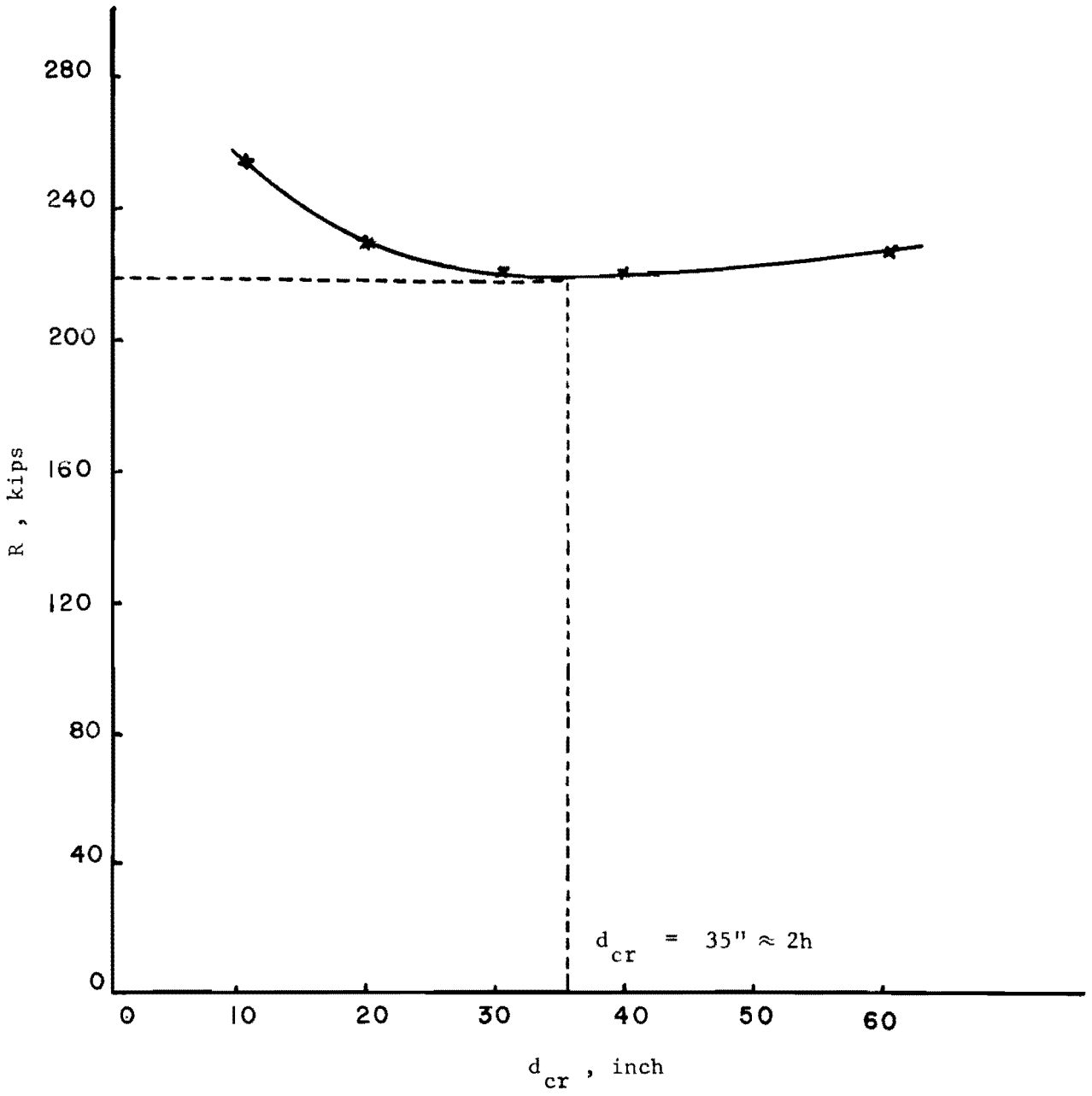

Fig 6.5. Effect of crack length.

height h should include the thickness of a composite slab if the shear capacity is to include the live load which must be resisted by the full composite cross section.

6.3 Design Procedure

On the basis of the two potential failure modes, one with a shear friction separation parallel to inclined strap reinforcement, and the other with a shear-compression separation from the corner of the notch into the flexural compression zone of the end block, a procedure for designing notched end reinforcement becomes apparent. Horizontal bars in the side faces of the end block above the notch plus bars welded to a bearing plate at the notch can be proportioned to satisfy bracket design recommendations of Sections 11.14 and 11.15 in the ACI Building Code. The size of inclined strap hangers then can be determined from the required capacity to balance ultimate forces from steel including straps that cross the potential shear compression crack.

A sample design will be used to illustrate the procedure. It is assumed that the sole purpose for using a notch is to allow a "standard" beam to be used with an elevated support shelf in order that a continuous top or bottom profile may be maintained in the structural assembly. Therefore it may be further assumed that an end block region with vertical and horizontal reinforcement adequate for shear is already designed. The design example illustrates only the modifications of end block details to accommodate the notch.

For this example a 54-in.-deep standard section of the Bureau of Public Roads (15) will be taken as the standard member for which a notched end is desired. The maximum span for this pretensioned girder is given as 70 feet for a 28-ft roadway. Details of all reinforcement, design loads and material strengths are given in the referenced document. All strands in the reference stringer are straight. In order to illustrate the role of draped strands it will be assumed that 14 strands are draped with two drape points 5 feet on either side of the midspan. Cross section details and strand drape dimensions are as shown in Figs 6.6a and 6.6b. Dimensions assumed at the notch also are given in Fig 6.6b.

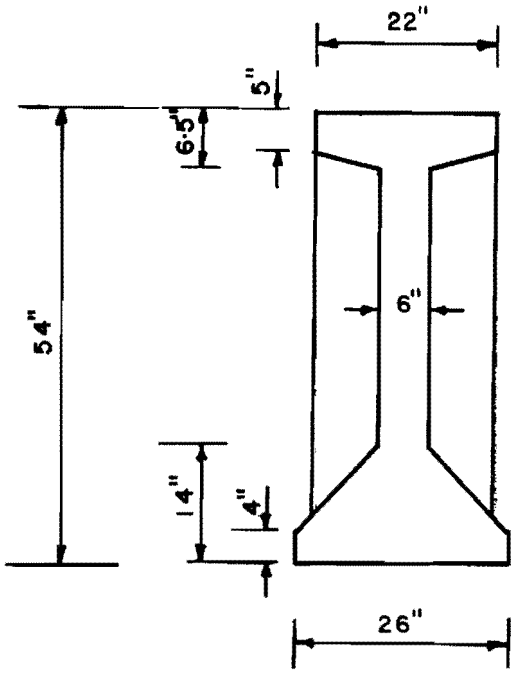

52 strands 1/2" , 250 ksi
(2 at top, 50 at bottom)

(a)

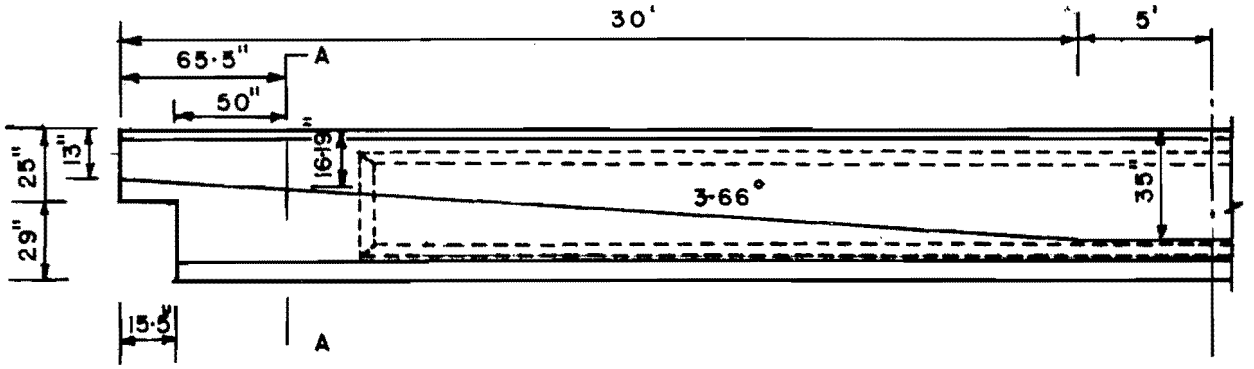

(b)

Fig 6.6. Details of 54-in.-deep beam - design example.

Calculations:

$d_{cr} = 2\,h = 2 \times 25 = 50$ in.

Depth of neutral axis
at 50 in. from notch = 9.5 in.

(For procedure for calculating depth, see Fig 6.4)

Inclination of crack $= \tan^{-1} \frac{15.5}{50} = 17.2^{o}$

The strap is positioned perpendicular to the crack but in any case the strap end at the top should be located above the center of the bearing for the stringer. See Fig 6.7a.

From the details of service loads given in the reference document ultimate load reaction at the notched end is calculated as

Reaction $= (1.35 \times 48.6) + 2.25\ (43.2 + 11.1)$

$= 188$ k

Longitudinal
force at bearing $= .2 \times 188 = 37.6$ k

Calculation of horizontal steel by shear friction analysis

A shear plane is assumed as parallel to the hanger strap. Refer to Fig 6.7b.

Applied shear force at crack $V_u = 179.6 + 11.0$

$= 190.6$ k

Applied normal force at crack $P_u = 55.6 - 35.9$

$= 19.7$ k

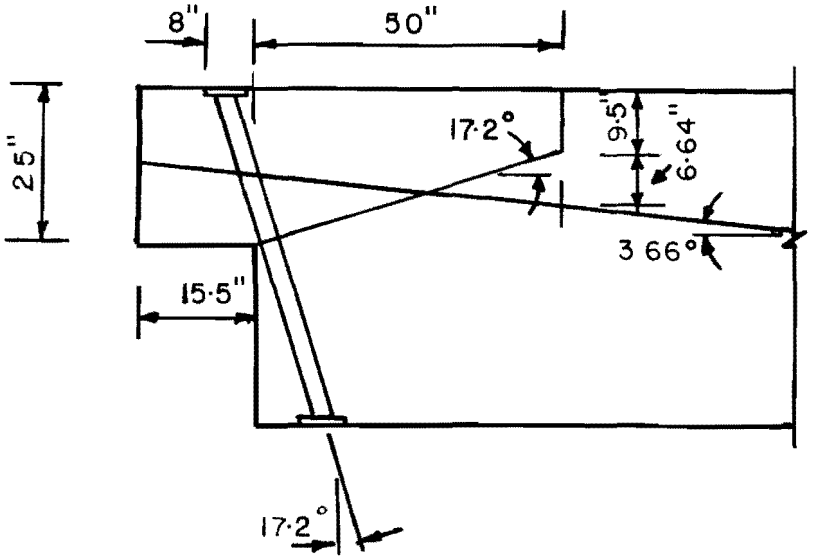

(a)

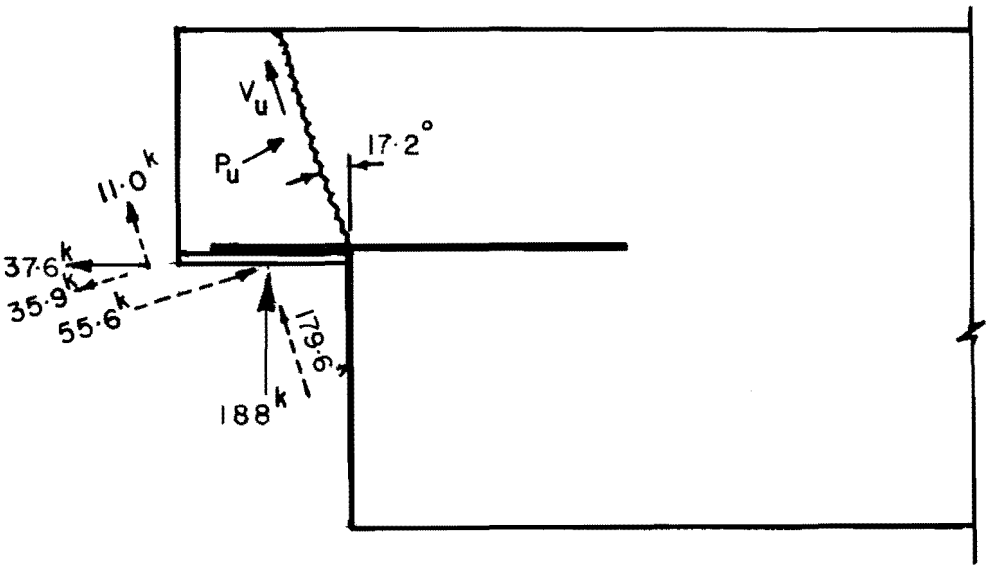

(b)

Fig 6.7. Shear friction - 54-in.-deep beam.

Check maximum v_u $= \frac{190.7 \cos 17.2}{24 \times 22}$

$= .345 < 0.840$ ksi O.K.

Required reinforcement A_{vf}

for the shear friction force $= \frac{1}{\phi F_y}\left(\frac{Vu}{\mu} - P_u\right)$

$= \frac{1}{.85 \times 60}\left(\frac{190.7}{1.4} - 19.7\right)$

$= 2.28$ in.^{2}

Strand contribution to A_{vf} $= \left[14(.08) \cos(17.2 + 3.7)\right]$

$= 3.04$ in.^{2} $\times \frac{152}{60}$

(or 1/3 A_{vf}, whichever is smaller)

Additional horizontal steel required $= \frac{2}{3} \times \frac{2.28}{\cos 17.2}$

$= 1.59$ in.^{2}

Specify 3 #7 bars welded to plate 1.80 in.^{2}

Calculation of hanger strap area (Fig 6.8a)

$(52.3 + 1.8) F = 188(58) + 37.6(21.83) - 6(.40)(26)(60)$
$- 14(.080)(60)(13.02) \cos 3.7 - 1.80(60)(20.39)$

Strap force, $F = 90.6$ k

With A36 steel,

$A_{stp} = \frac{90.6}{\phi 36} = 2.96$ in.^{2}

Use 4 straps 3 in. $\times$ 1/4 in. or 2 straps 3 $\times$ 1/2

Anchor plates for straps: See Fig 6.8b for relative amount of congestion at straps

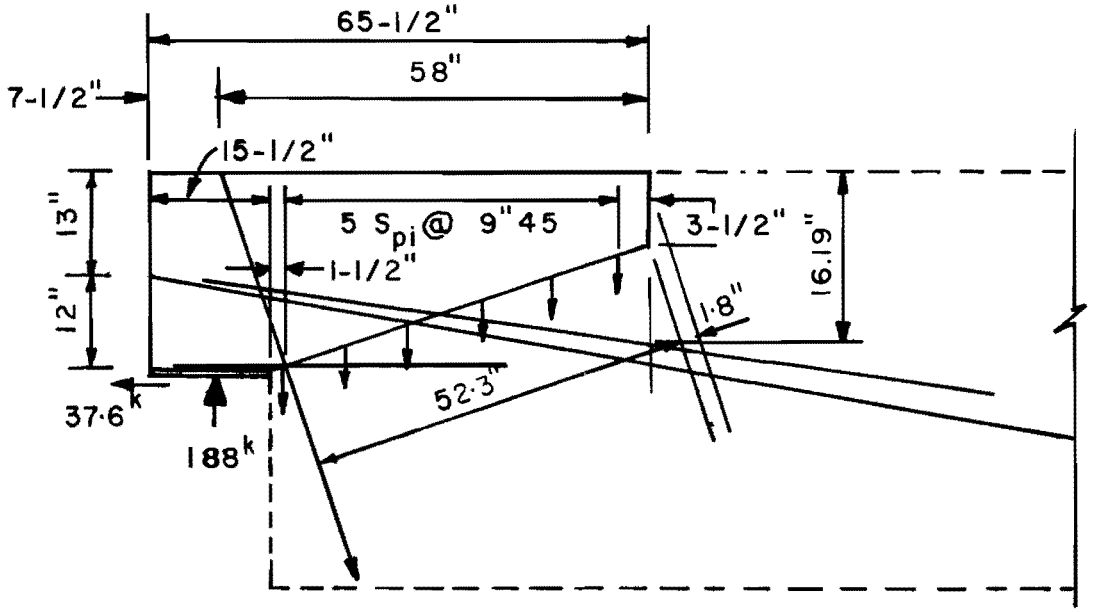

(a)

6"x1.5"x20" Plate

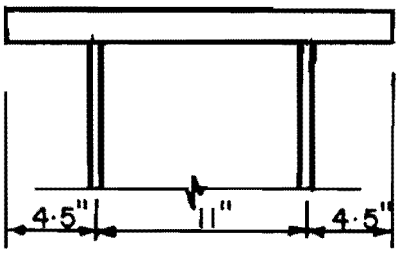

(b-1)

2 straps 1/2-inch thick
require heavier anchor plate

6"x.75"x20" Plate

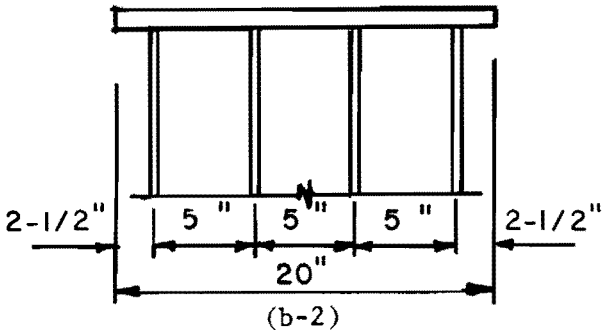

(b-2)

4 straps 1/4-inch thick
require thinner anchor plate

Fig 6.8. Analysis for strap area.

Moment on anchor plate $M_u = \frac{90.6}{20} \times \frac{(2.5)^2}{2} = 14.2$ in.-k

Thickness of 6-in. plate $= \sqrt{\frac{6 \times 14.2}{6(.85)(36.0)}} = 0.68$ in.

Use $6 \times \frac{3}{4} \times 20$-in. plate

6.4 Computer Methods

As indicated earlier in Chapter 2, various discrete element models of the notched end block were analyzed using the computer program 'LINFIX.' The following basic assumptions were made in modeling.

(1) A reinforced concrete member can be conceived of as a frame or truss consisting of members with stiffness properties concentrated along their centroidal axes.

(2) Each truss member is assumed to represent one-fourth of the concrete and one-half of the steel occurring within the area between the two adjacent truss members on either side of it, as indicated in Fig 6.9.

(3) Transformed section properties can be assigned to each member with appropriate values of E_c and E_s.

(4) The continuity between the end block and the rest of the beam can be represented by a set of supports. As indicated in Fig 2.6a, all the nodes on a vertical line at the left end are considered as supports with one hinge at the top node and the rest with rollers to allow for rotation and vertical deflection.

(5) Prestressing can be represented by external loads applied at appropriate joints. For a pretensioned beam these could be calculated in proportion to the distance from the end of the strand, assuming that the full prestress develops within a length of 50 diameters of the strand.

(6) On application of load, if the tensile force in a truss member exceeds the concrete capacity the member should

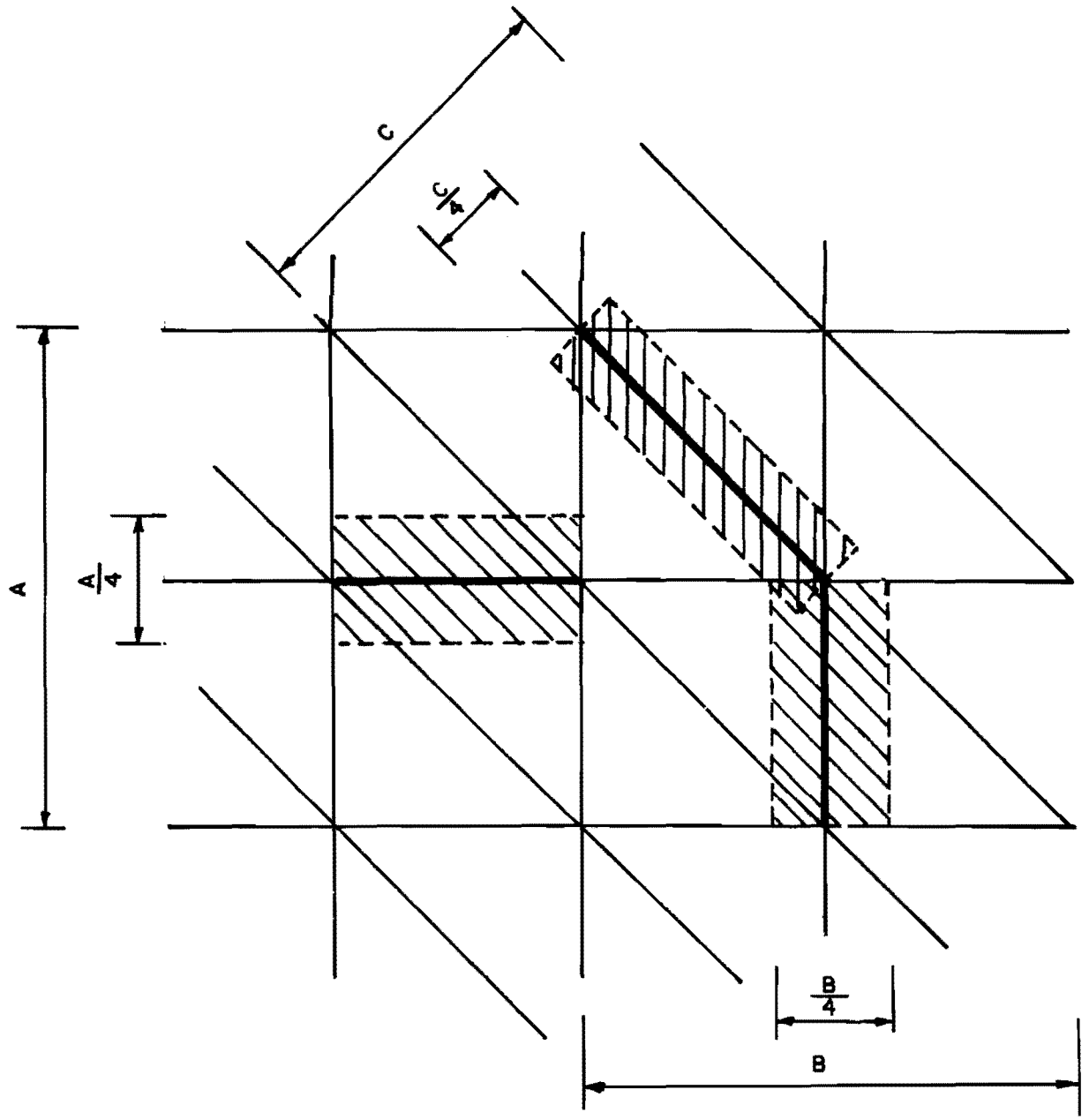

Fig 6.9. Area of concrete assigned for a truss member.

either be disconnected by assigning negligible values for its properties if the member consists of concrete alone; or be converted to a steel member by assigning the properties of the reinforcement.

Following the basic assumptions as described, the end block of the prototype beam was modeled in different patterns and analyzed using the computer program. Results for one of the models are contained in Appendix H. The hatched lines in Fig 6.10 are the truss members which are overtensioned beyond the tensile capacity of concrete. These were either reinforced in stages or disconnected depending upon their positions and the magnitude of stress in them. Results from this analysis also confirmed that the horizontal stirrups were not sharing much load and hence their quantity could be reduced.

The test specimen design with reduced reinforcement was analyzed. Appendix I contains computed member stresses. Figures 6.11 and 6.12 show the cracked members cross-hatched. The load applied was 50K followed by an additional 50K. Figure 6.13 shows an approximate layout of expected cracking. The cracks are assumed to form across the overtensioned members. The crack pattern obtained based on the analytical study is in general agreement with the test results shown in Fig 4.4.

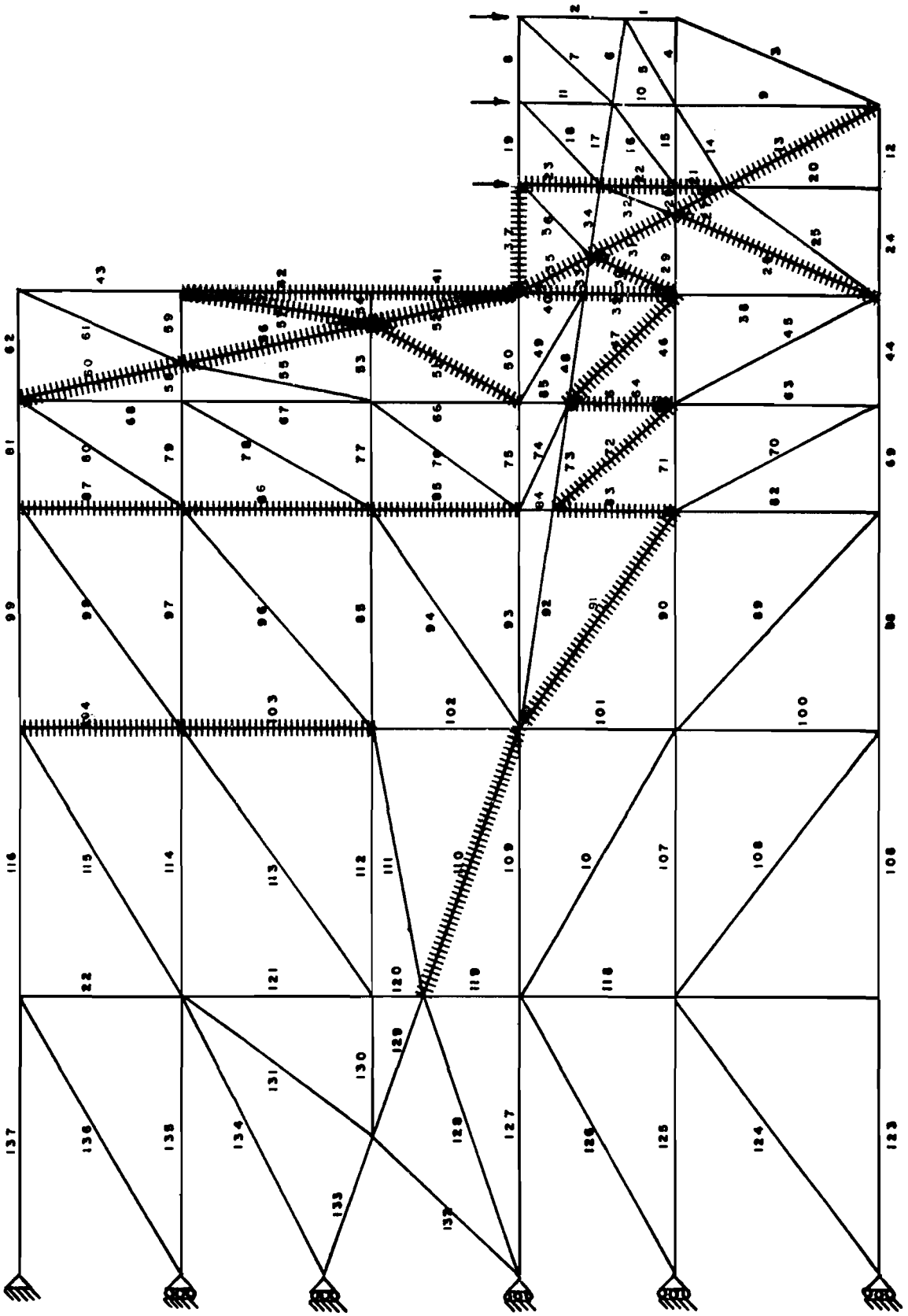

Fig 6.10. Computer analysis of prototype beam.

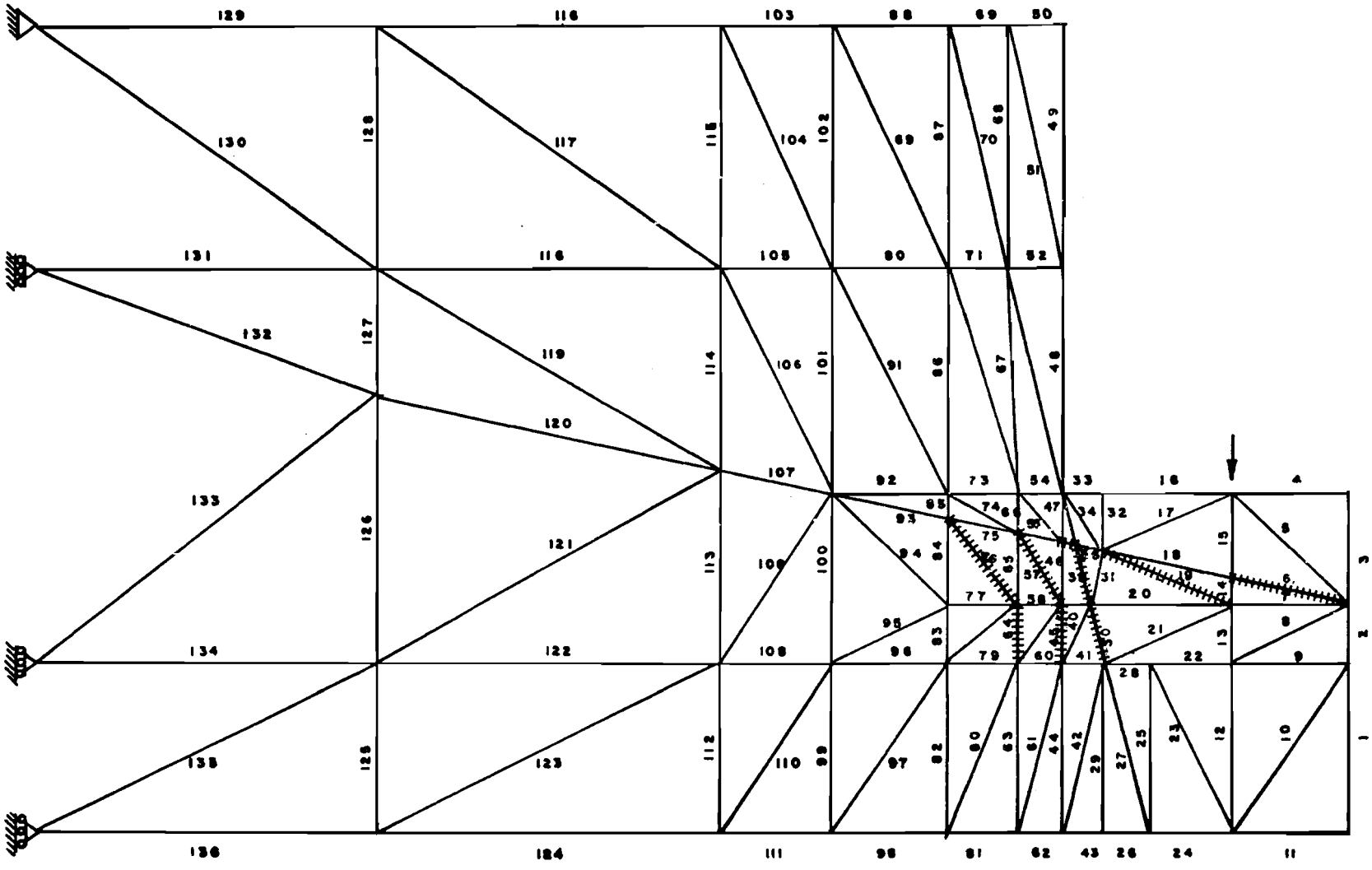

Fig 6.11. Specimen members cracked, first stage.

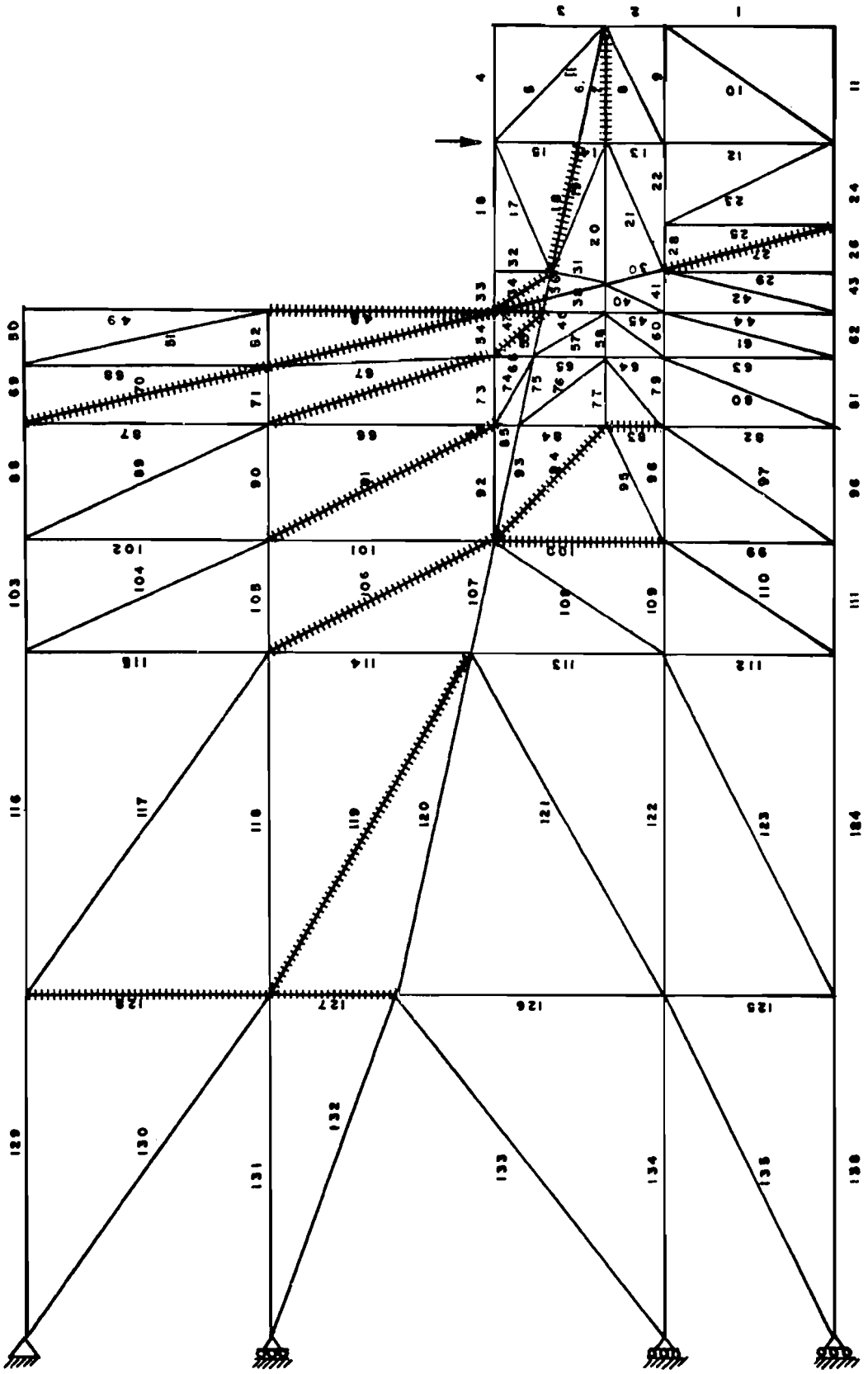

Fig 6.12. Specimen members cracked, second stage.

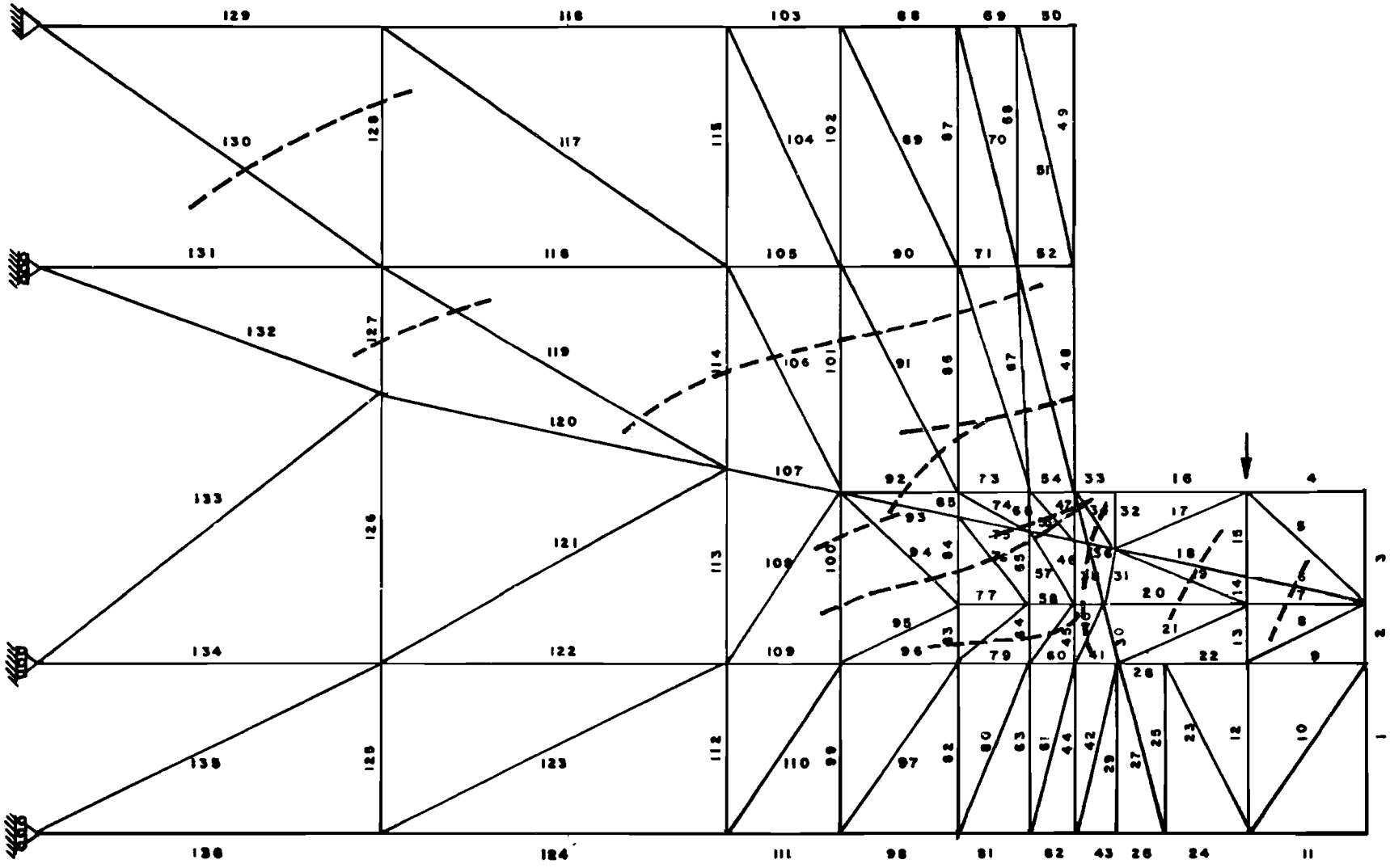

Fig 6.13. Cracks as predicted by computer analysis
(figure reversed for comparison with Fig 4.4).

CHAPTER 7. RECOMMENDATIONS

7.1 Analytical Study

A two-dimensional stress analysis of the notched block modeled by discrete elements is useful for identifying the load paths and resulting crack propagation. For problems of this nature it helps the designer to locate the tensile zones where reinforcement is necessary. However, this method does not appear practical for predicting the ultimate load capacity, nor for common design circumstances.

7.2 Test Study

Based on test results the following recommendations are made.

(1) Shear at the notched ends can be supported by provision of structural steel inclined straps plus horizontal bars welded to a bearing plate. The bearing plate and bars plus the inclined straps need not constrict the placement of concrete in the notched end region.

(2) A design with web plates was employed in order to transfer with steel plates the stress concentrations from the notched end into the region of full member depth. The use of two large web plates involved the minimum interruption of cross section space and the simplest details of reinforcement for the end block region. The web plate reinforcement performed adequately, resisting the total load applied before the beam itself failed in shear. However, there were more cracks and larger crack widths in the web plate reinforced end than in the strap and rebar reinforced end. It is felt that the web plate assembly also involves more expense than does the strap and rebar reinforcement detail.

7.3 Design of Notched End Reinforcement

Two mechanisms of potential failure should be considered in order to establish reinforcement requirements in the notched end region of a beam. The design procedure recommended here assumes that an end block region of a standard beam has been functioning successfully, and the same type member is to be modified for a notched end bearing. A steel strap hanger is to be inclined from the midpoint of the notched region above the bearing to the bottom of the end block region in the deep part of the beam.

7.3.1 Step 1

The bars that must be welded to the bearing plate can be designed on the basis of bracket shear friction requirements at an assumed shear plane along the exterior edge of the inclined strap hanger assembly. Additional horizontal bars into the end block above the notch should also fulfill bracket design recommendations.

7.3.2 Step 2

Retain the longitudinal spacing of vertical stirrups for the end block without a notch, and compute the required area of steel in inclined straps in order to resist forces on a free body of the flexural compression region of the notched end. The free body, as described in Chapter 6, is bounded by a potential crack from the root of the notch into the compression zone of the end block.

REFERENCES

1. Ali A. Hamoudi, Michael K. S. Phang, and Robert A. Bierweiler, "Diagonal Tension in Prestressed Concrete Dapped Beams," Journal of the ACI, Vol 72, July 1975, pp 347-350.

2. American Concrete Institute, "Building Code Requirements for Reinforced Concrete," ACI 318-71, Detroit, 1971.

3. Birkeland, P. W., and H. W. Birkeland, "Connections in Precast Concrete Construction," ACI Journal, Proceedings, Vol 63, No. 3, March 1966, pp 345-368.

4. Burns, Ned H., "Moment Curvature Relationships for Partially Prestressed Concrete Beams," Journal of the Prestressed Concrete Institute, Vol 9, No. 1, February 1964, pp 52-63.

5. Ferguson, P. M., "Reinforced Concrete Fundamentals," Third Edition, 1973.

6. Furlong, Richard W., Ferguson, Phil M., and Ma, John S., "Shear and Anchorage Study of Reinforcement in Inverted T-Beam Bent Cap Girders," Research Report No. 113-4, Center for Highway Research, The University of Texas at Austin, July 1971.

7. Gaston, J. R., and L. B. Kriz, "Connections in Precast Concrete Structures, Scarf Joints," Journal of the Prestressed Concrete Institute, June 1964, pp 37-59.

8. Joint ASCE-ACI Task Committee 426, "The Shear Strength of Reinforced Concrete Members," Journal of the Structural Division, American Concrete Institute, June 1973.

9. Kani, G. N. J., "The Riddle of Shear Failure and Its Solution," Journal of The American Concrete Institute, April 1964.

10. Lyn, T. W., "Design of Prestressed Concrete Structures," Second Edition, 1963.

11. Mattock, A. H., and N. M. Hawkins, "Research on Shear Transfer in Reinforced Concrete," Journal of the Prestressed Concrete Institute, Vol 17, No. 2, March-April 1972.

12. Prestressed Concrete Institute, "PCI Design Handbook, Precast and Prestressed Concrete," First Edition, 1972.

13. Priestly, M. J. N., "Tests on Notched Ends of Prestressed Concrete Bridge Beams," Report No. 289, Thorndon Overbridge Central Laboratories, Gracefield Lower Hutt, New Zealand, January 1968.

14. The Institution of Structural Engineers, London, "The Shear Strength of Reinforced Concrete Beams," A Report by the Shear Study Group, Series No. 49, January 1969.

15. U. S. Department of Commerce, Bureau of Public Roads, "Standard Plans for Highway Bridge Superstructures," Revised 1956.

16. Werner, M. P., and W. H. Dilger, "Shear Design of Prestressed Concrete Stepped Beams," Journal of the Prestressed Concrete Institute, Vol 18, No. 4, July-August 1973, pp 37-49.

APPENDIX A

APPENDIX A

Calculations of Loading at Notched End Bearing for the Prototype Girder

Loading HS-20

Span (c/c of bearings of simply supported girder) = 125 feet

Spacing of girders = 7 feet 6 inches

Slab thickness = 8 inches assumed

Lane width = 10 feet

Live load reaction with uniform loading case is found to be more than the standard truck loading.

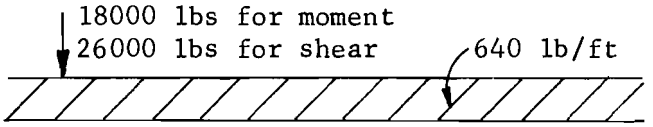

$$\text{L. L. Reaction} = \left(26000 + 640 \times \frac{125}{2}\right) \times \frac{1}{1000}$$

$$= 80 \text{ k}$$

Dead Load

Weight of slab, 8-in. thickness $= 7.5 \times \left(\frac{8 \times 12}{144}\right) \times 150$

$= 750$ lb/ft

Girder weight $= \frac{789}{144} \times 150 = 822$ lb/ft

Total = 1572 lb/ft

Dead load reaction $= 1.572 \times \frac{125}{2} = 98.25$ k

Total service load reaction $= 80 + 98.25 = 178.25$ k

Ultimate Load Reaction

Impact factor I $= \frac{50}{L + 125} = \frac{50}{125 + 125}$

$= .2$

Maximum ultimate load reaction $= 1.35D + 2.25(L + I)$

$= (1.35 \times 98.25) + 2.25(80 + .2 \times 80)$

$= 350$ k

APPENDIX B

APPENDIX B

Capacity/Stress Computations for Prototype Beam (see Fig B.1)

Moment Capacity

Using ACI Code equation 18-3,

$$f_{ps} = fpu\ (1 - .5\rho_p \frac{f_{pu}}{f'_c})$$

$$= 270\ (1 - .5 \times .005 \times \frac{270}{6.5})$$

$$= 242 \text{ ksi}$$

where

$$f_{pu} = 270 \text{ ksi}$$

$$\rho_p = \frac{37 \times .153}{26 \times 41.22}$$

$$= 0.0053$$

$$f'c = 6.50 \text{ ksi}$$

$$.85f'c \times a \times 26 = 37 \times .153 \times 242$$

$$a = 9.54 \text{ in.}$$ (1.02 in. below bottom of flange O.K.; since in the chamfered portion)

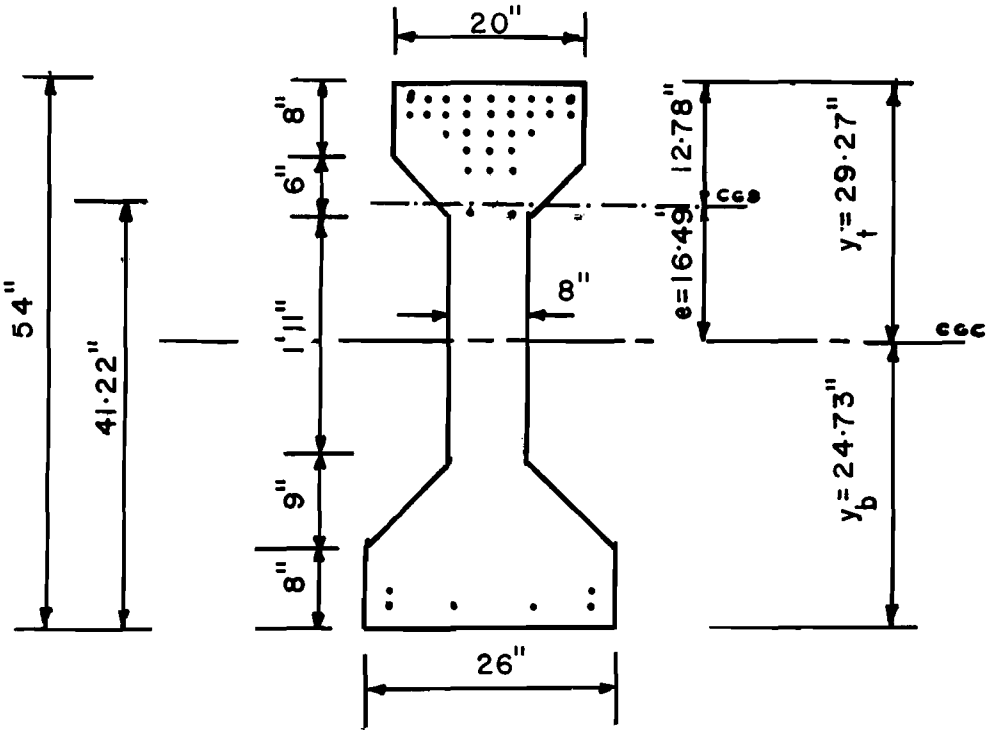

A = 789 in.^{2}

Y_b = 24.73 in.

Y_t = 29.27 in.

I = 258330 in.^{4}

e = 16.49 in.

37 strands

Fig B.1. Cross section of prototype beam.

$$M_u = (37 \times .153 \times 242)\ (41.22 - \frac{9.02}{2})$$

$$= 50300 \text{ in-kips}$$

Stresses at Service Load

Beam weight $= 789 \times \frac{150}{144} = .82$ k/ft

Moment $= .82 \times \frac{14^2}{2} \times 12 = 966$ in-kips

Moment due to applied load $= 178 \times 163 = 29014$ in-kips

Total M $= 30000$ in-kips

Prestressing force after all losses have occurred (25 percent losses) $= (189 \times .75) \times (37 \times .153)$

$= 802$ k

Top fibre stress, ft $= \left(\frac{802}{789}\right) + \left(\frac{802 \times 16.49 \times 29.27}{258330}\right) - \left(\frac{30000 \times 29.27}{258330}\right)$

$= -0.884$ ksi

Allowable (ACI Code)

$-6\sqrt{6500} = -.484$ ksi

Bottom fibre stress, f_b = $\left(\frac{802}{789}\right)$ $-\left(\frac{802 \times 16.49 \times 24.73}{258330}\right)$

$+\left(\frac{30000 \times 24.73}{258330}\right)$

= 2.6 ksi

Allowable (ACI Code)

$.45 \times 6.5$

= 2.925 ksi

Stresses at Transfer

Assuming initial losses of 10 percent, prestress at the time of release of strands

= $(270 \times .7) \times .9$

= 170.1 ksi

F = $170.1 \times 41 \times .153$ = 1067 k

Top fibre stress,

$f_t = \frac{F}{A} + \frac{F \times e \times Y_t}{I} = \frac{1067}{789} + \frac{1067 \times 16.49 \times 29.27}{258330}$

= 1.35 + 1.99

= 3.34 ksi (comp)

Allowable = $.6\ f'_{ci}$

= $.6 \times 6.5$

= 3.9 ksi

Bottom fibre stress,

$$f_b = \frac{F}{A} - \frac{F \times e \times Y_b}{I} = \frac{1067}{789} - \frac{1067 \times 16.49 \times 24.73}{258330}$$

$$= 1.35 - 1.68$$

$$= -0.33 \text{ ksi}$$

$$\text{Allowable} = \overline{-3\sqrt{f'_{ci}}}$$

$$= \frac{\overline{-3\sqrt{6500}}}{1000}$$

$$= -0.242 \text{ ksi}$$

APPENDIX C

APPENDIX C

Shear Capacity of Notched End - Prototype (Following ACI Provisions)
(see Fig C.1a, c, and d)

Shear Capacity at Section 1-1 (Fig C.1)

$$v_{ci} = .6\sqrt{f'_c} + \frac{V_d + \left(\frac{V_\ell M_{cr}}{M_{max}}\right)}{b_w d}$$

$f'_c = 5900$ psi

$V_d = 0$ (assumed)

$$\frac{M_{max}}{V_\ell} = P \times \frac{9}{p} = 9 \text{ inches}$$

$$M_{cr} = \frac{I}{Y_t}\left(6\sqrt{f'_c} + f_{pe} - f_d\right)$$

$$= \frac{26090}{12.7}\left(6\sqrt{5900} + 410 - 0\right)$$

$$= 1789052 \text{ in-lbs}$$

$v_{ci} = 861$ psi

(See Fig C.1c and d)

$$f_e = (21 \times .153 \times 189) \times .75 = 455.4 \text{ k}$$

$$\text{Prestress developed} = 455.4 \times \frac{15.5}{50 \times \frac{1}{2}} = 282 \text{ k}$$

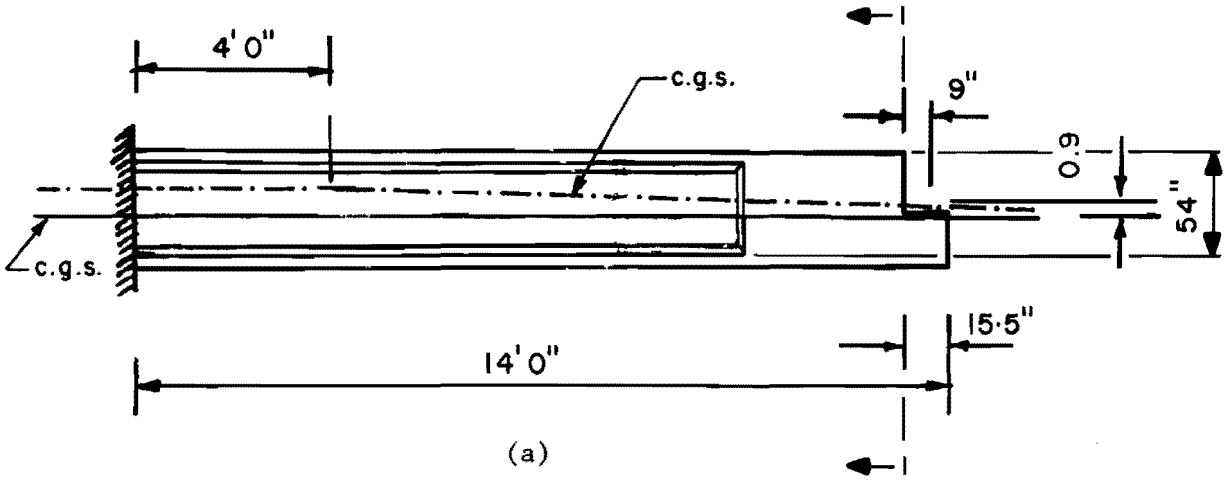

(a)

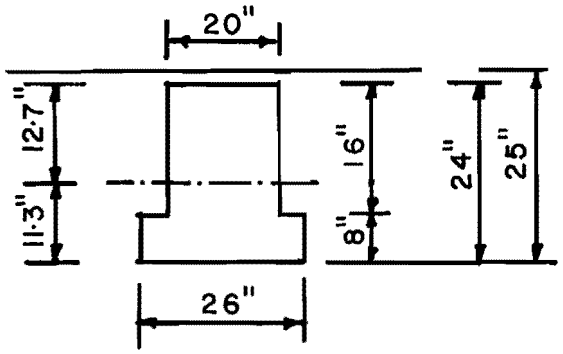

(b)

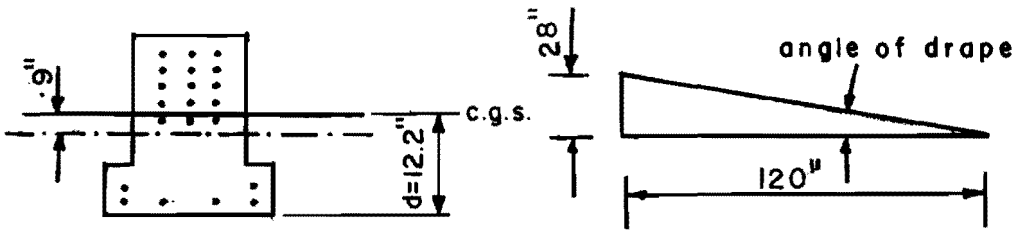

(c) (d)

Fig C.1. Notched end details - prototype.

$$f_{pe} = \left(\frac{282}{528} - \frac{282 \times .9 \times 12.7}{26090} \right) = .410 \text{ ksi}$$

$$f_{pc} = \frac{282}{528} \times 1000 = 534 \text{ psi}$$

Vertical component of strand force V_p

$$V_p = (15 \times .153 \times 189 \times .8) \times \frac{28}{120} \times \frac{15.5}{25} = 50 \text{ k}$$

$$v_{cw} = 3.5\sqrt{5900} + .3 \times 534 + \frac{50}{20 \times 12.2} \times 1000 = 634 \text{ psi}$$

Estimate total reaction capacity R by trial:

Try R = 500 k

$$v_u = \frac{500 \times 1000}{20 \times 12.2} = 2049 \text{ psi}$$

$$v_u - v_c = 2049 - 634 = 1415 \text{ psi}$$

$$A_s = \frac{(v_u - v_c)\, b_w s}{F_y}$$

Taking f_y = 36000 psi for hanger strap, A_s required for a space of 12 in.,

$$A_s = \frac{1415 \times 20 \times 12}{36000} = 9.43 \text{ in.}^2$$

Steel provided,

Straps = $4 \times 4 \times \frac{1}{2} = 8 \text{ in.}^2$

No. of vertical stirrups in 12 in.

$$= (3 \times .4) \frac{60000}{36000} = 2.0 \text{ in.}^2$$

Shear capacity can be taken as 500 k .

APPENDIX D

APPENDIX D

Calculations for Design of Specimen (see Figs D.1a, b, and c)

Stresses at Transfer

f'_{ci} = 5500 psi

F = 16 × 23 = 368 k

Midspan

$$f_b = \frac{368}{453} + \frac{368 \times 9.81 \times 18.31}{46{,}600} = .812 + 1.418$$

$= 2.23$ k (comp)

all = .6f'ci =

.6 × 5.5 =

3.3 ksi

$$f_t = \frac{368}{453} - \frac{368 \times 9.81 \times 15.69}{46{,}600} = .812 - 1.215$$

$= -.403$ k (tens)

$= -5.7f'_{ci}$

allow $\frac{-3\sqrt{5500}}{1000}$ =

$-.222$ k

(O.K. since this is a very temporary phase)

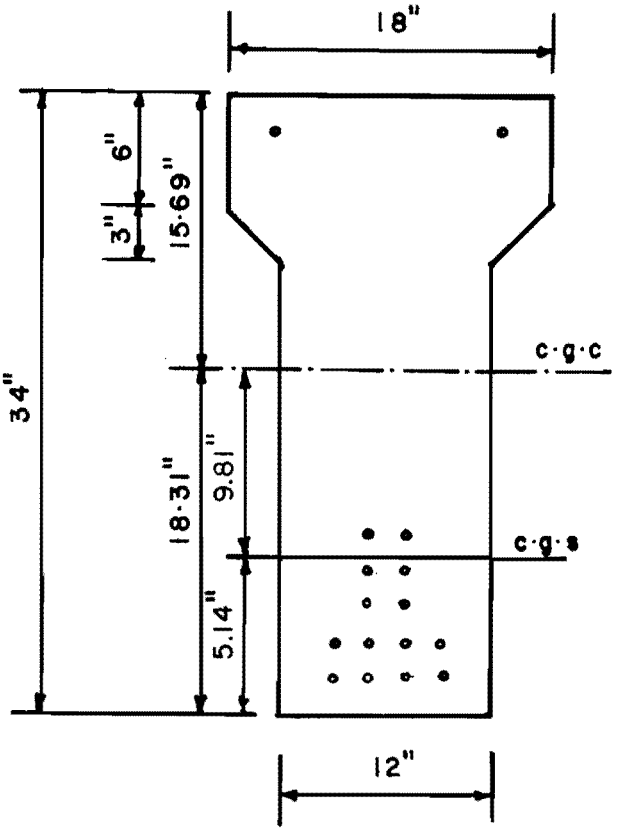

(a). Midspan

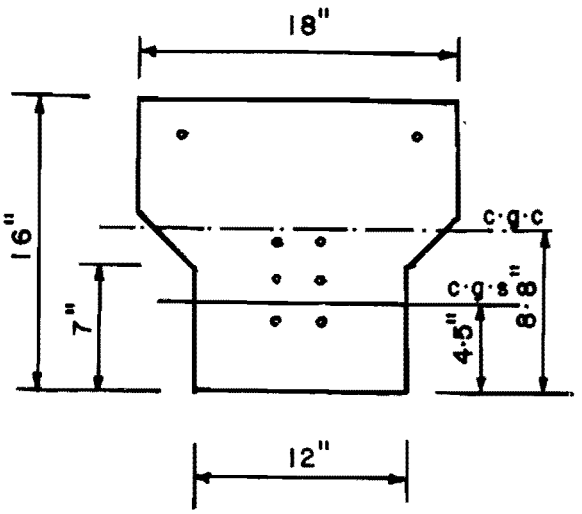

(b). Ends

$A = 453 \text{ in.}^2$

$Y_t = 15.69 \text{ in.}$

$Y_b = 18.31 \text{ in.}$

$I = 46600 \text{ in.}^4$

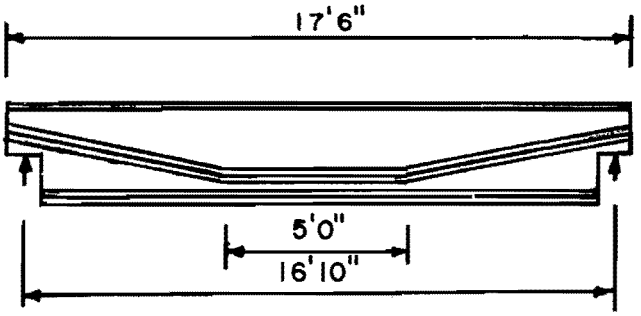

(c).

Prestressing:

2, 1/2" strands at top

14, 1/2" strands (6 draped) at bottom

All strands 270 ksi

Fig D.1. Section properties of specimen.

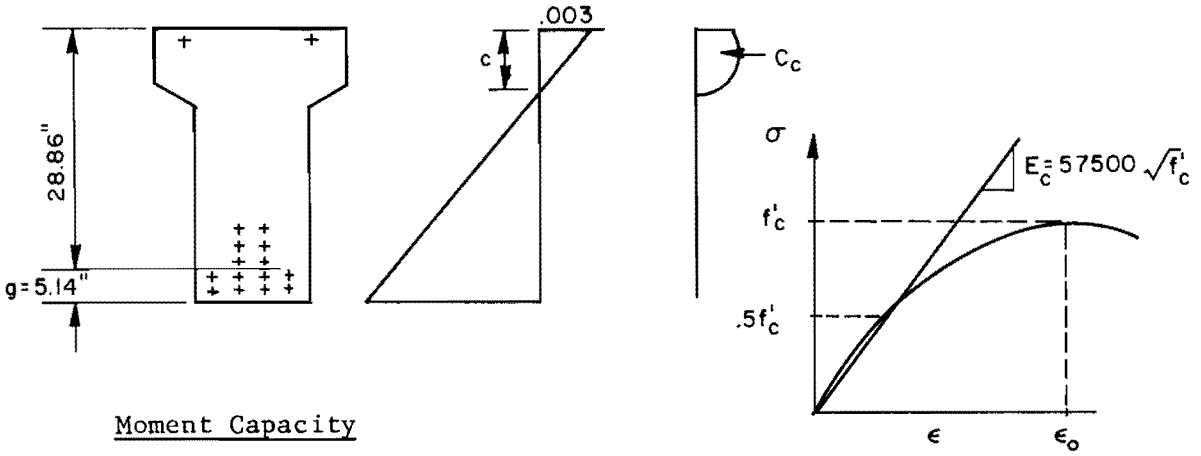

Moment Capacity

Compute ϵ_o

$$E_c = 57.5\sqrt{6500} = 4636 \text{ ksi}$$

$$4636 = \frac{3250}{\epsilon_{3250} \times 1000}$$

$$\epsilon_{3250} = \frac{3250}{1000 \times 4636} = .000701$$

$$3250 = 65000\left[2\left(\frac{\epsilon}{\epsilon_o}\right) - \left(\frac{\epsilon}{\epsilon_o}\right)^2\right] = 6500\,(2a - a^2)$$

$$\epsilon_o = .00239$$

For top fibre strain .003 , try c = 6.5 in. ;

$$\phi = \frac{.003}{6.5} = 461 \times 10^{-6}$$

$$C_c = bc^2 f'c \frac{\phi}{\epsilon_o}\left[1 - \frac{(\phi)(c)}{3t_o}\right]$$

$$= 18 \times 6.5^2 \times 6.5 \times \frac{461 \times 10^{-6}}{.00239}\left[1 - \frac{461 \times 10^{-6} \times 6.5}{3 \times .00239}\right]$$

$$= 555 \text{ kps}$$

$$\epsilon_s = \frac{.003\,(28.86 - 6.5)}{6.5} = 10320 \times 10^{-6}$$

Stresses After Initial Losses After Transfer
and Due to Self Weight of Beam (21 ^{k}/strand after losses)

$$F = 21 \times 16 = 336\ ^{k}$$

$$W_G = \frac{453 \times 150}{144 \times 1000} = .472\ ^{k}/ft\ ;\quad M_G = .472 \times \frac{16.83^2 \times 12}{8}$$

$$= 200 \text{ in-kips}$$

$$f_t = \frac{336}{453} - \frac{336 \times 9.81 \times 15.69}{46{,}600} + \frac{200 \times 15.69}{46{,}600}$$

$$= \underbrace{.742 - 1.11}_{-.368} + .067 = -.301 \text{ ksi}$$

$$f_b = \frac{336}{453} + \frac{336 \times 9.81 \times 18.31}{46{,}600} - \frac{200 \times 18.31}{46{,}600}$$

$$= \underbrace{.742 + 1.295}_{2.037} - .0786 = 1.958 \text{ ksi}$$

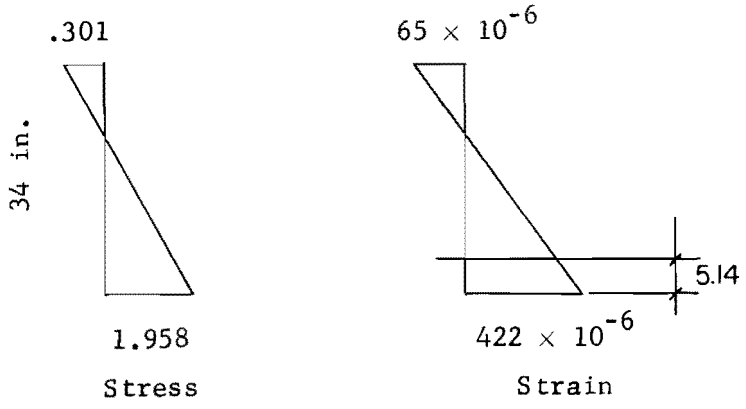

Initial strain in steel $= \frac{21 \times 1000}{.153 \times 27.5 \times 106} = 4990 \times 10^{-6}$

Strain (addl.) when conc. str. at steel level is zero $= \left[\frac{(34 - 5.14)(422 + 65)}{34} - 65\right] 10^{-6}$

$= 348 \times 10^{-6}$

Total strain in steel when conc. strain at steel level is zero $= 5338 \times 10^{-6}$

$\approx$

5350×10^{-6}

Total strain in steel $= (10320 + 5350)\ 10^{-6} =$

15670×10^{-6}

From load-elongation curve for 1/2-in. strands, Fig D.4

Load in one 1/2-in. strand for the above elongation = 40.5 k

T $= 40.5 \times 14 = 567$ k

O.K. for 560 k

$\bar{x} = c\left(\frac{8\epsilon_o - 3\phi c}{12\epsilon_o - 4\phi c}\right) = 6.5\left(\frac{8 \times .00239 - 3 \times 461 \times 10^{-6} \times 6.5}{12 \times .00239 - 4 \times 461 \times 10^{-6} \times 6.5}\right)$

$= 3.94$ in.

M $= 560\ (28.86 - 6.5 + 3.94) = 14728$ in-kips

M capacity $= 14728$ in-kips

$\underline{P_{cap}}$

(1) When loading points are 5 ft 0 in. apart

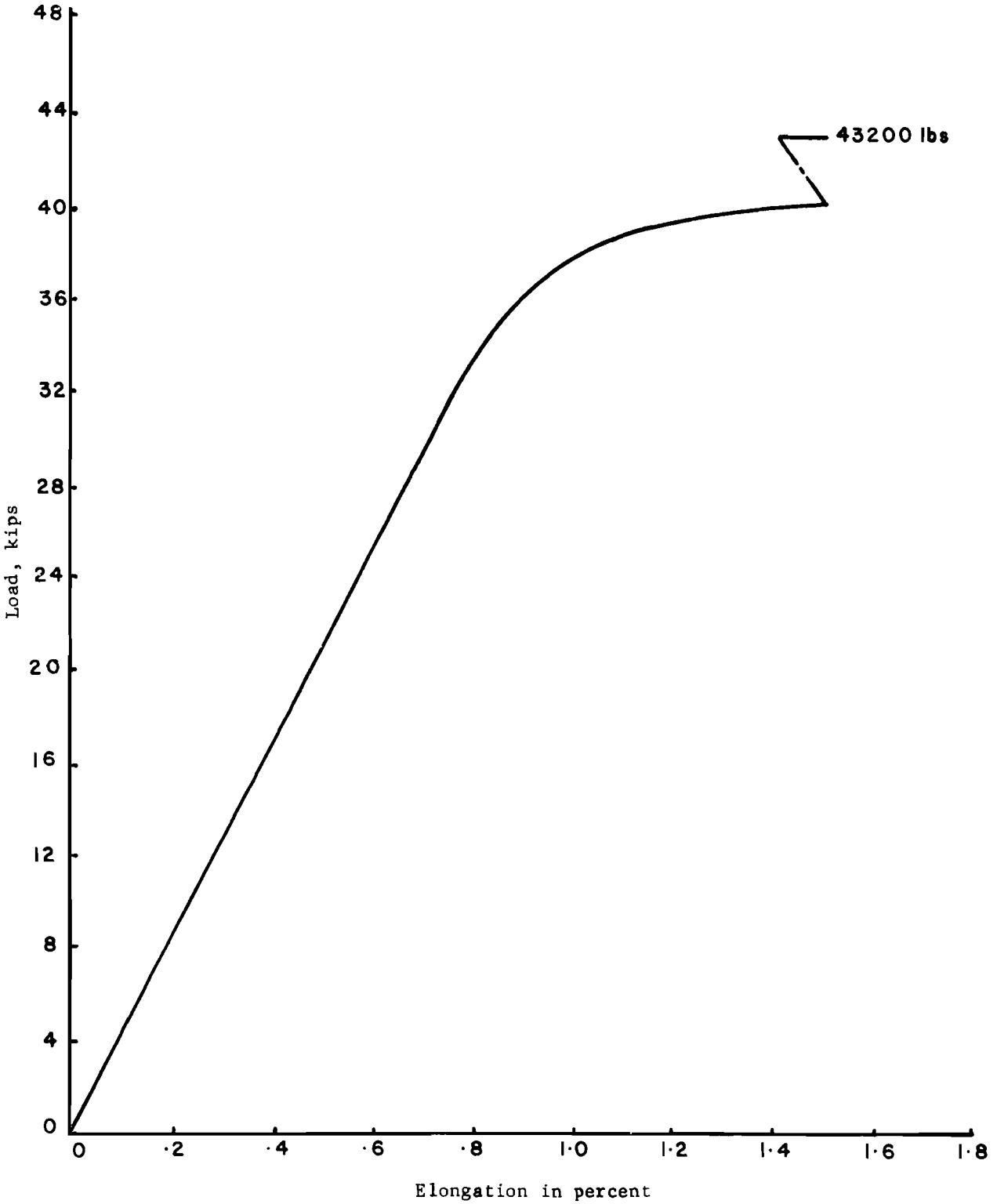

Fig D.4. Load elongation curve of 1/2-in. strands, 270 ksi.

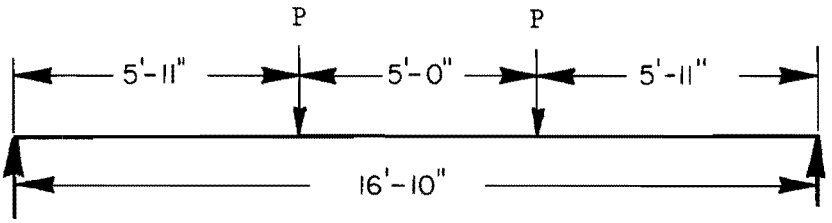

$$P_{cap} = \frac{14728}{5.917 \times 12} = 207.4 \text{ k}$$

(2) When loading points are 5 ft 9-1/2 in. apart

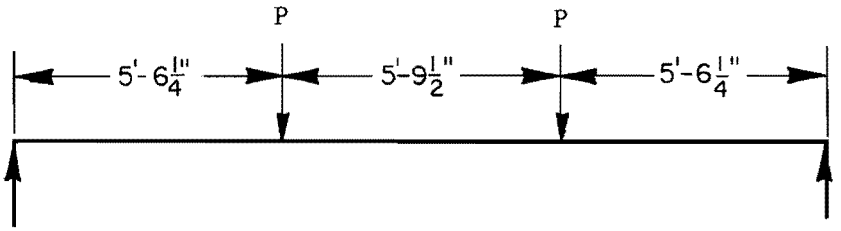

P = total load on one side

$$P_{cap} = \frac{14728}{5.52 \times 12}$$

$$= 222 \text{ k}$$

Moment Capacity Using ACI Equation

$$f_{ps} = fpu\ (1 - .5\ P_p\ \frac{fpu}{f'_c})$$

$$= 270\ (1 - .5 \times .00412 \times \frac{270}{6.5})$$

$$= 247 \text{ ksi}$$

$$f_{pu} = 270 \text{ ksi}$$

14 strands in flexural tension

$$P_p = \frac{14 \times .153}{18 \times 28.86} = .00412$$

$$f'_c = 6.5 \text{ ksi}$$

$$.85(f'_c) \times a \times 18 = 14 \times .153 \times 247 = 529$$

$$a = \frac{14 \times .153 \times 247}{.85 \times 6.5 \times 18} = 5.32$$

$$M = 529\ (28.86 - \frac{5.32}{2}) = 13860 \text{ in-kips}$$

Stresses at Service Load for the Model

Though there is no service load condition for a laboratory test, for comparison with the prototype a scaled service load is assumed.

Service load for prototype = 178 k

Scale of the model = 0.4

Service load for the model = 178 × 0.4

TABLE D.1

Section	Distance from Midspan, ft	Stages	M, in-kips	ϕ, 10^{-6} in./in.
1	0	Zero Moment	0	- 15.0
		Cracking	6724	15.9
		ϵ_c = .001	10693	98.0
		ϵ_c = .002	14105	267.0
		ϵ_c = .003	14728	461.0
2	5	Zero Moment	0	- 11.5
		Cracking	5917	15.9
		ϵ_c = .001	9104	100.0
		ϵ_c = .002	12386	267.0
		ϵ_c = .003	13260	448.0
3	8.34	Zero Moment	0	1.3
	(Notch)	Cracking	1703	9.2
		ϵ_e = .001	5223	172.0
		ϵ_e = .002	8624	345.0
		ϵ_e = .003	10537	500.0

The M - ϕ relationship is plotted in Fig D.5.

Using the M - ϕ relations at different sections of the beam, load-deflection calculations were carried out using the area-moment method of the ϕ-diagram. The load-deflection relationship for the two types of loading used for the specimen test, as analytically computed, are plotted, along with test values, in Fig 5.1.

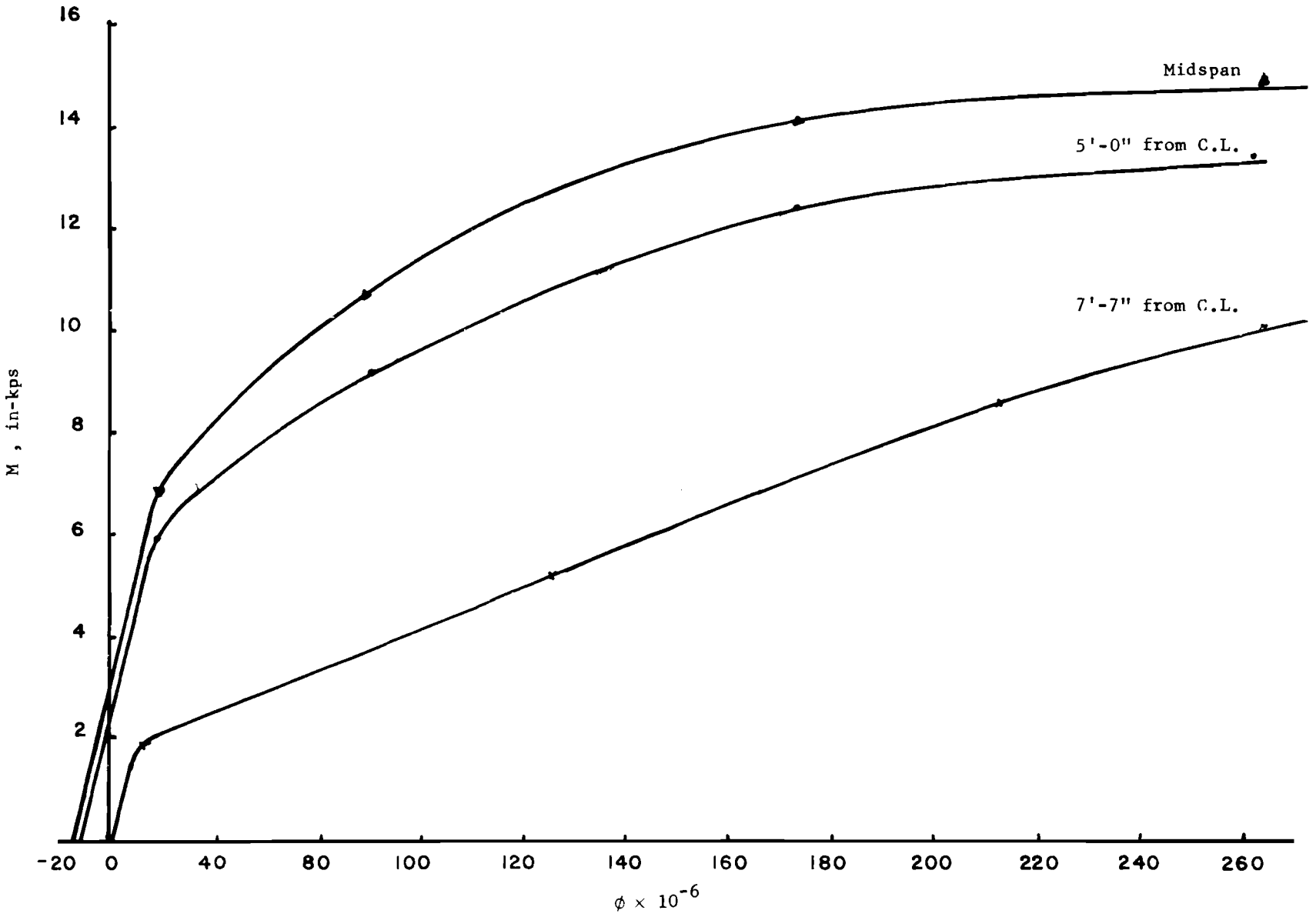

Fig D.5. M - ϕ diagram for model.

APPENDIX E

APPENDIX E

Estimated Shear Capacity at Notched End of the Model (Fig 3.2)

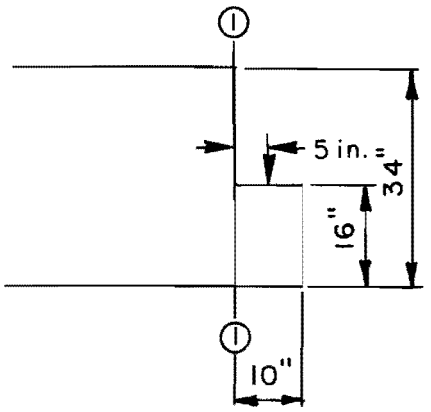

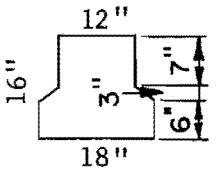

$A = 237 \text{ in.}^2$

$I = 4970 \text{ in.}$

$$v_{ci}, \text{ at Section } ① \quad ① = .6\sqrt{f'_c} + \frac{V_d + \left(\frac{V\ell\, M_{cr}}{M_{max}}\right)}{b_w d}$$

$f'_c = 6500 \text{ psi}$

$V_d = 0$

$$\frac{M_{max}}{V\ell} = P \times \frac{5}{P} = 5$$

$$M_{cr} = \left(\frac{I}{Y_t}\right)\left(6\sqrt{f'_c} + f_{pe} - f_d\right)$$

$$= \frac{4970}{8.8}\left(6\sqrt{6500} + 3080\right)$$

$$= 2012700 \text{ in./lb}$$

$$v_{ci} = .6\sqrt{6500} + \frac{2012700}{5 \times 12 \times 10}$$

$$= 3403 \text{ psi}$$

$f_d = 0$

$$f_{pe} = \frac{336}{237} + \frac{336 \times 2.8 \times 8.8}{4970}$$

$= 3.08 \text{ ksi}$

$d = 10 \text{ in.}$

$b_w = 12 \text{ in.}$

$\underline{v_{cw}}$

$$f_{pc} = \left(\frac{336}{237}\right) \frac{10}{50 \times 1/2} = .568 \text{ ksi}$$

$$V_p = \left(6 \times 21 \times \frac{16}{75}\right) \frac{10}{50 \times 1/2} = 10.75 \text{ k}$$

$$v_{cw} = 3.5\sqrt{f'_c} + .3f_{pc} + \frac{V_p}{b_w d}$$

$$= (3.5\sqrt{6500}) + (.3 \times 568) + \left(\frac{10750}{12 \times 10}\right) = 542 \text{ psi}$$

Steel provided in 12-in. space,

Straps	$4 \times 3 \times 1/4$	=	3 in.^{2}	of 36 ksi
Rebars	$3 \times .2$	=	.6	of 60 ksi

This can be taken as $3 + \left(.6 \times \frac{60}{36}\right) = 4$ in.^{2} of 36 ksi

$$\frac{A_s f_y}{b_w s} = v_u - v_c$$

$$\frac{4 \times 36000}{12 \times 12} = v_u - 542$$

$$v_u = 1542 \text{ psi}$$

$$V = v_u \times 6_w \times d$$

$$= 1.542 \times 12 \times 10$$

$$= \underline{185 \text{ k}}$$

Shear Capacity of the Saddle Plate End

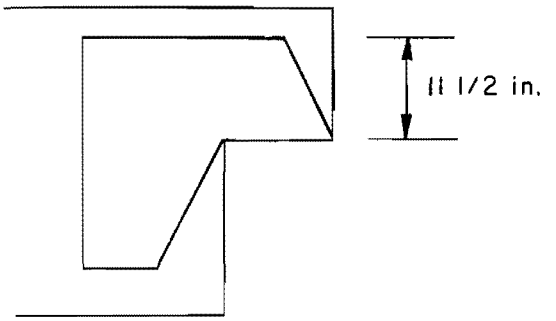

Concrete Capacity v_{cw} = .542 ksi

$V_c = 12 \times 10 \times .542$ = 65 k

Capacity Contributed by Plates = $A_s \times .4\ F_y$

$= \left(2 \times 11.5 \times \frac{3}{8}\right) \times .4 \times 36$

= 124 k

Total Shear Capacity = 189 k

APPENDIX F

APPENDIX F

Load Calculations for Stressing Operations

Stress required to be applied on strands for the specimen = .7 fpu - Time dependent losses (estimated as 16%)

$= .7 \times 270 \times \frac{84}{100}$

$= 162.54$ ksi

Length of strand from one grip to the other = 22 ft

Extension in 22 ft $= p \frac{L}{E_s}$

$= \frac{162.54 \times 22 \times 12}{29000}$

$= 1.479$ in.

Allowance for slip of grips estimated as = .313 in.

Total elongation required = 1.792 in.

Stress required to elongate the strand by 1.792 in. $= \frac{1.792 \times 29000}{22 \times 12}$

$= 196.8$ ksi

Load on one strand $= 196.8 \times .153$

$= \underline{\underline{30.11}}$ kps

APPENDIX G

APPENDIX G

PROGRAM LINFIX 6 - LINEAR ANALYSIS OF TWO DIMENSIONAL FRAMES - REV. 12-16
MODEL 1-1

TABLE 3.4 --- RESULTS - MEMBER STRESSES --- LOAD CASE 1

LOAD CASE LOAD-APPLIED AT JOINT , 100 KPS

MEM-	JOINTS		AXIAL STRESS (KP/(IN**2))
1	1	2	-2.960E-01
2	2	3	-3.813E-01
3	3	4	-1.372E-01
4	4	5	-1.247E-01
5	6	4	1.836E-01
6	6	3	-2.568E-01
7	7	3	1.987E-01
8	7	2	-5.439E-01
9	2	8	-8.779E-01
10	8	1	-1.945E-01
11	8	7	-1.446E+00
12	7	6	-5.488E-01
13	6	5	-1.490E-01
14	15	5	-3.479E-01
15	15	6	-7.628E-01
16	14	5	4.154E-01
17	14	6	-3.245E-01
18	14	7	-1.376E+00
19	13	6	8.935E-01
20	13	7	-3.417E-01
21	13	8	-1.832E+00
22	12	7	1.248E+00
23	12	8	3.485E-02
24	9	10	4.160E-01
25	10	11	7.821E-01
26	11	12	1.039E+00
27	12	13	5.851E-01
28	13	14	2.507E-01
29	14	15	1.265E-01
30	15	16	-7.535E-01
31	16	14	-7.957E-01
32	17	15	2.690E-01
33	17	14	-6.601E-01
34	17	13	-1.007E+00
35	18	14	6.816E-01
36	18	13	-6.081E-01
37	18	12	-6.678E-01
38	19	13	1.041E+00
39	19	12	3.187E-01
40	19	11	-2.149E-01
41	20	12	1.040E+00
42	20	11	2.076E-01
43	10	20	-3.384E-01
44	21	10	1.017E-01
45	9	21	-5.652E-01
46	22	9	-2.221E-01
47	22	21	2.813E-01
48	21	20	3.142E-01
49	20	19	8.538E-02
50	19	18	4.501E-01
51	18	17	3.664E-01
52	17	16	2.337E-01
53	16	29	-1.064E+00

54	29	17	-6,973E-01
55	28	16	-6,891E-03
56	17	28	-8,063E-01
57	28	18	-7,453E-01
58	27	17	3,399E-01
59	18	27	-6,179E-01
60	27	19	-7,830E-01
61	26	18	5,522E-01
62	19	26	-5,782E-01
63	23	20	7,547E-01
64	25	19	4,517E-01
65	20	25	5,578E-02
66	21	25	-6,150E-01
67	21	24	1,102E-01
68	22	24	-6,618E-01
69	22	23	-3,395E-01
70	23	24	1,429E-01
71	24	25	1,977E-01
72	25	26	4,254E-02
73	26	27	2,845E-01
74	27	28	2,471E-01
75	28	29	2,287E-01
76	29	30	-1,257E+00
77	30	28	-6,435E-01
78	31	29	-2,169E-01
79	28	31	-9,057E-01
80	31	27	-6,620E-01
81	32	28	1,016E-01
82	27	32	-6,950E-01
83	32	26	-6,899E-01
84	33	27	4,051E-01
85	26	33	-4,737E-01
86	33	25	-7,987E-01
87	34	26	7,640E-01
88	25	34	5,283E-03
89	34	24	-7,677E-01
90	24	35	1,808E-01
91	23	35	-7,006E-01
92	23	36	-3,308E-01
93	36	35	1,558E-01
94	35	34	4,568E-01
95	34	33	3,566E-01
96	33	32	3,147E-01
97	32	31	2,329E-01
98	31	30	2,128E-01
99	30	43	-1,427E+00
100	43	31	-4,078E-01
101	31	42	-9,486E-01
102	42	32	-3,562E-01
103	41	32	-7,114E-01
104	33	41	-4,673E-01
105	40	33	-4,442E-01
106	34	40	-6,833E-01
107	39	34	5,667E-02
108	35	39	-7,526E-01
109	38	35	3,298E-01
110	36	38	-8,251E-01
111	37	36	-4,067E-01
112	37	38	7,276E-01
113	38	39	1,534E+00
114	39	40	1,142E+00
115	40	41	6,313E-01

116	41	42	4.454E-01
117	42	43	3.267E-01
118	43	44	-1.475E+00
119	44	42	-1.332E-01
120	45	43	-5.055E-01
121	42	45	-1.138E+00
122	45	41	-2.667E-01
123	41	46	-8.414E-01
124	46	40	-3.462E-02
125	40	47	-9.031E-01
126	47	39	-2.177E-02
127	39	48	-1.623E+00
128	48	38	-3.051E-02
129	38	49	-2.070E+00
130	49	37	-5.710E-02
131	50	38	7.030E+00
132	37	50	-5.476E-01

PROGRAM LINFIX 6 - LINEAR ANALYSIS OF TWO DIMENSIONAL FRAMES - REV. 12-16
MODEL 1-1

TABLE 3.4 --- RESULTS - MEMBER STRESSES --- LOAD CASE 1

LOAD CASE -LOAD+APPLIED AT JOINT , 100 KPS

MEM-	JOINTS		AXIAL STRESS (KP/(IN**2))
1	1	2	-2.719E-01
2	2	3	-2.398E-01
3	3	4	-5.038E-02
4	4	5	-3.826E-02
5	6	4	8.197E-02
6	6	3	-2.753E-01
7	7	3	1.621E-01
8	7	2	-6.798E-01
9	2	8	-6.903E-01
10	8	1	-1.557E-01
11	8	7	-1.478E+00
12	7	6	-7.136E-01
13	6	5	-2.626E-01
14	15	5	-3.066E-01
15	15	6	-9.823E-01
16	14	5	6.036E-01
17	14	6	-1.770E-01
18	14	7	-1.799E+00
19	13	6	9.071E+00
20	13	7	-2.873E-01
21	13	8	-2.603E+00
22	12	7	2.091E+01
23	12	8	4.904E-01
24	9	10	1.413E-01
25	10	11	1.640E+01
26	11	12	3.542E+01
27	12	13	1.331E+01
28	13	14	8.245E-02
29	14	15	-1.126E-02
30	15	16	-9.792E-01
31	16	14	-1.322E+00
32	17	15	7.747E-01
33	17	14	-5.504E-01
34	17	13	-1.700E+00
35	18	14	1.417E+01
36	18	13	-8.262E-03
37	18	12	-1.416E+00
38	19	13	2.486E+01
39	19	12	8.364E-01
40	19	11	-2.300E-01
41	20	12	2.524E+01
42	20	11	6.185E-02
43	10	20	1.090E-01
44	21	10	-7.909E-02
45	9	21	-2.438E-01
46	22	9	-4.931E-01
47	22	21	3.343E-01
48	21	20	6.317E-01
49	20	19	7.184E-01
50	19	18	1.362E+00
51	18	17	9.842E-01
52	17	16	4.456E-01
53	16	29	-1.518E+00

54	29	17	-8.343E-01
55	28	16	4.145E-02
56	17	28	-8.556E-01
57	28	18	-6.491E-01
58	27	17	6.995E-01
59	18	27	-4.379E-01
60	27	19	-5.286E-01
61	26	18	1.018E+00
62	19	26	-3.770E-01
63	23	20	2.254E-02
64	25	19	1.033E+00
65	20	25	2.105E-01
66	21	25	-5.102E-01
67	21	24	1.086E-01
68	22	24	-5.688E-01
69	22	23	-7.593E-01
70	23	24	3.219E-01
71	24	25	5.482E-01
72	25	26	4.271E-01
73	26	27	4.316E-01
74	27	28	4.099E-01
75	28	29	3.423E-01
76	29	30	-1.680E+00
77	30	28	-6.027E-01
78	31	29	-4.222E-01
79	28	31	-9.342E-01
80	31	27	-4.805E-01
81	32	28	8.797E-02
82	27	32	-4.879E-01
83	32	26	-5.410E-01
84	33	27	6.918E-01
85	26	33	-1.136E-01
86	33	25	-8.282E-01
87	34	26	4.178E-02
88	25	34	3.856E-01
89	34	24	-8.159E-01
90	24	35	3.567E-01
91	23	35	-8.339E-01
92	23	36	-8.263E-01
93	36	35	9.148E-01
94	35	34	1.293E+00
95	34	33	9.870E-01
96	33	32	4.714E-01
97	32	31	2.272E-01
98	31	30	2.223E-01
99	30	43	-1.789E+00
100	43	31	-3.232E-01
101	31	42	-1.021E+00
102	42	32	-1.526E-01
103	41	32	-5.933E-01
104	33	41	-1.607E-01
105	40	33	-2.916E-01
106	34	40	-5.079E-01
107	39	34	1.212E-01
108	35	39	-9.982E-01
109	38	35	4.097E-01
110	36	38	-2.488E+00
111	37	36	3.788E-01
112	37	38	8.664E+01
113	38	39	4.568E+01
114	39	40	2.305E+01
115	40	41	6.916E+00

116	41	42	2.149E-01
117	42	43	2.649E-01
118	43	44	-1.735E+00
119	44	42	-1.538E-01
120	45	43	-5.911E-01
121	42	45	-1.120E+00
122	45	41	-3.136E-01
123	41	46	-5.544E-01
124	46	40	1.754E-02
125	40	47	-5.626E-01
126	47	39	9.475E-02
127	39	48	-1.711E+00
128	48	38	1.624E-01
129	38	49	-2.243E+00
130	49	37	5.670E-01
131	50	38	2.106E+02
132	37	50	-3.374E-01

PROGRAM LINFIx 6 - LINEAR ANALYSIS OF TWO DIMENSIONAL FRAMES - REV. 12-16
MODEL 1-1

TABLE 3.4 --- RESULTS - MEMBER STRESSES --- LOAD CASE 1

LOAD APPLIED 100 KPS

MEM-	JOINTS		AXIAL STRESS (KP/(IN**2))
1	1	2	-3.309E-01
2	2	3	-3.547E-01
3	3	4	-9.359E-02
4	4	5	-8.996E-02
5	6	4	1.537E-01
6	6	3	-3.288E-01
7	7	3	2.633E-01
8	7	2	-5.796E-01
9	2	8	-7.932E-01
10	8	1	-1.925E-01
11	8	7	-1.484E+00
12	7	6	-6.518E-01
13	6	5	-1.449E-01
14	15	5	-2.696E-01
15	15	6	-1.058E+00
16	14	5	5.950E+00
17	14	6	-2.156E-01
18	14	7	-1.943E+00
19	13	6	1.179E+01
20	13	7	-6.581E-02
21	13	8	-2.393E+00
22	12	7	2.837E+01
23	12	8	3.473E-01
24	9	10	1.860E-01
25	10	11	3.020E+01
26	11	12	6.534E+01
27	12	13	3.075E+01
28	13	14	2.998E-01
29	14	15	1.552E-01
30	15	16	-8.159E-01
31	16	14	-1.492E+00
32	17	15	6.140E+00
33	17	14	-7.987E-01
34	17	13	-1.974E+00
35	18	14	2.317E+01
36	18	13	2.412E-01
37	18	12	-4.487E-01
38	19	13	6.282E+01
39	19	12	4.712E+01
40	19	11	-7.917E-01
41	20	12	6.563E+01
42	20	11	2.032E-01
43	10	20	3.939E-02
44	21	10	1.993E-02
45	9	21	-3.134E-01
46	22	9	-4.666E-01
47	22	21	1.283E-01
48	21	20	1.561E+01
49	20	19	5.836E+00
50	19	18	3.952E+01
51	18	17	1.958E+01
52	17	16	1.692E-01
53	16	29	-1.790E+00

54	29	17	-1.511E+00
55	28	16	7.708E-01
56	17	28	-5.737E-01
57	28	18	-9.770E-01
58	27	17	2.047E+01
59	18	27	3.287E-01
60	27	19	-7.935E-01
61	26	18	2.879E+01
62	19	26	-7.699E-01
63	23	20	4.501E-02
64	25	19	1.102E+01
65	20	25	4.568E-01
66	21	25	-3.413E-01
67	21	24	-3.960E-02
68	22	24	-3.823E-01
69	22	23	-8.401E-01
70	23	24	1.041E+00
71	24	25	1.462E+00
72	25	26	1.370E+00
73	26	27	1.345E+00
74	27	28	1.237E+00
75	28	29	7.133E-01
76	29	30	-2.192E+00
77	30	28	-5.362E-01
78	31	29	-4.473E-01
79	28	31	-6.918E-01
80	31	27	-1.799E-01
81	32	28	5.427E-01
82	27	32	8.798E-02
83	32	26	-5.379E-01
84	33	27	9.052E+00
85	26	33	-3.989E-01
86	33	25	-4.280E-01
87	34	26	6.914E-02
88	25	34	2.861E-01
89	34	24	-9.596E-01
90	24	35	3.803E-01
91	23	35	-1.592E+00
92	23	36	-3.414E-01
93	36	35	3.108E+01
94	35	34	3.227E+01
95	34	33	2.478E+01
96	33	32	3.875E-01
97	32	31	9.237E-02
98	31	30	2.038E-01
99	30	43	-2.240E+00
100	43	31	-2.921E-01
101	31	42	-7.813E-01
102	42	32	-1.862E-01
103	41	32	-1.101E-01
104	33	41	-4.996E-01
105	40	33	1.056E-01
106	34	40	-6.331E-01
107	39	34	1.964E-01
108	35	39	-1.140E+00
109	38	35	2.620E-01
110	36	38	-2.398E+00
111	37	36	3.771E-01
112	37	38	1.021E+02
113	38	39	7.059E+01
114	39	40	4.607E+01
115	40	41	1.778E+01

116	41	42	2.040E-01
117	42	43	2.386E-01
118	43	44	-2.143E+00
119	44	42	-2.139E-01
120	45	43	-6.008E-01
121	42	45	-9.878E-01
122	45	41	-3.222E-01
123	41	46	-1.457E-01
124	46	40	1.294E-01
125	40	47	-3.296E-01
126	47	39	2.403E-01
127	39	48	-1.837E+00
128	48	38	3.604E-01
129	38	49	-2.520E+00
130	49	37	7.660E-01
131	50	38	2.143E+02
132	37	50	-3.848E-01

PROGRAM LINFIX 6 - LINEAR ANALYSIS OF TWO DIMENSIONAL FRAMES - REV. 12-16
MODEL 1-1

TABLE 3.4 --- RESULTS - MEMBER STRESSES --- LOAD CASE 1

LOAD APPLIED 100 KPS

MEM-	JOINTS		AXIAL STRESS (KP/(IN**2))
1	1	2	-3.439E-01
2	2	3	-3.816E-01
3	3	4	-1.156E-01
4	4	5	-1.132E-01
5	6	4	1.825E-01
6	6	3	-3.186E-01
7	7	3	2.605E-01
8	7	2	-5.624E-01
9	2	8	-8.150E-01
10	8	1	-2.004E-01
11	8	7	-1.458E+00
12	7	6	-6.603E-01
13	6	5	-1.498E-01
14	15	5	-3.106E-01
15	15	6	-1.104E+00
16	14	5	6.314E+00
17	14	6	-1.584E-01
18	14	7	-1.887E+00
19	13	6	1.182E+01
20	13	7	-6.870E-02
21	13	8	-2.343E+00
22	12	7	2.927E+01
23	12	8	3.130E-01
24	9	10	1.792E-01
25	10	11	2.739E+01
26	11	12	6.581E+01
27	12	13	3.337E+01
28	13	14	3.737E-01
29	14	15	1.530E-01
30	15	16	-8.801E-01
31	16	14	-1.424E+00
32	17	15	6.890E+00
33	17	14	-7.423E-01
34	17	13	-1.851E+00
35	18	14	2.566E+01
36	18	13	2.040E-01
37	18	12	-5.774E-01
38	19	13	6.562E+01
39	19	12	4.737E+01
40	19	11	-9.110E-01
41	20	12	6.610E+01
42	20	11	2.328E-01
43	10	20	5.611E-02
44	21	10	5.232E-03
45	9	21	-2.989E-01
46	22	9	-4.743E-01
47	22	21	1.341E-01
48	21	20	1.407E+01
49	20	19	4.135E+00
50	19	18	4.066E+01
51	18	17	2.567E+01
52	17	16	5.216E-01
53	16	29	-1.708E+00

54	29	17	-1.366E+00
55	28	16	5.011E-02
56	17	28	-4.780E-01
57	28	18	-1.277E+00
58	27	17	2.521E+01
59	18	27	3.380E-01
60	27	19	-9.864E-01
61	26	18	3.039E+01
62	19	26	-7.372E-01
63	23	20	3.951E-02
64	25	19	1.117E+01
65	20	25	5.040E-01
66	21	25	-3.030E-01
67	21	24	-6.217E-02
68	22	24	-3.904E-01
69	22	23	-8.511E-01
70	23	24	8.166E-01
71	24	25	1.274E+00
72	25	26	1.228E+00
73	26	27	1.201E+00
74	27	28	9.984E-01
75	28	29	2.132E+01
76	29	30	-2.184E+00
77	30	28	-4.724E-01
78	31	29	5.136E-01
79	28	31	-1.023E+00
80	31	27	-1.867E-01
81	32	28	3.419E-01
82	27	32	1.170E-01
83	32	26	-6.014E-01
84	33	27	9.427E+00
85	26	33	-3.646E-01
86	33	25	-5.264E-01
87	34	26	7.899E-02
88	25	34	4.587E-01
89	34	24	-1.069E+00
90	24	35	3.999E-01
91	23	35	-1.897E+00
92	23	36	-2.320E-01
93	36	35	3.679E+01
94	35	34	3.022E+01
95	34	33	2.860E+01
96	33	32	4.441E-01
97	32	31	2.184E-01
98	31	30	3.487E-01
99	30	43	-2.280E+00
100	43	31	-3.681E-01
101	31	42	-7.737E-01
102	42	32	-2.433E-01
103	41	32	-1.594E-01
104	33	41	-5.332E-01
105	40	33	1.757E-01
106	34	40	-7.674E-01
107	39	34	4.115E-01
108	35	39	-1.742E+00
109	38	35	4.359E-01
110	36	38	-3.788E+00
111	37	36	1.361E+00
112	37	38	2.629E+02
113	38	39	8.351E+01
114	39	40	5.798E+01
115	40	41	2.386E+01

116	41	42	3,074E-01
117	42	43	2,564E-01
118	43	44	-2,227E+00
119	44	42	-2,275E-01
120	45	43	-5,959E-01
121	42	45	-1,037E+00
122	45	41	-3,224E-01
123	41	46	-1,735E-01
124	46	40	2,000E-01
125	40	47	-3,617E-01
126	47	39	3,180E-01
127	39	48	-1,908E+00
128	48	38	4,137E-01
129	38	49	-1,599E+00
130	49	37	3,208E+00
131	50	38	1,970E+00
132	37	50	1,371E-01

APPENDIX H

APPENDIX H

PROGRAM LINFIX 6 - LINEAR ANALYSIS OF TWO DIMENSIONAL FRAMES - REV. 12-16
MODEL 120

TABLE 3.4 --- RESULTS - MEMBER STRESSES --- LOAD CASE 1

LOAD CASE TOTAL LOAD 340 KPS

MEM-	JOINTS		AXIAL STRESS (KP/(IN**2))
1	1	2	-8.864E-01
2	2	3	-1.145E+00
3	1	4	-1.642E+00
4	1	5	-4.867E-01
5	2	5	-6.195E-01
6	2	6	9.336E-02
7	3	6	-6.078E-01
8	3	7	1.880E-01
9	4	5	-1.342E-01
10	5	6	-7.245E-01
11	6	7	-1.217E+00
12	4	8	-1.132E+00
13	4	9	9.286E+00
14	5	9	-1.664E+00
15	5	10	-7.115E-01
16	6	10	-1.032E+00
17	6	11	2.597E-01
18	7	11	-6.420E-01
19	7	12	3.509E-01
20	8	9	5.020E-01
21	9	10	7.358E+00
22	10	11	5.461E+00
23	11	12	-1.027E+00
24	8	14	-1.223E+00
25	9	14	-1.001E+00
26	13	14	-1.592E-01
27	9	13	7.934E+00
28	10	13	-1.597E+00
29	13	15	-3.089E+00
30	17	13	5.629E-02
31	13	16	1.973E+01
32	11	13	2.098E-01
33	16	17	-1.068E-01
34	11	16	4.355E-01
35	16	18	3.032E+01
36	12	16	-1.164E+00
37	12	18	1.102E+01
38	14	15	4.286E-01
39	15	17	2.964E+01
40	17	18	3.526E+01
41	18	19	3.802E+01
42	19	20	3.728E+01
43	20	21	3.495E-01
44	14	24	-1.597E+00
45	25	14	1.463E-01
46	15	25	-2.278E+00
47	15	26	5.428E-02
48	17	26	-8.855E-01
49	27	17	2.883E-01
50	18	27	1.899E-01
51	22	27	4.565E-02
52	18	22	3.362E+01
53	22	28	2.651E-01

54	19	22	1.619E-02
55	28	23	5.371E-02
56	22	23	3.089E+01
57	22	20	1.036E-01
58	23	29	-6.236E-01
59	20	23	-1.055E-01
60	23	30	2.303E+01
61	21	23	-5.855E-01
62	21	30	-8.350E-01
63	24	25	2.304E-01
64	25	26	2.756E+01
65	26	27	1.833E+01
66	27	28	1.792E+01
67	28	29	1.965E+01
68	29	30	1.772E+01
69	24	31	-1.603E+00
70	32	24	6.453E-02
71	25	32	-2.282E+00
72	33	25	6.336E-02
73	26	33	-5.632E-01
74	34	26	-2.931E-01
75	27	34	7.914E-02
76	28	34	3.632E-01
77	28	35	1.884E-01
78	29	35	-7.767E-01
79	29	36	-1.666E-01
80	30	36	-1.624E+00
81	30	37	-7.016E-01
82	31	32	5.336E-01
83	32	33	1.693E+01
84	33	34	-2.530E-01
85	34	35	1.404E+01
86	35	36	1.557E+01
87	36	37	2.576E+01
88	31	38	-1.396E+00
89	39	31	-5.988E-01
90	32	39	-2.348E+00
91	40	32	2.996E-02
92	33	40	-3.426E-01
93	34	40	-3.115E-01
94	35	40	-1.153E+00
95	35	41	4.408E-01
96	36	41	-2.051E+00
97	36	42	4.755E-01
98	37	42	-2.960E+00
99	37	43	-6.508E-01
100	38	39	1.251E+01
101	39	40	-6.210E-01
102	40	41	-1.783E-01
103	41	42	2.463E+01
104	42	43	2.832E+01
105	38	34	4.929E-01
106	45	38	-2.785E+00
107	39	45	-4.173E+00
108	46	39	6.500E-01
109	40	46	-1.362E+00
110	40	47	3.583E-02
111	41	47	-6.326E-01
112	41	48	4.612E-01
113	42	48	-2.361E+00
114	42	49	4.818E-01
115	43	49	-1.354E+00

116	43	50	1,021E-01
117	44	45	-1,688E-01
118	45	46	-9,185E-01
119	46	47	-8,596E-01
120	47	48	-9,402E-01
121	48	49	-2,149E-01
122	49	50	3,793E-02
123	44	52	-9,005E-01
124	45	52	-1,586E+00
125	45	53	-2,756E+00
126	46	53	-1,606E+00
127	46	54	-1,934E+00
128	47	54	-1,563E+00
129	47	51	1,016E-01
130	48	51	1,349E-01
131	49	51	2,261E-01
132	51	54	0,
133	51	55	0,
134	49	55	-8,214E-01
135	49	56	-4,713E-01
136	50	56	-2,147E-01
137	50	57	3,699E-01

APPENDIX I

APPENDIX I

PROGRAM LINFIX 6 - LINEAR ANALYSIS OF TWO DIMENSIONAL FRAMES - REV, 12-16
MODEL 200

TABLE 3,4 --- RESULTS - MEMBER STRESSES --- LOAD CASE 1

LOAD APPLIED 50 KPS

MEM-	JOINTS		AXIAL STRESS (KP/(IN**2))
1	1	2	-3,361E-02
2	2	3	-2,686E-01
3	3	4	-2,015E-02
4	9	4	-9,440E-02
5	9	3	-7,233E-01
6	8	3	5,797E+00
7	7	3	5,685E-01
8	6	3	-5,388E-01
9	6	2	-2,144E-01
10	2	5	-2,618E-01
11	5	1	-1,194E-03
12	5	6	-3,459E-01
13	6	7	-8,655E-01
14	7	8	-8,931E-01
15	8	9	-1,382E+00
16	16	9	-6,157E-01
17	15	9	-7,111E-01
18	15	8	4,306E-01
19	15	7	2,361E-02
20	14	7	-2,142E-01
21	13	7	-2,105E+00
22	11	6	-6,926E-01
23	11	5	1,744E-01
24	10	5	-1,654E-01
25	10	11	5,974E-02
26	12	10	-3,775E-01
27	10	13	2,846E-01
28	13	11	-4,927E-01
29	12	13	1,866E-01
30	13	14	8,903E+00
31	14	15	-5,879E-01
32	15	16	1,344E-02
33	22	16	-6,356E-01
34	15	22	-1,919E-01
35	20	22	4,354E-01
36	20	15	-1,682E+00
37	21	20	1,030E+01
38	14	20	6,668E+00
39	19	14	-2,748E+00
40	18	14	-1,566E+00
41	18	13	-3,540E-01
42	13	17	-4,340E-02
43	17	12	-3,801E-01
44	17	18	1,184E-01
45	18	19	8,309E+00
46	19	21	8,160E-02
47	21	22	3,259E-01
48	22	23	4,067E-01
49	23	24	2,103E-01
50	31	24	-2,270E-01
51	23	31	3,346E-01
52	30	23	-4,477E-02
53	22	30	2,160E-01

54	29	22	-4,061E-01
55	29	21	-6,055E-02
56	28	21	-3,096E-01
57	28	19	2,249E-06
58	27	19	-1,885E+00
59	26	19	-1,165E+00
60	26	18	-4,815E-01
61	18	25	-1,355E-01
62	25	17	-3,842E-01
63	25	26	1,550E-01
64	26	27	1,073E+01
65	27	28	-8,758E-02
66	28	29	1,792E-01
67	29	30	1,620E-01
68	30	31	1,382E-01
69	38	31	-5,465E-01
70	38	30	3,943E-01
71	37	30	-6,151E-01
72	37	29	-8,433E-02
73	36	29	-4,494E-01
74	36	28	-6,067E-01
75	35	28	-7,888E-01
76	35	27	1,476E-06
77	34	27	-1,348E+00
78	33	27	-1,030E+00
79	33	26	-6,127E-01
80	26	32	-2,432E-01
81	32	25	-3,935E-01
82	32	33	2,258E-01
83	33	34	5,880E-01
84	34	35	2,033E-01
85	35	36	2,255E-02
86	36	37	-9,938E-03
87	37	38	7,418E-02
88	43	38	-8,648E-01
89	43	47	-7,142E-01
90	42	37	-6,430E-01
91	42	36	-3,153E-01
92	41	36	-8,811E-01
93	41	35	-9,428E-01
94	41	34	3,226E-01
95	40	34	-9,065E-01
96	40	33	-7,768E-01
97	33	39	-2,282E-01
98	39	32	-4,275E-01
99	39	40	1,060E-01
100	40	41	1,655E-01
101	41	42	-1,873E-02
102	42	43	-9,376E-02
103	48	43	-1,296E+00
104	48	42	1,413E-01
105	47	42	-7,474E-01
106	47	41	-3,938E-01
107	46	41	-1,841E+00
108	45	41	-7,120E-01
109	45	40	-7,960E-01
110	44	40	-1,991E-01
111	44	39	-5,624E-01
112	44	45	1,677E-02
113	45	46	6,220E-02
114	46	47	-1,677E-01
115	47	48	-9,231E-02

116	53	48	-2,024E+00
117	53	47	-3,594E-01
118	52	47	-1,032E+00
119	52	46	-2,599E-01
120	51	46	-6,747E-01
121	50	46	-8,828E-01
122	50	45	-7,441E-01
123	49	45	-6,987E-01
124	49	44	-7,865E-01
125	49	50	1,238E-01
126	50	51	3,387E-01
127	51	52	3,438E-01
128	52	53	3,383E-01
129	57	53	-1,709E+00
130	57	52	7,688E-07
131	56	52	-1,782E+00
132	56	51	-4,108E-01
133	55	51	-6,450E-02
134	55	50	-1,403E+00
135	54	50	-2,197E-01
136	54	49	-1,345E+00

PROGRAM LINFIX 6 - LINEAR ANALYSIS OF TWO DIMENSIONAL FRAMES - REV. 12-16-
MODEL 200

TABLE 3.4 --- RESULTS - MEMBER STRESSES --- LOAD CASE 1

LOAD APPLIED 100 KPS

MEM-	JOINTS		AXIAL STRESS (KP/(IN**2))
1	1	2	-3.255E-02
2	2	3	-3.743E-01
3	3	4	-3.365E-02
4	9	4	-1.899E-02
5	9	3	-8.965E-01
6	8	3	1.366E+01
7	7	3	9.150E+00
8	6	3	-7.749E-01
9	6	2	-1.050E-01
10	2	5	-4.918E-01
11	5	1	1.170E-02
12	5	6	-9.953E-01
13	6	7	-2.524E+00
14	7	8	-2.630E+00
15	8	9	-2.927E+00
16	16	9	-7.911E-02
17	15	9	-2.857E+00
18	15	8	1.714E+01
19	15	7	9.650E-02
20	14	7	4.259E-01
21	13	7	-3.945E+00
22	11	6	-4.856E-01
23	11	5	6.202E-01
24	10	5	-4.427E-01
25	10	11	-2.195E-01
26	12	10	-7.222E-01
27	10	13	7.344E+00
28	13	11	2.978E-01
29	12	13	3.252E-01
30	13	14	2.413E+01
31	14	15	-9.478E-01
32	15	16	2.857E-02
33	22	16	3.663E-02
34	15	22	3.844E-07
35	20	22	9.097E+00
36	20	15	-2.355E+00
37	21	20	3.538E+01
38	14	20	1.823E+01
39	19	14	-2.688E+00
40	18	14	-3.290E+00
41	18	13	-1.885E-01
42	13	17	-5.223E-01
43	17	12	-7.367E-01
44	17	18	4.901E-01
45	18	19	1.540E+01
46	19	21	-1.569E-04
47	21	22	6.177E+00
48	22	23	4.502E+00
49	23	24	6.200E-02
50	31	24	-1.987E-01
51	23	31	3.385E-01
52	30	23	-7.960E-02
53	22	30	7.684E+00

54	29	22	-7,913E-02
55	29	21	8,512E-01
56	28	21	1,853E-01
57	28	19	8,453E-06
58	27	19	-1,767E+00
59	26	19	-2,655E+00
60	26	18	-4,351E-01
61	18	25	-3,657E-01
62	25	17	-7,622E-01
63	25	26	4,763E-01
64	26	27	2,273E+01
65	27	28	-3,227E-01
66	28	29	1,503E-01
67	29	30	1,108E-01
68	30	31	-1,317E-01
69	38	31	-5,102E-01
70	38	30	4,808E+00
71	37	30	-8,078E-02
72	37	29	9,489E-01
73	36	29	1,709E-02
74	36	28	1,113E-01
75	35	28	-2,298E-01
76	35	27	6,522E-06
77	34	27	-1,735E+00
78	33	27	-2,306E+00
79	33	26	-6,851E-01
80	26	32	-7,410E-01
81	32	25	-7,888E-01
82	32	33	3,892E-01
83	33	34	2,117E+01
84	34	35	-4,120E-03
85	35	36	-3,560E-02
86	36	37	-4,161E-01
87	37	38	-1,489E-01
88	43	38	-1,108E+00
89	43	47	-1,165E+00
90	42	37	-3,400E-02
91	42	36	9,754E-01
92	41	36	-3,298E-01
93	41	35	-4,101E-01
94	41	34	4,714E-07
95	40	34	-1,623E+00
96	40	33	-6,541E-01
97	33	39	-8,591E-01
98	39	32	-9,087E-01
99	39	40	4,148E-01
100	40	41	6,681E-01
101	41	42	-4,598E-01
102	42	43	-5,161E-01
103	48	43	-1,453E+00
104	48	42	-9,730E-02
105	47	42	1,059E-01
106	47	41	7,807E-01
107	46	41	-1,063E+00
108	45	41	-1,160E+00
109	45	40	-9,197E-01
110	44	40	-4,402E-01
111	44	39	-1,202E+00
112	44	45	9,183E-02
113	45	46	2,937E-01
114	46	47	8,897E-02
115	47	48	-7,234E-01

116	53	48	-2,313E+00
117	53	47	4,628E+00
118	52	47	-1,956E+00
119	52	46	3,255E-07
120	51	46	-5,859E-01
121	50	46	-1,397E+00
122	50	45	-8,346E-01
123	49	45	-1,099E+00
124	49	44	-1,463E+00
125	49	50	1,958E-01
126	50	51	5,492E-01
127	51	52	5,922E+01
128	52	53	1,144E+02
129	57	53	-5,640E-01
130	57	52	8,178E-06
131	56	52	-1,956E+00
132	56	51	7,953E-02
133	55	51	-9,479E-02
134	55	50	-2,020E+00
135	54	50	-3,530E-01
136	54	49	-2,125E+00